UNIVERSITY OF WITWATERSRAND
SCHOOL OF PATHOLOGY
DEPARTMENT OF VIROLOGY

Design of soluble HIV-1 Env trimers from highly neutralisation-resistant HIV-1 strains for the isolation of broadly neutralising antibodies.

Danielle Martin
(Student number: 2589758)

Supervisors:

Dr Thandeka Moyo-Gwete
Senior Medical Scientist at the National Institute of Communicable Diseases
Senior Researcher at the University of the Witwatersrand

Dr Dale Kitchin
Senior Medical Scientist at the National Institute of Communicable Diseases
Researcher at the University of the Witwatersrand

Dr Nonhlanhla N Mkhize
Senior Medical Scientist at the National Institute of Communicable Diseases
Researcher at the University of the Witwatersrand

Prof. Penny Moore
Research Professor, University of Witwatersrand
Director: Antibody Immunity Research Unit (AIRU), an extramural unit of the South African Medical Research Council and National Institute of Communicable Diseases (NICD)

September 2025

A Dissertation submitted to the Faculty of Health Sciences,
University of Witwatersrand, Johannesburg, in fulfilment of the requirements
for the degree of Master of Science Medicine (Virology)

Declaration

UNIVERSITY OF THE WITWATERSRAND, JOHANNESBURG

FACULTY OF HEALTH SCIENCES

PLAGIARISM DECLARATION TO BE SIGNED BY ALL HIGHER DEGREE STUDENTS

SENATE PLAGIARISM POLICY: APPENDIX ONE

I Danielle Martin (Student number: 2589758) am a student registered for the degree of MSc (Med) Virology in the academic year 2025.

I hereby declare the following:

- I am aware that plagiarism (the use of someone else's work without their permission and/or without acknowledging the original source) is wrong.
- I confirm that the work submitted for assessment for the above degree is my own unaided work except where I have explicitly indicated otherwise.
- I have followed the required conventions in referencing the thoughts and ideas of others.
- I understand that the University of the Witwatersrand may take disciplinary action against me if there is a belief that this is not my own unaided work or that I have failed to acknowledge the source of the ideas or words in my writing.
- I have included as an appendix a report from "Turnitin" (or other approved plagiarism detection) software indicating the level of plagiarism in my research document.

Signature: _____ Date: 25/09/2025

For my parents, Renee and Wayne Martin,

and

In memory of my dear grandmother

Lorna Kathleen De Klerk

4 February 1945 - 7 January 2025

Acknowledgements

First and foremost, I would like to express my sincerest gratitude to my incredible supervisors for guiding me and for generously sharing their expertise—personally and professionally. I am truly honoured to have been supervised by Prof Penny Moore – thank you for the opportunity to join the Antibody Immunity Research Unit (AIRU) and for fostering the inspiring the supportive work culture, Dr Nono Mkhize – thank you for your unwavering encouragement and reassurance, Dr Thandeka Moyo-Gwete – thank you for challenging me to push beyond what I thought possible and sparking my newfound passion for structural biology, and Dr Dale Kitchin – thank you for always reminding me to prioritise my well-being and be detail orientated.

I would also like to thank the brilliant medical scientists, I was privileged to work alongside at AIRU, for all the training, advice, chats and encouragement. Special mention to the following people for their assistance: Rudolph Serage and Alaine Marsden – B cell receptor analysis, Donald Mhllanga – assistance with expression of antibodies for screening, Haajira Khaldine – assistance with single dilution antibody neutralisation screening and Sebotsana Rasebotsa - antibody isolation.

I would also like to thank Dr Jeremy Woodward, Claire Van Den Berg and Mohamed Jaffer from the Electron Microscopy Unit (EMU) at the University of Cape Town, for their assistance with single-particle electron microscopy and training, funded by the Chan Zuckerberg Initiative. Additional thanks to Dr Karen Davies at the electron Bio-Imaging Centre (eBIC) unit at the Diamond Light Source, for her support with cryogenic electron microscopy.

I gratefully acknowledge the financial support provided by the National Research Foundation (NRF) and the Poliomyelitis Research Foundation (PRF), and to IAVI who funded this research through the Investigator-Initiated Research (IIR) program, awarded to Dr Dale Kitchin and Dr Thandeka Moyo-Gwete. I also extend my heartfelt appreciation to the participants and investigators of both the CAPRISA clinical trials and IAVI ADVANCE Surveillance Project, without whom this research would not be possible.

Finally, I would like to thank my family for their prayers, encouragement, and unwavering support. To my parents—thank you for allowing me to follow my passions, for instilling in me the value of hard work, and for making it possible for me to reach this point. To my wonderful friends—thank you for the laughter, joy, motivation, and inspiring me with your relentless work ethic.

Presentations

Martin, D., Moore, PL., Mkhize, NN., Kitchin, D., Moyo-Gwete, T. “Ultra-bNAb: Using ultra-resistant HIV Envs to isolate next generation bNAbs”, CAPRISA strategic planning meeting (1 March 2023), Oral presentation; Durban, South Africa.

Martin, D., Mzindle N, Naidoo, T., Rasebotsa, S., Moore, PL., Mkhize, NN., Kitchin, D., Moyo-Gwete, T. “Design of soluble HIV-1 Env trimers from highly neutralisation-resistant HIV-1 strains for the isolation of broadly neutralising antibodies”, Molecular Biosciences Research Trust (MBRT) research day (7 December 2023), Poster presentation; Johannesburg, South Africa.

Martin, D., Mzindle N, Naidoo, T., Rasebotsa, S., Moore, PL., Mkhize, NN., Kitchin, D., Moyo-Gwete, T. “Design of soluble HIV-1 Env trimers from highly neutralisation-resistant HIV-1 strains for the isolation of broadly neutralizing antibodies”, “The role of CryoEM in discovering new drugs and vaccines” workshop (19 August 2024), Oral presentation; Cape Town, South Africa.

Martin, D., Mzindle N, Naidoo, T., Rasebotsa, S., Van Den Berg, C., Woodward, J., Moore, PL., Mkhize, NN., Kitchin, D., Moyo-Gwete, T. “Design of soluble HIV-1 Env trimers from highly neutralisation-resistant HIV-1 strains for the isolation of broadly neutralising antibodies”, University of Witwatersrand Faculty of Health Sciences Research Day (5 September 2024), Poster presentation; Johannesburg, South Africa.

Abstract

The emergence of circulating HIV-1 strains with decreased sensitivity to clinically relevant broadly neutralising antibodies (bNAbs) poses a significant challenge, suggesting that current bNAbs may lose efficacy against future variants. This highlights the need for new bNAbs capable of neutralising resistant viruses. This study aimed to isolate novel bNAbs using a soluble trimer based on the envelope protein (Env) of a difficult-to-neutralise HIV-1 isolate with intrinsic resistance to several existing bNAbs. A soluble Env trimer derived from the FRESH1388 transmitted founder virus was successfully engineered with multiple stabilising mutations and expressed in mammalian cells. Binding assays revealed the V3 loop – an immunodominant, non-bNAb epitope – was overexposed on this trimer. However further stabilisation within the V3 region reduced this exposure and limited off-target antibody binding. Structural characterisation confirmed that the modified trimer, FRESH1388-2P-316W, adopted a closed, native-like conformation. This trimer was used in cell sorting to isolate 252 memory B cells from a CAPRISA cohort participant living with HIV-1, CAP287 – an individual with previously unmapped responses and 61% neutralisation breadth. Antibodies were expressed from sequenced B cell receptors (BCRs) and screened for neutralisation activity. Multiple clonal lineages were identified from 94 productively rearranged BCRs, with the largest lineage using a rarely used IGHV3-13. Ten antibodies were screened against a diverse subtype six-virus panel and the FRESH1388 virus. Four novel bNAbs were discovered, with breadth up to 67%, and three were able to neutralise FRESH1388. This study demonstrates the potential of resistant Env trimers to isolate novel bNAbs with promising neutralisation profiles.

Table of Contents

Declaration ii

Acknowledgements iii

Presentations iv

Abstract v

List of Abbreviations ix

List of Figures xi

List of Tables xii

1 Introduction 1

1.1 HIV-1 pandemic 1

1.1.1 Antiretrovirals for HIV-1 treatment and prevention 2

1.2 The HIV-1 virion 4

1.2.1 The genetics and structure of HIV-1 4

1.2.2 Infection and replication of HIV-1 5

1.3 The immune response to HIV-1 6

1.3.1 Antibody development and diversity 6

1.3.2 Development of neutralising and broadly neutralising antibodies in HIV infection 8

1.3.3 Broadly neutralising antibody epitopes 9

1.4 Evolving neutralisation resistance among HIV-1 viruses 10

1.5 Isolation of broadly neutralising antibodies 12

1.5.1 Previously isolated broadly neutralising antibodies and clinical relevance 12

1.5.2 Native-like soluble envelope trimers 14

1.6 Rationale 16

1.7 Project aim and objectives 17

1.7.1 Aim and hypothesis 17

1.7.2 Objectives 17

2 Methods 18
2.1 Screening for neutralisation resistance in African viruses 18
2.1.1 Isolate selection 18
2.1.2 Env-pseudotyped virus production 18
2.1.3 HIV pseudovirus neutralisation assay 19
2.2 Design and subcloning of SOSIP trimer plasmids 19
2.2.1 Design of soluble HIV-1 trimers 19
2.2.2 Subcloning and expression of the DS-SOSIP.664 plasmids 20
2.2.3 Mutagenesis 20
2.3 Expression and purification of trimers 21
2.4 Trimer characterisation 22
2.4.1 Luminex binding antibody multiplex assay 22
2.4.2 Negative stain electron microscopy 22
2.4.3 Cryogenic electron microscopy 23
2.5 B cell isolation 24
2.5.1 Screening of participant plasma 24
2.5.2 Fluorescently activated cell sorting 24
2.6 Antibody Isolation 25
2.6.1 cDNA synthesis 26
2.6.2 Immunoglobulin enrichment and sequencing 26
2.6.3 V(D)J sequence analysis 27
2.6.4 Linear cassette assembly 28
2.6.5 Antibody expression and screening 29
2.7 Characterisation of prioritized antibodies 30
2.7.1 Selection of priority CAP287 antibodies 30
2.7.2 Screening prioritised CAP287 antibodies for neutralisation breadth 30
3 Results 31

3.1 Defining the neutralisation phenotype of difficult-to-neutralise isolates 31
3.2 Screening CAPRISA participant plasma for neutralisation of difficult-to-neutralise isolates 33
3.3 Design, expression and characterisation of the FRESH1388 trimers 35
3.3.1 Expression of FRESH1388 trimers 35
3.3.2 Antigenicity of the FRESH1388-2P trimer 37
3.3.3 Expression of V3-stabilised FRESH1388 trimers 39
3.3.4 Antigenicity of V3-stabilised FRESH1388 trimers 41
3.3.5 Structural characterisation of the FRESH1388-2P-316W trimer 43
3.4 Antibody isolation from sorted B cells of participant CAP287 47
3.4.1 Isolation of B cells and immunogenetics of paired heavy and light chain sequences 47
3.4.2 Preliminary antibody screening 51
3.4.3 Antibody selection 51
3.4.4 Neutralisation breadth of prioritised CAP287 antibodies 53
4 Discussion 55
5 Conclusion 64
References 65
Appendix A - CAPRISA letter of support 90
Appendix B - Ethics clearance certificate 91
Appendix C - Turnitin report 92
Appendix D - Supplementary materials 93

List of Abbreviations

AA: amino acids

AIDS: acquired immunodeficiency syndrome

ART: antiretroviral therapy

ARV: antiretroviral

BAMA: binding antibody multiplex assay

BCR: B cell receptor

β-ME: β-mercaptoethanol

bNAb: broadly neutralising antibody

CATNAP: Compile, Analyze, and Tally NAb Panels

CD4bs: CD4 binding site

cDNA: complementary DNA

CDR: complementary determining region

CDRH3: CDR3 of the heavy chain

CDRL3: CDR3 of the light chain

CRFs: circulating recombinant forms

Cryo-EM: cryogenic electron microscopy

DMEM: Dulbecco's Modified Eagle Medium

DNA: deoxyribonucleic acid

Env: envelope

FBS: fetal bovine serum

FP: fusion peptide

FR: framework region

HIV: human immunodeficiency virus

GNL: Galanthus Nivalis Lectin

HEK: Human embryonic kidney

IC_{50}: half-maximal inhibitory concentration

ID_{50}: half-maximal inhibitory dilution

Ig: immunoglobulin

IgG: immunoglobulin G

IGHV: immunoglobulin variable heavy chain

IGKV: immunoglobulin variable kappa chain

IGLV: immunoglobulin variable lambda chain

mAb: monoclonal antibody

MFI: mean fluorescence intensity

MPER: membrane proximal external region

mRNA: messenger ribonucleic acid

NAb: neutralising antibody

nNAb: non-neutralising antibody

NS-EM: negative staining electron microscopy

OD450: optical density at 450 nm

PCR: polymerase chain reaction

PEP: post-exposure prophylaxis

PLWH: people living with HIV

PrEP: pre-exposure prophylaxis

RATPIg: Rapid Assembly, Transfection and Production of Immunoglobulins

RLU: relative light unit

RNA: ribonucleic acid

SEC: size-exclusion chromatography

SHIV: simian-human immunodeficiency virus

SHM: somatic hypermutation

WHO: world health organization

V: variable

VH: variable heavy

VL: variable light

URFs: unique recombinant forms

List of Figures

Figure 1.1: Global distribution of HIV-1 group M subtypes and recombinants..... 1

Figure 1.2: Yearly new global HIV-1 infections..... 2

Figure 1.3: The HIV-1 genome and viral particle..... 5

Figure 1.4: Schematic of the immunoglobulin 2D structure..... 7

Figure 1.5: BNAb epitopes on the HIV-1 Env..... 10

Figure 2.1: RATPIg workflow..... 26

Figure 3.1: Design and size-exclusion chromatography (SEC) profiles of soluble FRESH1388 trimers..... 36

Figure 3.2: Luminex binding data of the various antibodies targeting bNAb and non-bNAb epitopes on the FRESH1388-2P trimer..... 38

Figure 3.3: Design and purification of the V3- stabilised FRESH1388 trimers..... 40

Figure 3.4: Comparative luminex binding data of the bNAb and non-bNAb antibodies to the FRESH1388-2P trimer and V3 stabilised FRESH1388 trimers..... 42

Figure 3.5: Negative-stain electron microscopy of soluble FRESH1388 trimers relative to BG505 trimer..... 44

Figure 3.6: 3D models based on particles of the FRESH1388-2P-316W trimer observed through NS-EM and cryo-EM..... 46

Figure 3.7: Flow cytometry plots of cells sorted from participant CAP287..... 48

Figure 3.8: High-throughput neutralisation screening data of expressed antibodies and immunogenetic data of paired heavy and light chain sequences..... 50

List of Tables

Table 3.1: Neutralisation of difficult-to-neutralise isolates, from the IAVI ADVANCE study, by bNAbs and non-bNAbs targeting multiple Env epitopes. 32

Table 3.2: CAPRISA participant plasmas, from the CAPRISA 002 and 004 cohorts, were screened for neutralisation of the difficult-to-neutralise isolates. 34

Table 3.3: Immunogenetic and neutralisation screening data of antibodies selected for further characterisation. 52

Table 3.4: Neutralisation breadth and potency of the prioritised CAP287 antibodies against a six-virus heterologous panel and FRESH1388. 54

1 Introduction

1.1 HIV-1 pandemic

The human immunodeficiency virus (HIV) is a retrovirus that is part of the lentivirus sub-family and is the cause of acquired immune deficiency syndrome (AIDS) (Barré-Sinoussi *et al.*, 1983; Gallo *et al.*, 1984; Desrosiers and Letvin, 1987). There are two types of HIV: HIV-1, the main contributor to the global HIV burden and HIV-2, which is endemic to West Africa (Sharp and Hahn, 2011). HIV-1 is highly diverse and comprises four groups: M (for major), N (for non-M), O (for outlier) and P, of which group M is globally dominant (Barré-Sinoussi *et al.*, 1983; Gallo *et al.*, 1984; Popovic *et al.*, 1984; De Leys *et al.*, 1990; Gürtler *et al.*, 1994; Simon *et al.*, 1998; Plantier *et al.*, 2009; Sharp and Hahn, 2011). Group M consists of the following subtypes or clades: A, B, C, D, F, G, H, J and K, and recombinants of these subtypes are known as circulating recombinant forms (CRFs) or unique recombinant forms (URFs) (Robertson *et al.*, 2000; Hemelaar *et al.*, 2019; Gartner *et al.*, 2020). Prevalence of the group M subtypes and recombinants varies around the world (**Figure 1.1**), with subtype C being the most dominant in sub-Saharan Africa, contributing to more than 45% of new infections globally (Buonaguro, Tornesello and Buonaguro, 2007; Gartner *et al.*, 2020).

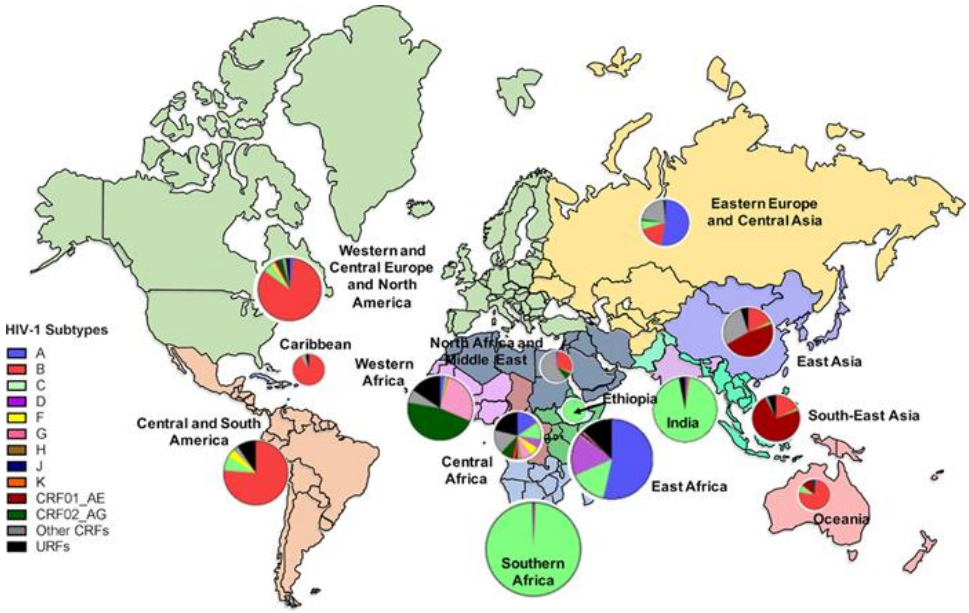

Figure 1.1: Global distribution of HIV-1 group M subtypes and recombinants. Pie charts depict the presence of each subtype in different regions, with the size of each chart indicating the respective region's contribution to the global HIV-1 burden. (Source: Gartner et al., 2020)

In 1982, the first case of HIV-1 was recorded and since then an estimated 88.4 million people have been infected with HIV (Abdool Karim *et al.*, 2009; UNAIDS, 2024). In 2023, according to the World Health Organization (WHO) and United Nations Programme on HIV and AIDS (UNAIDS), there were approximately 1.3 million new infections and an estimated 39.9 million people living with HIV (PLWH) with roughly 30.7 million accessing antiretroviral therapy (ART) (UNAIDS, 2024; WHO, 2024). Furthermore, due to the socio-economic conditions within sub-Saharan Africa, high numbers of HIV-1 infections continue to accrue annually (Abdool Karim *et al.*, 2009; Kharsany and Abdool Karim, 2016). With the implementation of ART and improvements to antiretroviral (ARV) drugs, there has been a reduction in the number of global new infections per year (**Figure 1.2**) (UNAIDS, 2024). However an increase in the number of infections was still observed in 28 countries, effectively highlighting the need for more preventative measures in order to reach the 2030 target of ending the AIDS pandemic (UNAIDS, 2024).

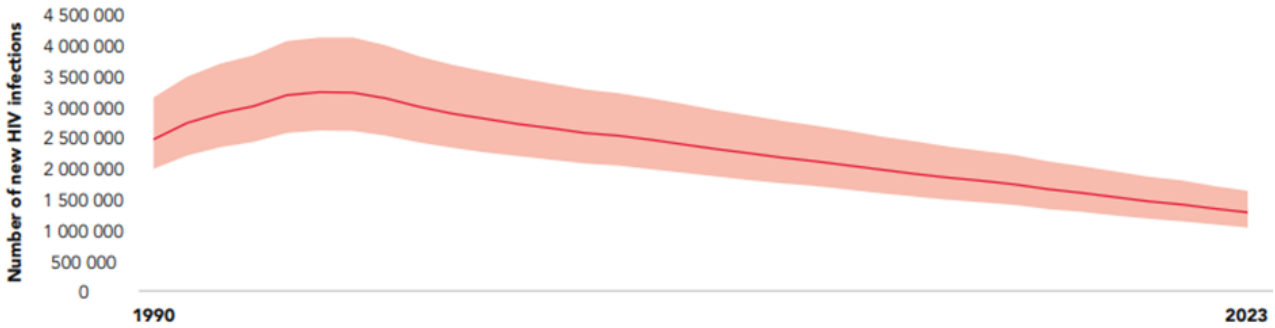

Figure 1.2: Yearly new global HIV-1 infections.
Total new infections observed from 1990 to 2023. (Source: UNAIDS, 2024)

1.1.1 Antiretrovirals for HIV-1 treatment and prevention

The current approved form of treatment for HIV-1 is ART, which involves several regimens of antiretroviral (ARV) drugs that target various stages in the HIV-1 replication cycle, thereby controlling disease progression (Palella *et al.*, 1998; Arts and Hazuda, 2012). The first ARV was discovered in 1987 and now over 40 ARVs, belonging to five different drug classes, based on their target within the HIV-1 replication cycle, have been developed (Fischl *et al.*, 1987; Tseng, Seet and Phillips, 2015). Initial monotherapy ART involved daily oral uptake, however this drove rapid viral resistance and subsequent treatment failure, leading to the development of combination ART (cART), which includes three ARVs from two distinct drug classes (HIV-CAUSAL Collaboration *et al.*, 2010).

Although ART has revolutionised HIV treatment, several challenges exist, including: long-term toxicity with ART, poor adherence to ART, social stigma, adverse effects, drug interactions and accessibility (Kontomanolis *et al.*, 2017; Chawla *et al.*, 2018; Serrão *et al.*, 2019; Thavarajah, Hønge and Wejse, 2024). Simplified treatments were therefore recommended to improve adherence, reduce drug interactions and improve quality of life (Tseng, Seet and Phillips, 2015). This was followed by the evolution of pre-exposure prophylaxis (PrEP) and post-exposure prophylaxis (PEP), using ARV drugs in those at risk of acquiring HIV-1, to prevent infection (Kelesidis and Landovitz, 2011; Tseng, Seet and Phillips, 2015; Sivay *et al.*, 2017; Massud *et al.*, 2019).

A significant development in ARV medicine was the development of long acting (LA) ARVs, including lenacapavir, cabotegravir, dapivirine and rilpivirine (Ullah Nayan *et al.*, 2023). Additionally various drug delivery systems, such as injections, vaginal rings (VR) or topical applications, have been explored as part of clinical trials for treatment and prevention (Cobb *et al.*, 2020; Deodhar *et al.*, 2022). Recently, promising results came from clinical trials investigating the use of lenacapavir as a preventative given subcutaneously twice yearly or intramuscularly once yearly (Bekker *et al.*, 2024; Kelley *et al.*, 2024; Jogiraju *et al.*, 2025). Lenacapavir was well tolerated, and proved effective and safe in the prevention of HIV-1 among both males and females.

While existing LA ARVs have proven to be effective at prevention, additional improvements are needed to simplify administration, decrease drug-drug interactions and improve accessibility. Several experimental therapies in development, including ultra-long-acting (ULA) ARVs, ARV nanoformulation, implants, microarray patches (MAP) and VRs have addressed these challenges (Deodhar *et al.*, 2022; Ullah Nayan *et al.*, 2023). Additionally several approved LA ARVs have varying pharmacokinetic effects between persons, in part due to difficulties in administration, and therefore could select for drug resistance mutations (Ullah Nayan *et al.*, 2023). Furthermore, the inability of ARVs to cure infection or eliminate the viral reservoir is unfavourable, and interrupted treatment leads to the re-emergence of the virus and increases drug-resistance (Chun *et al.*, 1999; Zhang *et al.*, 2016). Moreover, the costs of such treatments have been starkly highlighted by recent funding cuts. Global HIV-1 prevalence, although decreasing, it is still high, highlighting the need for more effective treatments and prevention approaches (Palella *et al.*, 1998; Zhang *et al.*, 2016).

1.2 The HIV-1 virion

1.2.1 The genetics and structure of HIV-1

HIV-1 is a retrovirus encoded by ~ 9 kb single-stranded RNA (ssRNA) genome, consisting of nine genes that encode for the various viral enzymes and structural or accessory proteins required for viral replication (**Figure 1.3**) (Frankel and Young, 1998; Peng *et al.*, 2023). The *vif*, *vpr*, *vpu*, *tat*, *rev* and *nef* genes encode for accessory proteins, and assist in transporting the viral genome out of the nucleus into the cytoplasm and aid in the viral replication cycle (Frankel and Young, 1998). The *gag*, *pol* and *env* genes encode structural and enzymatic proteins (Frankel and Young, 1998). Gag proteins include the nucleocapsid, capsid and matrix proteins which form protective layers around the viral genome (Epstein and Greene, 1991; Freed, 2001). The *pol* gene encodes for the three enzymes: reverse transcriptase which is responsible for making viral DNA from viral RNA; integrase which incorporates the viral DNA into the host cellular genome, and protease which cleaves viral proteins into functional components (Frankel and Young, 1998; Freed, 2001). The *env* gene encodes for the glycoprotein (gp) 160 protomer which forms the Envelope (Env) protein embedded in the virus membrane and which mediates host cell entry (Freed, 2001).

The trimeric HIV Env protein is formed by the cleavage of three gp160 protomers into gp120 and gp41 subunits (Frankel and Young, 1998). It is essential for infection as it binds to the receptor and co-receptor, and mediates membrane fusion (Wyatt and Sodroski, 1998). The Env is the sole target of neutralising antibodies (NAbs), which are generally strain-specific, but over time can develop neutralisation breadth/cross-reactivity, yielding broadly neutralising antibodies (bNAbs) (Wyatt and Sodroski, 1998), described in more detail below (section 1.3.2). Viral genetic diversity is constantly generated during infection through recombination and random mutations, due to the error-prone nature of the HIV reverse transcriptase enzyme (Mansky and Temin, 1995; Frost *et al.*, 2005). Mutations and recombination in the *env* gene can result in reduced neutralisation by autologous NAbs, and would be selected for, resulting in the generation of viral escape mutants (Bar *et al.*, 2012; Hemelaar, 2012).

Aside from sequence variation, the Env protein is a flexible and dynamic protein, moving between open and closed conformations thereby altering the accessibility to epitopes by NAbs (Munro *et al.*, 2014; Pugach *et al.*, 2015) and preventing neutralisation of the virus. Additionally, the glycan shield, composed of many host sugar or glycan residues, can diminish accessibility at certain epitopes for NAbs (Wei *et al.*, 2003). However, several of these glycans have proven important for binding and neutralisation by bNAbs, described in 1.3.2 (Behrens *et al.*, 2016).

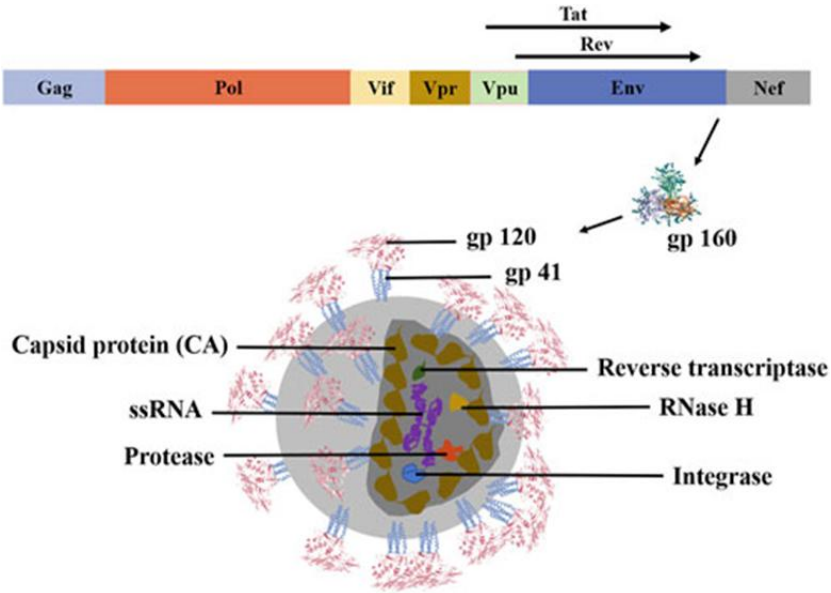

Figure 1.3: The HIV-1 genome and viral particle.
Genes encoding HIV-1 with the production of gp160 protomer for the HIV-1 Env trimer. Inside the HIV-1 viral particle is the ssRNA with several enzymes, all encapsulated by the lipid bilayer and protective protein layers including the capsid and nucleocapsid. (Source: Peng *et al.*, 2023)

1.2.2 Infection and replication of HIV-1

Viral infection occurs through the attachment of the gp120 Env subunit to the CD4 cell receptor, followed by conformational changes and binding to co-receptors: C-C chemokine receptor type 5 (CCR5) or CX-C chemokine receptor type 4 (CXCR4), found on the cell surface (Frankel and Young, 1998; Wyatt and Sodroski, 1998). This triggers conformational changes in the gp41 Env subunit, allowing for membrane fusion and entry of the viral particle into the cell (Weissenhorn *et al.*, 1996). The viral genome is then converted into DNA by the viral reverse transcriptase enzyme and guided into the cell nucleus by Vpr proteins (Freed, 2001). In the nucleus of the host cell, the integrase enzyme incorporates the viral DNA into the host chromosome, resulting in a provirus which will either remain dormant (creating latent reservoirs) or undergo replication (Rojas-

Celis *et al.*, 2019). If the provirus is replicated, Tat proteins enhance transcription of viral mRNA, which is transported by Rev proteins out of the nucleus and into the cytoplasm (Epstein and Greene, 1991; Gaynor, 1992). The Gag proteins are produced and the virus is assembled near the plasma membrane of the cell (Gaynor, 1992). New viral particles then bud off the cell, and this is moderated by Vpu proteins that weaken the interaction of cell receptors and new viral particles (Murakami, 2008).

1.3 The immune response to HIV-1

1.3.1 Antibody development and diversity

Immunoglobulins, also known as antibodies, are composed of two heavy and light chains that contain one variable domain and one to three constant domains (**Figure 1.4**) (Schroeder and Cavacini, 2010). Both the heavy and light (kappa or lambda) chains have one variable domain and one constant domain at the N-terminus, forming the antigen-binding fragment (Fab) responsible for binding specific antigens and potential neutralisation of the antigen (Schroeder and Cavacini, 2010). The variable domain for the heavy chain is encoded for by *variable* (*V*), *diversity* (*D*) and *joining* (*J*) genes while the light chain variable region is encoded by *V* and *J* genes only (Tonegawa, 1983). In addition to the Fab region, the heavy chains have two constant domains which form the crystallizable fragment (Fc) which determines the antibody classes (Schroeder and Cavacini, 2010). Furthermore the Fc portion has a number of functions including regulation of antibody half-life and activation of immune cells for clearance of the pathogens through binding of Fc receptors on effector cells (Schroeder and Cavacini, 2010). More specifically these clearance mechanisms include antibody-dependent cellular cytotoxicity (ADCC), complement dependent cytotoxicity (CDC), antibody-dependent cellular trogocytosis (ADCT) and antibody-dependent cellular phagocytosis (ADCP) (Schroeder and Cavacini, 2010; Richardson *et al.*, 2018).

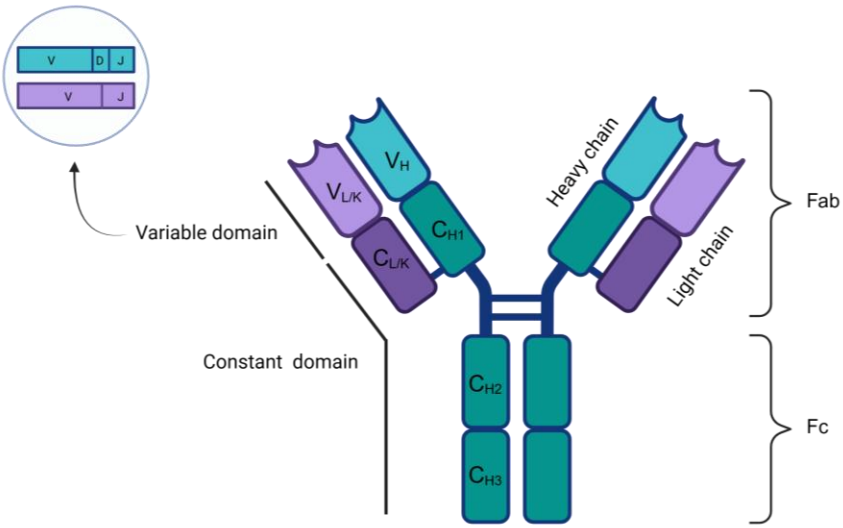

Figure 1.4: Schematic of the immunoglobulin 2D structure.
The Y-shaped immunoglobulin is formed by various domains (variable and constant) and regions (Fab and Fc). Furthermore the Variable domain is composed of *V(D)J* genes which form the antibody binding region also known as the paratope. Created using BioRender (https://BioRender.com).

The variable domain comprises four framework regions (FR) that alternate with and provide structural support to three complementary determining regions (CDR) which are highly variable and are largely responsible for antigen binding (Schroeder and Cavacini, 2010; Gąciarz and Ruddock, 2017). More specifically, the *V* gene segment encodes the FR1, CDR1, FR2, CDR2, FR3 and the amino-terminal portion of the CDR3 regions. The *D* gene encodes the middle of the CDR3 while the J gene encodes the carboxy-terminal of the CDR3 and FR4. There are multiple *V*, *D* and *J* gene segments at the VH, Vλ and Vκ loci and during B cell development the variable domain genes undergo *V(D)J* recombination which results in the joining of random *V*, *D* and *J* gene segments, generating diversity in the variable region (Tonegawa, 1983). Furthermore after exposure to the antigen, antibodies can undergo class switch recombination (CSR) or isotype switching and somatic hypermutation (SHM) (Dudley *et al.*, 2005). The heavy chain constant region determines the antibody class and during CSR the constant region is altered, resulting in an antibody with different effector functions (Dudley *et al.*, 2005). In the germinal centres, SHM increases the affinity of an antibody for binding to a particular antigen, through the introduction of multiple mutations into the variable domain of either the heavy and/or light chains (Dudley *et al.*, 2005). This is followed by affinity maturation which selects for antibodies with the best affinity for the circulating antigen. Antibodies

can undergo multiple rounds of SHM and affinity maturation, thus enhancing the binding or recognition of an antigen (Dudley *et al.*, 2005).

1.3.2 Development of neutralising and broadly neutralising antibodies in HIV infection

PLWH develop strain-specific NAbs between 12 and 20 weeks post-infection (Li *et al.*, 2006; Gray *et al.*, 2007). These antibodies target variable regions on the Env protein which often change due to mutational diversity or shifting of the glycan shield (Wei *et al.*, 2003). While strain-specific NAbs can neutralise viruses against which they were elicited they are not considered broad as they only target the virus which caused the infection, known as an autologous virus (Moore, 2018).

The development of new antibodies that can recognize viruses that have escaped autologous neutralisation drives viral diversity, essentially resulting in an “arms-race” between the virus and immune system (Bar *et al.*, 2012; Bonsignori *et al.*, 2017). The continual exposure to evolving Env antigens during chronic infection over many years, results in multiple rounds of affinity maturation, which in some instances leads to the development of bNAbs (Bhiman *et al.*, 2015; Landais and Moore, 2018; Griffith and McCoy, 2021).

Broadly neutralising antibodies (bNAbs) target conserved epitopes on the Env and are capable of neutralising heterologous viruses of different subtypes and geographic origins (Moore *et al.*, 2011). These antibodies only develop in 20-30% of PLWH, with chronic infection, however continual viral escape renders them ineffective in controlling their infections (Simek *et al.*, 2009; Gray *et al.*, 2011; Moore *et al.*, 2011) The reason that bNAbs only develop in a small number of infected people is thought to be due to a number of factors. Firstly, studies have shown that bNAb precursor B cells generally exist at a low frequency in the naive B cell repertoire, with many of these precursors having unusual characteristics (Havenar-Daughton *et al.*, 2018). Second, distinctive bNAb initiating Envs or transmitted/founder Envs are required to engage the rare precursors to induce bNAb lineages, with the potential to develop breadth (Bhiman *et al.*, 2015). Third, extensive viral diversity during chronic infection is required to generate changes around the antibody epitopes, which will further drive the antibody evolution by affinity maturation (Liao *et al.*, 2013; Doria-Rose *et al.*, 2014). Furthermore, this can drive viral escape from autologous antibodies and therefore select for antibodies which can withstand escape mutations

(Bhiman *et al.*, 2015; Doria-Rose *et al.*, 2016). Finally, high viral load together with low $CD4^+$ T cell count early during infection is associated with the development of this neutralisation breadth (Gray *et al.*, 2011).

Furthermore bNAbs have unique characteristics. This includes the long length of the third complementary-determining region of the heavy chain (CDRH3), allowing access to any recessed epitopes on the HIV-1 Env, but are only rarely found in the naive repertoire (Havenar-Daughton *et al.*, 2018; Griffith and McCoy, 2021; Gruell and Schommers, 2022). These properties are considered to be autoreactive and thus B cells with BCRs containing these characteristics are often eliminated during various stages of B cell development by immune tolerance mechanisms (Williams *et al*., 2017; Landais and Moore, 2018). However during HIV-1 infection these B cells, and thus bNAbs, are allowed to develop due to dysregulation of the immune system resulting in impaired or relaxed tolerance mechanisms (Moody *et al*., 2016).

1.3.3 Broadly neutralising antibody epitopes

Epitopes targeted by bNAbs are conserved on HIV-1 trimers, and include the CD4-binding site (CD4bs), V2-apex, V3-glycan site, the gp120/gp41 interface, the membrane proximal external region (MPER) of gp41, the fusion peptide (FP) and the silent face (**Figure 1.5**) (Kumar, Singh and Luthra, 2023). Isolation of antibodies targeting these various epitopes has allowed for the classification of bNAbs into “classes”, especially those targeting the V2-apex or CD4bs, with antibodies from multiple donors exhibiting similar heavy variable (V) gene usage, targeting the same contact residues on the Env, having similar angles of approach or sharing common structural features (Scheid *et al.*, 2011; Wu *et al.*, 2011; Zhou *et al.*, 2013; Andrabi *et al.*, 2015; Gorman *et al.*, 2016; Moore *et al.*, 2017).

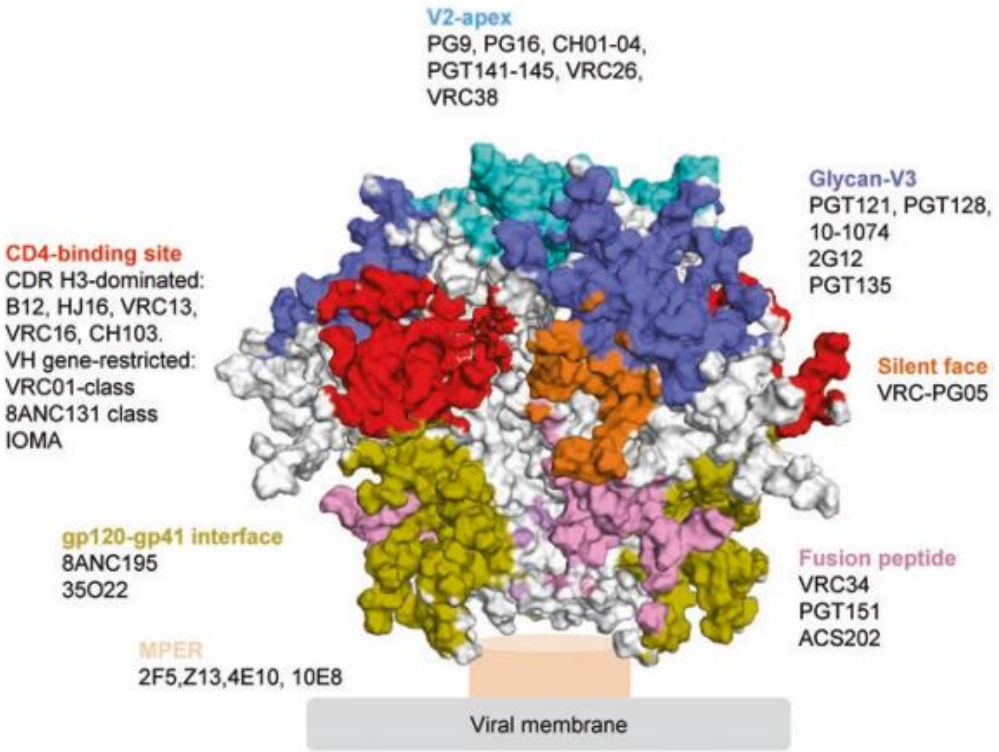

Figure 1.5: BNAb epitopes on the HIV-1 Env.
Known bNAb epitopes include the CD4-binding site (CD4bs), V2-apex, V3-glycan site, the gp120/gp41 interface, silent face, the membrane proximal external region (MPER) of gp41 and the fusion peptide (FP). Examples of antibodies and antibody classes specific for each epitope are listed under each epitope name. Image source: (Zhou and Xu, 2018).

1.4 Evolving neutralisation resistance among HIV-1 viruses

Over time, HIV-1 has evolved to exhibit reduced sensitivity to bNAbs (Bouvin-Pley *et al.*, 2013, 2014; Rademeyer *et al.*, 2016). Bouvin-Pley *et al.* (2014) assessed neutralisation sensitivity of subtype B pseudotyped viruses of the French epidemic, previously described by (Bouvin-Pley *et al.*, 2013). Several bNAbs targeting the CD4bs, V2-apex, V3-glycan, interface and MPER epitopes were tested against the pseudotyped viruses and an overall decrease in neutralisation sensitivity was observed from the historical viruses to (then) contemporary viruses, spanning 1987 to 2010 (Bouvin-Pley *et al.*, 2014). The decrease in neutralisation sensitivity was not epitope specific but observed for multiple epitopes on the gp120 subunit. In contrast there was no decrease in sensitivity noted for bNAbs targeting the MPER, which may be due to low tolerance to mutations within the MPER (Bouvin-Pley *et al.*, 2014). Overall this suggests selective pressure specifically focused on the gp120 epitopes (Bouvin-Pley *et al.*, 2014).

Similarly, Rademeyer *et al.* (2016), assessed the neutralisation sensitivity of 200 pseudotyped viruses from subtype C isolates within southern Africa, collected over 13 years and divided into three time periods from 1998 to 2010. These isolates were tested against five bNAbs targeting the CD4bs (VRC01), V2-apex (CAP256-VRC26.25 and PG9), V3-glycan (PGT128) and MPER (4E10). Significant reductions in neutralisation sensitivity to 4E10, VRC01 and PG9, was observed, suggesting that in this study the selective pressure was directed at both the gp120 and gp41 subunits (Rademeyer *et al.*, 2016).

Building on this, Mkhize *et al.* (2023) compared neutralisation sensitivity of historical and contemporary subtype C viruses against a panel of eight bNAbs in clinical development. The historical pseudotyped viruses were based on the 200 subtype C panel described above by Rademeyer *et al.* (2016) and contemporary pseudotyped viruses were based on subtype C viruses from the placebo arm of the Antibody Mediated Prevention (AMP) trials (HVTN703/HPTN081), isolated between 2016 to 2020 (Corey *et al.*, 2021; Mkhize *et al.*, 2023). The bNAbs tested targeted the CD4bs (VRC01, VRC07-523LS and 3BNC117), V3-glycan (PGT121 and 10-1074), V2-apex (CAP256-VRC26.25 and PGDM1400) and MPER (4E10). Recent viruses were found to be significantly less sensitive to the VRC07-523LS and CAP256-VRC26.25 bNAbs. Additionally, neutralisation sensitivity was reduced for VRC01, 3BNC117 and PGDM1400, however this was not significant.

As subtype C is also dominant in India, Mullick *et al.* (2021) tested the neutralisation sensitivity of 71 Indian pseudotyped viruses, collected from 1999 to 2014, against VRC01, CAP256-VRC26.25, PGDM1400 and PGT121. When compared to global isolates from other subtypes found on the CATNAP (Compile, Analyze, and Tally NAb Panels) database (https://www.hiv.lanl.gov/content/index), the Indian subtype C viruses appeared more sensitive to VRC01 than all other subtypes and more resistant to CAP256-VRC26.25 compared to African subtype C viruses (Mullick *et al.*, 2021). Additionally, assessment of trends in neutralisation sensitivity between Indian and African subtype C isolates, sampled from 1990 to 2016, revealed reduced sensitivity to PGT121, VRC01 and PGDM1400 over time among both groups. Furthermore, the Indian isolates conversely had decreased sensitivity to CAP256-VRC26.25 whereas African isolates had increased sensitivity. Subsequently, Sutar *et al.* (2025) compared neutralisation

sensitivity of contemporary African and Indian subtype C viruses. Both groups had a significant decrease in sensitivity to V2-apex targeting bNAbs, CAP256-VRC26.25 and ePGDM1400v9, which is consistent with observations by Rademeyer *et al.* (2016), however a new observation was the increased sensitivity to PGT121 (Sutar *et al.*, 2025).

Most recently, as part of the International AIDS Vaccine Initiative (IAVI) ADVANCE Virus Surveillance study, African viruses from early infection, <100 days post infection (dpi), isolated between 2006 and 2020, were screened against potent bNAbs targeting the V2-apex (CAP256-VRC26.25 and ePGDM1400v9), MPER (10E8.V4), V3-glycan (ePGT121v1 and BG18) and CD4bs (N6 and 1-18) epitopes (Kitchin *et al.*, unpublished data). A significant reduction in neutralisation sensitivity was observed for the two V2-apex targeting bNAbs (Kitchin *et al.*, unpublished data), which aligns with the findings of both Mkhize *et al.* (2023) and Sutar *et al.* (2025). All these studies demonstrated decreased bNAb sensitivity however the coverage remained the same. Nonetheless the evolving resistance towards these bNAbs, across subtypes, is concerning as it indicates that existing bNAbs, particularly those of clinical relevance, may not be effective against circulating or future circulating strains which would have evolved even more.

1.5 Isolation of broadly neutralising antibodies

1.5.1 Previously isolated broadly neutralising antibodies and clinical relevance

Numerous bNAbs have been isolated using varying methods and techniques (McCoy and Burton, 2017; Sanders and Moore, 2017). The earliest bNAbs, termed “first-generation bNAbs”, were isolated by phage display or B cell immortalization and tested in several preclinical trials in non-human primates and in human clinical trials (Thavarajah, Hønge and Wejse, 2024). These antibodies included b12, 2G12, 4E10, 2F5 and F105, which were well tolerated overall, however the emergence of escape mutants meant that these bNAbs could not clear the virus or maintain viral suppression (Trkola *et al.*, 2005).

Second-generation bNAbs were discovered through the advancement and development of techniques such as single B cell sorting, functional screening assays and improved design of HIV-1 antigens, including soluble Env trimers (Wibmer, Moore and Morris, 2015). Native-like trimers mimic the native-Env, found on the viral membrane, in terms of conformation, shape, epitope presentation and allowed for the isolation of trimer-specific bNAbs that target the V2-apex epitope (Sok *et al.*, 2014). Second-generation bNAbs were

more potent and broad compared to first-generation bNAbs (Julg and Barouch, 2019), and were shown to be safe for use when administered to people living with or without HIV-1 (Thavarajah, Hønge and Wejse, 2024).

These bNAbs were tested in both monotherapy (single bNAb) and combination therapy (two or more bNAbs) clinical trials. Monotherapy therapeutic trials demonstrated that individual bNAbs could not maintain viral suppression, as the virus was able to quickly mutate and escape the single bNAb, resulting in viral rebound (Thavarajah, Hønge and Wejse, 2024). Consequently combination therapy trials were conducted, involving two or more bNAbs that targeted different epitopes. The first clinical trials combined 3BNC117 and 10-1074, and showed that the combination of two or more bNAbs could maintain viral suppression for longer with less viral rebound (Bar-On *et al.*, 2018; Mendoza *et al.*, 2018).

Passive infusion of bNAbs has been shown to reduce viraemia in human trials (Caskey *et al.*, 2015, 2017) and provide protection against simian-human immunodeficiency virus (SHIV) challenge in animal models (Mascola *et al.*, 2000; Moldt *et al.*, 2012; Pegu *et al.*, 2014). These antibodies could potentially be used as prophylactics, to prevent infection by viruses, and therapeutics, to slow viral progression and evolution (Halper-Stromberg *et al.*, 2014; Thavarajah, Hønge and Wejse, 2024). Proof of concept for the use of bNAbs as prevention was demonstrated by the recently conducted Antibody Mediated Prevention (AMP) trials (also known as HVTN 703/HPTN 081 and HVTN 704/HPTN 085). The AMP trial tested the VRC01 bNAb in at-risk women from sub-Saharan Africa or men from the Americans and Europe, and proved that VRC01 was effective in the prevention of HIV-1 infection when participants were exposed to a VRC01-sensitive virus (Corey *et al.*, 2021).

In addition, HIV-1 vaccines are being developed with the goal of eliciting bNAbs (Haynes *et al.*, 2023). However, in animal studies, SOSIP.664 trimers derived from various HIV-1 clades elicited neutralising antibodies (NAbs) primarily against autologous tier 2 viruses, while bNAbs generated against heterologous viruses were largely limited to tier 1 strains (Sanders *et al.*, 2015). Therefore this remains a significant challenge, as bNAbs possess unique features and require co-evolution with the virus—allowing for extensive somatic hypermutation (SHM) and affinity maturation, as previously described in section 1.3.2. Although no effective HIV-1 vaccine has yet been licensed, some promising results have emerged from human trials. Notably, the RV144 trial conducted in Thailand demonstrated

a modest reduction in HIV-1 transmission through the induction of V2-apex–directed antibodies using a regimen of four priming immunogens followed by two booster doses of a gp120 subunit vaccine (Rerks-Ngarm *et al.*, 2009; Haynes *et al.*, 2012b). This study indicates that vaccines inducing high levels of V1V2-directed antibodies, and low levels of Env-specific IgA antibodies, could decrease the risk of HIV-1 infection (Haynes *et al.*, 2012b). Further, proof-of-concept studies have shown that the germline-targeting immunogens, eOD-GT8 (Jardine *et al.*, 2016) - can successfully bind VRC01-class precursor B cells in humans (Leggat *et al.*, 2022) and recently the same was shown for BG505 SOSIP.v4.1-GT1.1 (Caniels *et al.*, 2025). Considering breadth develops after years of virus-antibody co-evolution current vaccine strategies under development typically includes a priming immunogen – a soluble Env that can bind to the bNAb precursors – followed by sequential immunisation with immunogens that select for improbable mutations (Haynes *et al.*, 2012a; Wiehe *et al.*, 2018). The use of soluble Env trimers is critical especially as booster immunogens, as it facilitates the elicitation of bNAbs targeting quaternary epitopes.

1.5.2 Native-like soluble envelope trimers

To create native-like trimers, several stabilisation strategies have been employed. Most commonly, these involve replacing the REKR cleavage site with an RRRRRR (R6) motif to enhance cleavage efficiency (Binley *et al.*, 2002); introducing cysteine residues at positions 501 and 605 (referred to as SOS) to form a disulfide bond - preventing the dissociation of gp120 and $gp41_{ECTO}$ (Binley *et al.*, 2000; Sanders *et al.*, 2000) and lastly incorporating an isoleucine to a proline substitution (referred to as IP) at residue 559 to break the helix and help with trimer formation (Sanders *et al.*, 2002). These modifications together resulted in the gp140 SOSIP construct (Sanders *et al.*, 2013). However, the hydrophobic MPER region resulted in trimer aggregation, thus a more soluble trimer (SOSIP.664) was designed where the construct was truncated after residue 664 (Klasse *et al.*, 2013).

To improve the stabilisation of the SOSIP.664 trimers, the DS-SOSIP.664 was created through introducing cysteine point substitutions at residues 201 and 433, which forms a disulphide bond to prevent CD4-induced triggering, which results in the trimer being in an open conformation (Joyce *et al.*, 2017). Moreover, proline substitutions at residues 568 and 569, referred to as the “2P” mutation, added to SOSIP.664 and DS-SOSIP.664

constructs were shown to further stabilise the trimers (Joyce *et al.*, 2017; Wrapp *et al.*, 2023). Other stabilising mutations have been developed for particular regions of the soluble Env trimer and can be used to improve trimer expression or alter antigenicity by increasing hydrophobicity, changing charge or increasing the number of disulfide bonds (Torrents de la Peña and Sanders, 2018). These trimers are designed to have a native-like conformation, displaying bNAb epitopes.

Several stabilised HIV-1 Env trimer constructs have been designed based on various isolates (Guenaga *et al.*, 2015); however, the gold-standard Env is BG505 SOSIP.664, based on the Env of a clade A isolate (Sanders *et al.*, 2013). Structural characterisation of the BG505 SOSIP.664 trimer revealed that the trimer is highly stable and found mainly in the closed conformation (Sanders *et al.*, 2013). To confirm the trimer conformation, techniques including binding assays (Veillette *et al.*, 2014) and hydrogen deuterium exchange (HDX) (Guttman *et al.*, 2015) can be used. However the binding assays require sensitivity to trimer-specific antibodies and HDX requires large reaction volumes. An alternative approach is the use of structural biology, in particular negative stain electron microscopy (NS-EM), which allows for visualisation of the trimer and identification of various conformations (Julien *et al.*, 2013a; Khayat *et al.*, 2013; Sanders *et al.*, 2013; Pugach *et al.*, 2015; Verkerke *et al.*, 2016; Kumar *et al.*, 2019, 2024). Furthermore the progress of structural biology in terms of cryogenic-EM (cryo-EM) and X-ray crystallography has allowed for the visualisation of trimers at atomic resolution, allowing for more accurate analysis of trimer shape and conformation (Julien *et al.*, 2013b; Lyumkis *et al.*, 2013). The advancement within this field has contributed toward the structure based design of HIV-1 antigens for various uses such as vaccine design, antibody isolation and understanding antibody-Env interactions (Kwong and Mascola, 2018).

1.6 Rationale

HIV-1 vaccines capable of eliciting bNAbs or antibody-mediated protection through passive immunization could be key for prevention of HIV-1 infection (Corey *et al.*, 2021; Caniels *et al.*, 2025; Willis *et al.*, 2025). However, recent studies have identified evolving resistance towards existing bNAbs (Bouvin-Pley *et al.*, 2014; Rademeyer *et al.*, 2016; Mkhize *et al.*, 2023), which suggests that existing bNAbs may lose efficacy against future circulating strains. Therefore, novel bNAbs are required to expand coverage to more difficult-to-neutralise viruses.

Several soluble Env trimers used in the isolation of bNAbs have not been based on difficult-to-neutralise viruses (Sok *et al.*, 2014; van Gils *et al.*, 2016; Kumar *et al.*, 2019; Schommers *et al.*, 2020). However the evolving resistance to existing bNAbs and development of multi-bNAb class resistance (Kitchin *et al.*, unpublished data), necessitates a new approach. We hypothesize that novel bNAbs, capable of neutralising these resistant viruses, could be isolated using a soluble Env trimer, derived from a highly neutralisation-resistant virus, as a B cell sorting bait. Due to inherent resistance of the viral isolate to existing bNAbs, the soluble trimer would be highly selective for B cells with BCRs capable of binding to difficult-to-neutralise viruses, either by targeting novel epitopes or through novel binding mechanisms to neutralisation escaped epitopes. Antibodies derived from these B cells could be used in combination with existing bNAbs to increase the virus coverage of bNAb mediated prevention and treatment regimens.

1.7 Project aim and objectives

1.7.1 Aim and hypothesis

This project aimed to use SOSIP trimers derived from highly neutralisation-resistant Envs to isolate bNAbs, with novel epitope specificities or binding modalities, from PLWH with broad plasma antibody responses.

1.7.2 Objectives

1) Identify and characterise the neutralisation phenotype of difficult-to-neutralise viruses using bNAbs targeting the CD4bs, V1/V2 apex, V3-glycan, MPER, interface and FP epitopes.
2) Design, express and purify a soluble SOSIP trimer based on an Env protein from a difficult-to-neutralise virus.
3) Characterise the antigenicity and structure of soluble SOSIP trimer protein by single particle electron microscopy.
4) Use the expressed soluble trimers as FACS baits to singly sort B cells from an unmapped PLWH with a broad plasma antibody response.
5) Isolate and sequence the BCRs from the singly sorted B cells, and evaluate the corresponding antibodies for neutralisation activity.
6) Ten isolated monoclonal antibodies, prioritised based on single-dilution neutralisation activity and immunogentic characteristics, were characterised according to neutralisation breadth and potency against a multi-subtype six-virus panel and the difficult-to-neutralise isolate.

2 Methods

2.1 Screening for neutralisation resistance in African viruses

2.1.1 Isolate selection

Preliminary data from the IAVI ADVANCE Virus Surveillance study, involved assessing the neutralisation sensitivity of 192 viruses from South Africa, Uganda, Kenya, Zambia and Rwanda. These viruses were isolated less than 100 dpi and screened against six potent bNAbs targeting the V2-apex, V3-glycan and CD4bs epitopes. The isolates were ranked according to overall neutralisation sensitivity and three most difficult-to-neutralise isolates were selected (**Table S2.1**). These isolates were: FRESH1388 (subtype C virus from South Africa), PC220898 (subtype D virus from Kenya) and PC235205 (subtype C virus from Zambia).

2.1.2 Env-pseudotyped virus production

As previously described by Montefiori (2009), Env-pseudotyped viruses were produced using Human embryonic kidney (HEK) 293T cells. Within a sterile cryotube, 500 µL of Dulbecco's Modified Eagle Medium (DMEM) (Gibco) was combined with 48 µg transfection reagent, PEI MAX® (Kyfora Bio®). Next, 8 µg of both HIV-1 Env plasmid and PSG3ΔEnv backbone plasmid were added, followed by a 30 min incubation at room temperature. After the incubation, the transfection mixture was added to 6 x 10^6 cells/ml HEK293T cells grown in 20 ml growth media (GM) which consisted of DMEM with 10% Fetal Bovine Serum (FBS) (Hyclone), 25 mM HEPES buffer (Gibco) and 50 µg/ml gentamicin (Sigma-Aldrich). Transfected cells were incubated for 48 hours at 37°C with 5% CO_2 and 95% humidity. The pseudovirus was containing supernatant was harvested, filtered using a 0.45 µm nitrocellulose filter (Satorious) to remove cell debris and the FBS concentration was adjusted to 20%, to prevent aggregation of pseudovirus particles. The mixture was then mixed thoroughly through inversion, aliquoted into 1 ml aliquots and frozen at -80°C until later use.

2.1.3 HIV pseudovirus neutralisation assay

To assess the neutralisation sensitivity of the Env-pseudotyped viruses to antibodies, an HIV pseudovirus-based neutralisation assay, described by Montefiori (2009), was used. The antibody panel consisted of 19 bNAbs that targeted several epitopes including CD4bs (N6, 1-18, VRC01-23-LS, VRC07-523LS, 3BNC117, b12), V1/V2 apex (CAP256-VRC26.25, ePGDM14000v9), V3-glycan site (BG18, ePGT121v1, 10-1074), the gp120/gp41 interface (35O22), membrane-proximal external region (MPER) (4E10, 10E8v4, 2F5) and fusion peptide (FP) (VRC34, AIRU_F8, DFPHa01). The assay was performed as follows: GM was added to a 96-well flat-bottom plate. In row H, antibodies were added, excluding columns 1 and 2, which were reserved for cell and virus controls, respectively. Antibodies were prepared at an initial concentration of 50 µg/ml and serially diluted three-fold from row H to row A. Pseudovirus was added to all wells, except the cell control, to give an acceptable range of 20 000 to 50 000 relative light units (RLU) in the virus control. Following a one hour incubation in a humidified 37°C, 5% CO_2 incubator, TZM-bl cells (1×10^6 cells/ml) were then added to all wells, followed by a 24-hour incubation under the same conditions. After this, 130 µl of DMEM was added to each well, and plates were incubated for an additional 24 hours. Following the final incubation, 100 µl of media was removed from each well and replaced with 100 µl of Bright-Glo luciferase substrate (Promega). The plate was incubated for two minutes in a dark hood, then 150 µl from each well was mixed and transferred to a 96-well black plate. RLUs were measured using a luminometer, and either the half-maximal inhibitory concentration (IC_{50}) or half-maximal inhibitory dilution (ID_{50}) was calculated using an in-house Excel macro spreadsheet.

2.2 Design and subcloning of SOSIP trimer plasmids

2.2.1 Design of soluble HIV-1 trimers

Soluble DS-SOSIP.664 trimers were designed based on three difficult-to-neutralise Envs identified by the screening of the IAVI ADVANCE isolates. Modifications were added to the virus envelope sequence to design these trimers. These include the replacement of the REKR cleavage site with an RRRRRR (R6) motif to improve cleavage (Binley *et al.*, 2002), the introduction of a helix-breaking point substitution, I559P, which would assist in trimer formation (Sanders *et al.*, 2002) and cysteine

substitutions at residues at 501C and 605C (SOS) to prevent dissociation of the gp120 and $gp41_{ECTO}$ (Binley *et al.*, 2000; Sanders *et al.*, 2000). Furthermore, truncation of the sequence past residue 664, for increased solubility (Klasse *et al.*, 2013) and additional cysteine substitutions at residues 201C and 433C (DS) formed a disulphide bond, which prevents the trimer being from adopting an open conformation (Joyce *et al.*, 2017). Moreover, at the 5′ end a modified signal sequence (MPMGSLQPLATLYLLGMLVASVLAAENLWVTVYYG) replaced the native signal sequence, to allow for the efficient translocation of the protein out of the cell. The 3′ end was completed by the following sequence: GGSGGSGGLNDIFEAQKIEWHEHHHHHH including a glycine-serine linker, Avi tag, for biotinylation, and His tag for purification of the protein using a nickel-charged resin. The three DS-SOSIP.664 constructs were codon-optimised, for optimal expression in human cell culture, and synthesised by GenScript, then subsequently subcloned into the pVRC8400 backbone using restriction cloning. Sequences were confirmed by Sanger dideoxy sequencing.

2.2.2 Subcloning and expression of the DS-SOSIP.664 plasmids

The codon-optimised DS-SOSIP.664 encoding constructs were obtained from GenScript, cloned into pUC57, which had sites for restriction enzymes, Xba1 and BamH1, at the ends of the trimer insert. The trimer insert was excised from the pUC57 plasmid backbone by restriction digest using the Xba1 and BamH1 restriction enzymes and purified using QIAquick Gel Extraction Kit (Qiagen), as per the manufacturer's instructions. The insert was then subcloned into the pVRC8400 plasmid using the Rapid DNA ligation kit (Roche). Cells were transformed by the new plasmids, then cultured on agar plates overnight and colonies were selected for sequencing.

2.2.3 Mutagenesis

Additional stabilising mutations were introduced into the FRESH1388 constructs by site-directed mutagenesis using the QuikChange Lightning Site-Directed or QuikChange Lightning Multi Site-Directed Mutagenesis Kits (Agilent Technologies) as per the manufacturer's instructions. The first set of mutations include two proline substitutions, denoted 2P, at residues 558 and 559, in order to break the helices at those residues (Wrapp *et al.*, 2023). Furthermore, hydrophobic packing in the V3

region, of FRESH1388-2P, was increased in three separate constructs. The constructs included alanine to tryptophan substitution at residue 316 (denoted 316W) (de Taeye *et al.*, 2015; de Taeye *et al.*, 2018) and two methionine substitutions at residues 300 and 302 along with a leucine substitution at residue 320 (denoted 3M) (Chuang *et al.*, 2017). The final mutant included all the mutations from the 316W and 3M constructs, and was denoted 4M. Primers used to introduce these mutations were designed using the Agilent QuikChange Primer Design tool. Competent cells were then transformed, as described in 2.2.2, with the addition of the mutant plasmids.

2.3 Expression and purification of trimers

The SOSIP proteins were expressed in Human Embryonic Kidney 293F cells (HEK293F). OPTIPRO Serum Free Media (Gibco) was combined with 350 µg DS-SOSIP.664 plasmid, 210 µg furin plasmid, for the cleavage of the gp160 subunit, and 150 µg BirA plasmid, for *in vitro* biotinylation, and 2.4 mg PEI-max transfection reagent. The transfection mixture was incubated for 20 min before being added to a 1 l culture of 2 x 10^6 HEK293F suspension cells, which was incubated for six days at 37°C, 70% humidity and 8% CO_2. The cultures were then centrifuged at 1935 g for 30 min at 4°C and the supernatant was passed through a 0.2 µm nitrocellulose filter for clarification.

For all trimers, with the exception of FRESH1388-2P-316W, the supernatant was passed through a Nickel Sepharose resin (Cytiva™) column. The protein was then eluted using an elution buffer (57 mM NaH_2PO_4, 300 mM NaCl, 235 mM Imidazole pH 7). The FRESH1388-2P-316W supernatant was passed through a Galanthus Nivalis Lectin (GNL) column and the protein was eluted with 1M mannose. To exclude aggregates, monomers and dimers, further purification by size exclusion chromatography (SEC), using a HiLoad 16/600 Superdex 200 column (Cytiva™), was performed. Fractions of the purified trimers were pooled and passed through a negative selection column, to obtain the trimers in the correct, closed conformation. The negative selection column contained CNBr-activated-Sepharose 4B resin (Cytiva™) coupled with the 447-52D mAb. The 447-52D mAb binds the V3-loop on a trimer which is exposed when the trimer is in its open conformation and thus the flow-through will contain trimers in the desired closed conformation. The purified protein was collected and the concentration was measured using a NanoDrop ND-1000

Spectrophotometer (ThermoScientific) before being aliquoted and frozen by liquid nitrogen for storage at -80°C.

2.4 Trimer characterisation

2.4.1 Luminex binding antibody multiplex assay

The binding antibody multiplex assay (BAMA), previously described by Tomaras *et al.*, 2008 and Yates *et al.*, 2014, is a high throughput, luminex-based assay, which was used to determine the antigenicity of the various SOSIP trimers. Briefly, MAGplex beads (Luminex Corp) were activated and then coupled with different SOSIP trimers. In a 96-Well, Cell Culture-Treated, Flat-Bottom, Half-Area Microplate (Corning™), the coupled beads were incubated with the various antibodies and plasma, starting at concentration of 5 µg/ml or 1:100 dilution, respectively. Palivizumab, an antibody targeting the F protein on the respiratory synticial virus (RSV), was made in-house and used as a negative control starting at 5 µg/ml. A total of 21 antibodies targeting neutralising, non-neutralising and broadly neutralising epitopes were tested for binding to each SOSIP trimer. The bead-antibody mixture was then incubated for one hour, with shaking at 300 rpm. A phycoerythrin (PE) conjugated anti-IgG antibody (0.65 µg/ml) was added to the bead-antibody mixture and the fluorescence was measured using the Bio-Plex 200 multiplex system (BioRad). The mean fluorescence intensity (MFI) was reported by the Bio-Plex Manager™ software (version 6.2 build 175) and the area under the curve (AUC) was calculated using Graphpad Prism v9.3.0.

2.4.2 Negative stain electron microscopy

Negative stain electron microscopy (NS-EM) was used to identify whether the trimers in the sample occurred predominantly in the closed or open conformation. I performed NS-EM on the FRESH1388-2P-316W trimer while NS-EM for BG505 and FRESH1388-2P trimers were performed by Claire Van Den Berg, at the University of Cape Town (UCT) Electron Microscopy Unit (EMU). Briefly, carbon coated copper grids (Agar Scientific) were glow discharged, for 30 s at 25 mA using a EMS100 Glow Discharge Unit (Electron Microscopy Sciences), to increase hydrophilicity before the sample was added. Upon preparation of the grids, 3.5 µL of protein sample was loaded and the grid was washed twice with water and stained twice with 2% uranyl acetate (Agar Scientific). The grid was loaded onto a FEI Tecnai F20 field emission

transmission electron microscope (TEM) (Thermo Fisher Scientific) operating at 200 kV with DE-16 direct detection camera (Direct Electron) in integrating mode. The protein sample was imaged at 14 000X magnification at a defocus of -1.5 µm. Image processing was performed using Relion v4 (Scheres, 2012). Particles were then selected manually from contrast transfer function (CTF) corrected images and subjected to 2D classification. The best classes showing highest resolution and different particle orientations were selected and used to generate an initial *de novo* map via Stochastic Gradient Descent (SGD) (Punjani *et al.*, 2017). This was refined in Relion v4 and interpreted by docking the Protein Data Bank (PDB) model of BG505 (PDB ID: 8TNG) using Chimera X version 1.8. The percentage of trimers in either the open or closed conformations were calculated by counting the number of particles in the corresponding 2D-class averages of the final five classes.

2.4.3 Cryogenic electron microscopy

Cryogenic electron microscopy (Cryo-EM) was used to investigate the structure of the FRESH1388-2P-316W trimer by capturing the trimer in its native state using rapid freezing. Grids were prepared by the University of Cape Town (UCT) Electron Microscopy Unit (EMU). After screening for ice thickness, concentration and sample aggregation, the grids were shipped within seven days using a Worthington dry shipper to the electron Bio-Imaging Centre (eBIC) at Diamond Light Source in the United Kingdom (South African eBIC access bi36795-2). Dr Karen M. Davies assisted in clipping and loading the grids into Titan Krios 4 (mo7). Grids were imaged with the assistance of Claire van Der Berg using EPU (Thermo Fisher Scientific) at 300kV and 105 000X magnification (0.829 Å/pixel) at a dose of 31 e/Å^2 over 45 frames, C2 aperture: 50 µm and energy filter slit width of 20 eV over a defocus range of -0.75 µm to -3.0 µm. Real-time pre-processing was conducted at Diamond to adjust collection parameters and the raw data was downloaded for processing in Relion v4 according to standard practices ("New tools for automated cryo-EM single-particle analysis in RELION-4.0," 2021). A 3D-model was generated and refined by Dr Jeremy Woodward, using Relion v4, and further visualised using Chimera X version 1.8.

2.5 B cell isolation

2.5.1 Screening of participant plasma

To determine which participants had neutralisation activity toward the difficult-to-neutralise isolates, plasma from unmapped CAPRISA participants were selected for screening. These participants were from the CAPRISA 002 and 004 cohorts that were conducted in Durban, South Africa (Loggerenberg *et al.*, 2008; Abdool Karim *et al.*, 2010). Selected plasma samples were from chronically infected donors, collected from two or three years post-infection and had neutralisation breadth >30% against an 18-virus panel (**Table S2.2**). Screening for neutralisation of the difficult-to-neutralise isolates was done using the HIV pseudovirus neutralisation assay, described in 2.1.4, however in place of antibodies, plasma samples were added at a 1:10 initial dilution and underwent a five-fold serial dilution thereafter.

2.5.2 Fluorescently activated cell sorting

Memory B cells from the cryopreserved PBMCs of CAP287 were single sorted using fluorescently activated cell sorting (FACS). A cocktail of HIV-1 SOSIP.664 trimers were fluorescently labelled with fluorochromes Alexa Fluor™ 647 streptavidin conjugate (SA-AF647) (Thermo Fisher Scientific) and PE Streptavidin phycoerythrin conjugate (SA-PE) (Thermo Fisher Scientific), at a 1:2 molar ratio of fluorochrome to trimer, and used as sorting baits to isolate Env-specific B cells. Specifically, the FRESH1388-2P-316W trimer was conjugated to SA-PE and the cocktail of stable HIV-1 trimers (including BG505, CAP255 and CE1086C trimers) were conjugated to SA-AF647.

To evaluate the quality and determine optimal volumes of the sorting baits to use, the binding of positive (N6 – 200 µg/ml) and negative (17b – 50 µg/ml) control antibodies, to the conjugated proteins, was assessed. Briefly anti-Ig coated beads (Spherotech) were incubated with the control antibodies and subsequently incubated with different volumes (15 µl, 5 µl, 1.5 µl, and 0.5 µl) of fluorochrome conjugated sorting baits, starting at a concentration of 100 µg/ml. For the sort a volume of 15 µl was used as it showed the highest MFI.

Prior the sort, the PBMCs mixture were stained with a LIVE/DEAD Fixable Aqua Dead Cell Stain Kit (Thermo Fisher Scientific) to differentiate live cells from dead cells. This was followed by staining with several surface marker antibodies including: IgD-FITC, CD3-APC-CY7, CD14-APC-CY7, CD16-APC-CY7, CD19-PE-CY7, and CD20-PE-Cy7 (all supplied by BD Biosciences). Then cells were incubated with 25 µl each of the SA-AF647 and SA-PE fluorophore conjugated antigens. Furthermore, the cells were incubated with the HIV-1 trimers and the SARS-CoV-2 spike antigen, which was used to exclude cells that bound non-specifically to the trimer. The mixture was loaded onto the cell sorter and acquisition was started. HIV-1 trimer specific B cells were sorted if positive for CD19 and CD20 cell surface markers however negative for CD3, CD14, CD16 and IgD cell surface markers. The cells were singly sorted into wells containing 5 µl of 1% 2-mercaptoethanol in TCL buffer (Qiagen) and then kept on dry ice before being stored -80°C.

2.6 Antibody Isolation

Rapid Assembly, Transfection and Production of Immunoglobulins (RATPIg), described by Lima *et al.* (2022), was performed to rapidly isolate and screen mAbs for neutralisation activity without the need for molecular cloning. The method consists of four main steps: complementary DNA (cDNA) synthesis, Immunoglobulin (Ig) enrichment and sequencing, linear cassette synthesis and functional screening (**Figure 2.1**). Sequences for all primers described below are provided in **Table S2.3**.

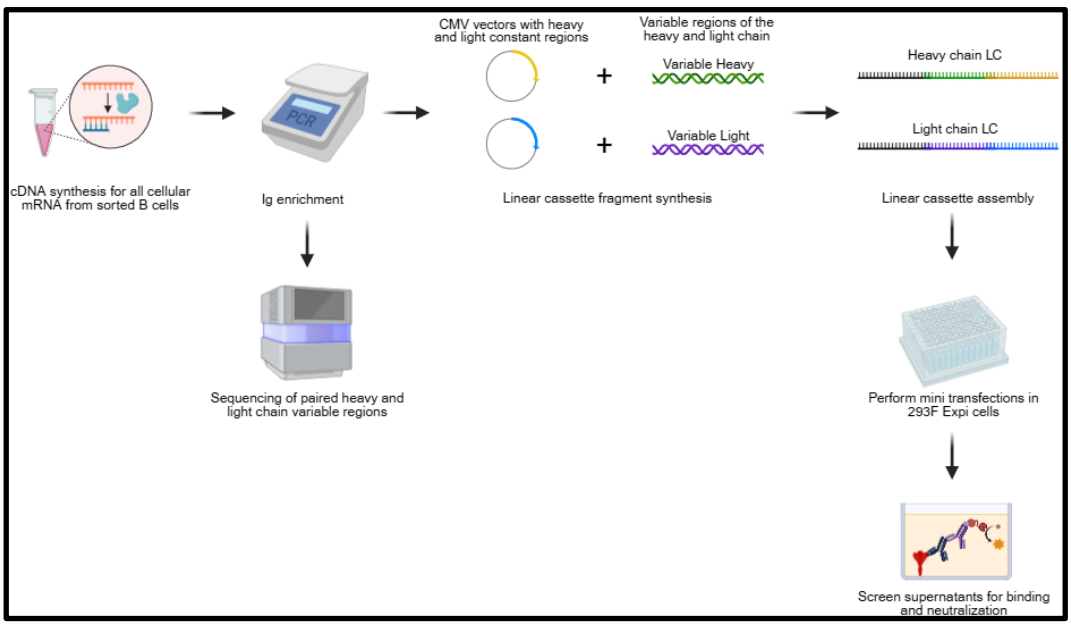

Figure 2.1: RATPIg workflow.
RNA released from isolated B cells was converted into cDNA from which the antibody heavy and light chain variable regions were enriched and sequenced. Heavy and light chain linear cassettes consisting of a CMV promoter, the amplified variable regions, antibody constant regions and a polyadenylation sequence, were constructed through Gibson cloning. Antibodies were expressed in small volume 293F Expi cell cultures, followed by screening the culture supernatant for virus neutralisation and Env binding.

2.6.1 cDNA synthesis

Total cellular mRNA was reverse transcribed into cDNA using the SMART-Seq2 5′ RACE (Rapid Amplification of cDNA Ends) protocol (Picelli *et al.*, 2014). Cell lysates were thawed, and mRNA was purified using RNAClean XP beads (Beckman Coulter) according to the manufacturer's instructions. The SMART-Seq2 method employs a template-switching mechanism mediated by SMARTScribe Reverse Transcriptase (Takara Bio), a modified Moloney Murine Leukaemia Virus enzyme, to synthesize full-length cDNA. A poly(dT) primer (TSoligo2_polydT) anneals to the mRNA 3′ poly(A) tail, while the template switching oligo (A-tag TSO) adds a defined sequence to the 5′ end of the cDNA, enabling cDNA amplification. The preparation of the cDNA synthesis reactions and cycling parameters are described in **Tables S2.4** and **S2.5**. The SeqAmp DNA polymerase (Takara Bio) was used to amplify cDNA, according to the manufacturers protocol using a forward primer (Primer II A), which binds to the 5' sequence added by the A-tag TSO, and a reverse primer (TSoligo2) which binds to a 3' sequence added by the TSoligo2_polydT primer. The preparation of the cDNA amplification reactions and cycling parameters are described in **Tables S2.6** and **S2.7**. Amplified cDNA was purified using AMPure XP beads (Beckman Coulter), as per the manufacturer's instructions, and residual primers and deoxynucleotide triphosphates (dNTPs) were removed with the EXO-CIP RAPID PCR clean-up kit (New England Biolabs), according to the manufacturer's protocol.

2.6.2 Immunoglobulin enrichment and sequencing

The variable regions of the heavy and light chains were amplified from cDNA using a universal forward primer (Primer II A) - bound to the 5′ end sequence introduced by the A-tag TSO and IgA/IgG or Igκ/Igλ reverse primer pool, that bound at the 5′ end of CH1 or Cκ/Cλ, respectively. Reactions were prepared with a 2× SuperFi II master mix (Invitrogen™) as per the manufacturer's instructions, and the reaction mixture and cycling conditions are shown in **Table S2.8** and **S2.9.** Subsequently, the Ig enrichment

amplicons were purified using AMPure XP beads (Beckman Coulter) as per the manufacturer's instructions.

The concentrations of the enriched heavy and light chain variable region amplicons were measured using the Qubit Flex Fluorometer (Invitrogen™) using the Qubit 1X dsDNA High Sensitivity (HS) assay kit (Invitrogen™), and their fragment size was assessed using the D5000 ScreenTape Assay on a TapeStation 4200 instrument (Agilent).

Heavy and light chain amplicons were normalised to a concentration of 10ng/ul and paired amplicons derived from the same sorted B cell were pooled for sequencing. The DNA Prep tagmentation kit (Illumina), together with Unique Dual (UD) indexes (Integrated DNA Technologies), were used to prepare the indexed sequencing libraries from the amplicon pools. Using this approach each heavy and light chain amplicon pool derived from the same B cell received a unique index pair during the library preparation, allowing sequencing reads to be mapped back to individual B cells. Sequencing was conducted at the NICD sequencing core facility on an Illumina NextSeq instrument, using 2×150bp paired-end reads with the NextSeq 500/550 Mid Output Kit v2.5 (Illumina 20024905, 300-cycles), to obtain 40GB of total data (500 000 reads per B cell).

2.6.3 V(D)J sequence analysis

Illumina sequencing reads were demultiplexed using bcl2fastq (Illumina) to produce two paired-end FASTQ files for reads derived from each sorted B cell. TrimGalore (https://github.com/FelixKrueger/TrimGalore/tree/master), a wrapper script for CutAdapt and FastQC, was used to trim low quality base calls and remove Illumina adaptor sequences from sequencing reads, prior to further analysis. TRUST4 (Song *et al.*, 2021) was used for the *de novo* assembly of heavy and light chain variable region contigs. IgBLAST (Ye *et al.*, 2013) was used to map contiguous to IMGT (Giudicelli *et al.*, 2006) reference sequences and for V, D and J gene, and CDR3 annotation. The annotated heavy and light chain variable region sequences were output from IgBLAST in an adaptive immune receptor repertoire (AIRR) formatted table for further analysis. B cell receptors (BCR) were assigned to clonotypes based on CDRH3 sequence similarity using the spectral clustering method in the SCOPer R

package (Nouri and Kleinstein, 2018, 2020). The complete analysis workflow was automated using Nextflow (https://www.nextflow.io/) and is available on request (https://github.com/NICD-AIRU/RATPIg).

2.6.4 Linear cassette assembly

For the assembly of linear cassettes, the CMV promoter and heavy and light chain constant region fragments were amplified from a donor pVRC8400 (CMVR) expression plasmid, containing either an antibody heavy or light chain insert. Constant region fragments included the pVRC8400-derived polyadenylation sequence at their 3' end. Separate PCR reactions were set-up for the isolation of each cassette fragment, and are described in **Table S2.10**. To isolate the heavy and light chain constant region, forward primers used were specific for the 5′ end of the heavy chain (IgHC_FWD) or light chain (IgLC_FWD) constant region and the same reverse primer was used for the 3′ end of the constant regions (TBGH REV). The CMV promoter was obtained from the CMVR backbone using a VRC_CMV_FWD (forward) primer and a CMV_SPLICE_TSO_REV (reverse) primer. All reactions were prepared using the 2× SuperFi II master mix (Invitrogen™), following the manufacturer's protocol and occurred under the same conditions described in **Table S2.11**, after which the fragments were purified using AMPure XP beads (Beckman Coulter).

Following amplification, linear cassette component DNA fragments were evaluated on a 1% (w/v) agarose gel and fragments of the correct size were excised and purified using the QIAquick Gel Extraction Kit (Qiagen). A DpnI digestion was performed to remove any plasmid template DNA before final bead purification with AMPure XP beads (Beckman Coulter). The size of the purified cassette fragments were confirmed using the D5000 ScreenTape Assay on a TapeStation 4200 instrument (Agilent) and the concentration was measured using the Qubit Flex Fluorometer (Invitrogen™) using the Qubit 1X dsDNA High Sensitivity (HS) assay kit (Invitrogen™). The concentration of each fragment for each component was diluted to 1 ng/µl, using nuclease-free water.

The linear cassettes for the heavy and light chains were prepared in separate 96-well plates, using Gibson cloning to assemble the CMV promoter, Ig enrichment and constant region fragments. Assembly reactions were prepared using the NEBuilder HiFi DNA Assembly Master Mix (New England Biolabs) according to the

manufacturer's instructions. Briefly, equimolar amounts of each component were used at 0.01 pmol per assembly. After a 1 hour incubation at 50°C, the linear cassettes were amplified using the VRC_CMV_FWD primer and TBGH_Rev primer and the reaction mixture and cycling parameters are described in **Table S2.12** and **S2.13,** respectively. Upon completion of the cassette amplification a final round of purification was performed using AMPure XP beads (Beckman Coulter). The final size and concentration was assessed as described above.

2.6.5 Antibody expression and screening

Expi293 cells (Thermo Fisher Scientific) were co-transfected with natively paired heavy and light chain linear expression cassettes, in individual wells in a 96-well deep-well plate. The transfection mixtures were prepared using equimolar amounts of 215 fmol of paired heavy and light chain linear cassettes in 70 µl OptiMEM-I (Thermo Fisher Scientific), and filtered through a 0.2 µm filter. OptiMEM-I, with 6% ExpiFectamine 293 Transfection reagent (Thermo Fisher Scientific), was added to each well followed by ~23 300 cells, per well, as per the manufacturer's instructions. The plate was incubated at 37°C, ≥80% humidity and 8% CO_2, on a shaker at 1100 rpm. After 18 hours, 38.5 µl of an enhancer cocktail was added to each well, composed of 9.1% Enhancer 1 (Thermo Fisher Scientific) and 90.9% Enhancer 2 (Thermo Fisher Scientific). The plate was incubated for a further 4 days after which antibody containing supernatants were harvested and filtered through a 0.2 µm filter. Transfection controls included in the plate included a no-template control (NTC), and expression plasmids for a SARS-CoV-2 antibody (AIRU-946.C4) and an HIV-1 specific antibody (N6).

Neutralisation screening was done using the pseudovirus-neutralisation assay, described above in 2.1.4, however single-dilutions of each antibody supernatant were screened instead of 3-fold serial dilutions of an antibody. Pseudoviruses used in the screening include: SF162, BG505, CE1086C, CAP255.4D and FRESH1388. Luminescence was measured for each plate, as described above, and the percentage inhibition was calculated for each supernatant. Based on luminescence from the NTC wells the threshold for background infection inhibition was set to 35%.

2.7 Characterisation of prioritized antibodies

2.7.1 Selection of priority CAP287 antibodies

Antibodies were prioritised based on prominent clonotypes, neutralisation screening data and interesting bNAb features such as long CDRH3s or high levels of SHM (Landais and Moore, 2018; Griffith and McCoy, 2021). Ten antibodies were selected and synthesised by GenScript through their GenScript Turbo Cho service.

2.7.2 Screening prioritised CAP287 antibodies for neutralisation breadth

Breadth and potency of the prioritised antibodies was assessed using a six-virus panel, described by Simek *et al.*, (2009), in the pseudovirus neutralisation assay described in 2.1.4. The six-virus panel was originally designed to predict neutralisation breadth of plasma samples and is a heterogeneous panel consisting of diverse subtypes and a circulating recombinant virus. More specifically this includes isolates 94UG103 (subtype A), 92BR020 (subtype B), JRCSF (subtype B), IAVIC22 (subtype C), 93IN905 (subtype C) and 92TH021, (CRF01_AE). In addition the neutralisation of the difficult-to-neutralise isolate, FRESH1388, by each mAb was also assessed.

3 Results

3.1 Defining the neutralisation phenotype of difficult-to-neutralise isolates

For this project, we aimed to more accurately define the neutralisation phenotypes of three viral isolates, previously identified as being difficult-to-neutralise from the IAVI-ADVANCE study (Kitchin et al, unpublished), using a panel of 19 bNAbs targeting six bNAb epitopes including the CD4bs, V2-apex, V3-glycan, interface, FP and MPER.

Overall the PC220898 virus (subtype D) was the most neutralisation-resistant, only being neutralised by 4/19 bNAbs (**Table 3.1**). More specifically the PC220898 isolate was sensitive to bNAbs targeting the V2-apex, and bNAbs 35022 (interface-specific) and 10E8v4 (MPER-specific). The FRESH1388 virus (subtype C) was neutralised by 5/19 bNAbs, specifically N6 (CD4bs-specific), 10E8v4 (MPER-specific) and all those targeting the V3-glycan (BG18, PGT121 and 101074) (**Table 3.1**). Interestingly, the FRESH1388 isolate showed complete resistance at the V2-apex and interface epitopes, which are the two trimer-specific epitopes. Lastly, the PC235205 virus (subtype C) was neutralised by 7/19 bNAbs and was sensitive to all bNAbs targeting the V2-apex (**Table 3.1**). Additionally, two of the broadest and most potent bNAbs known, N6 and 1-18, could not neutralise the PC220898 isolate, while only N6 could weakly neutralise the FRESH1388 isolate, further demonstrating the difficult-to-neutralise phenotype of these isolates. Lastly, PC235205 was sensitive at the CD4bs epitope, as it was neutralised by N6 and 1-18, and was the only isolate neutralised by b12, a first generation bNAb with relatively low potency and breadth compared to more recently isolated bNAbs (Hraber *et al.*, 2014).

Additionally, neutralisation by antibodies 17b and 447-52D was evaluated against all three isolates, to determine if the isolates were sensitive to weakly neutralising and non-neutralising antibodies, which would indicate the Env is exposing non-conserved epitopes and in an open conformation (**Table 3.1**). The 17b targets the CD4 inducible site (CD4i) which is only exposed when CD4 is bound to the Env protein and 447-52D is a non-neutralising antibody that targets the V3-loop. No neutralisation (IC_{50} > 50

µg/ml) by 17b or 447-52D was observed for any of the viruses, which indicates the viruses are not sensitive to these non-bNAbs.

The geometric mean titre (GMT) was calculated for each virus, using the IC_{50} values of all bNAbs and non-bNAbs, to provide an overall measure of sensitivity of the isolate. The most resistant isolate was PC220898 (GMT = 14.1 µg/ml), followed by FRESH1388 (GMT = 13 µg/ml) and lastly PC235205 (GMT = 11 µg/ml). Considering the error of the neutralisation assay is as high as three-fold, these titers are not considered significantly different and all isolates were regarded as fairly resistant.

Overall the results from the expanded bNAb panel confirmed the initial screening data (Kitchin *et al*, unpublished), demonstrating that all three isolates showed resistance to bNAbs across multiple epitope specificities. However, it is notable that none of the isolates were completely neutralisation resistant, with each virus showing sensitivity to all bNAbs targeting the V2-apex or V3-glycan.

Table 3.1: Neutralisation of difficult-to-neutralise isolates, from the IAVI ADVANCE study, by bNAbs and non-bNAbs targeting multiple Env epitopes.

		Subtype Year Virus	C 2017 FRESH1388	D 2009 PC220898	C 2008 PC235205
	Epitopes	**Antibody**	**IC_{50} (µg/ml)**		
bNAbs	**CD4 binding site**	N6	0,20	50	5
		1-18	50	50	0,59
		VRCO1-23-LS	50	50	50
		VRCO7523LS	50	50	50
		3BNC117	50	50	50
		b12	50	50	16
	V2-apex	ePGDM1400v9	50	0,002	0,01
		CAP256VRC265	50	0,004	0,01
	V3-glycan	BG18	0,12	50	50
		ePGT121v1	0,02	50	50
		101074	0,06	50	50
	Fusion peptide	VRC34	50	50	50
		F8	50	50	50
		DFPHa01	50	50	50
	Interface	35O22	50	5	50
		PGT151	50	50	0,54
	MPER	4E10	50	50	50
		10E8v4	5	0,59	3
		2F5	50	50	50
non-bNAbs	**CD4 inducible site**	17b	50	50	50
	V3-loop	447-52D	65	50	50
		GMT (µg/ml)	13	14	11

Potent neutralisation

No neutralisation

3.2 Screening CAPRISA participant plasma for neutralisation of difficult-to-neutralise isolates

To determine which participant PBMCs to prioritize for antibody isolation, CAPRISA 002 and 004 participant plasma samples (n=20), from three years post infection and with known neutralisation breadth (Gray *et al.*, 2007; Moore *et al*. unpublished data), were screened for neutralisation activity toward the three difficult-to-neutralise isolates (**Table 3.2**). Overall, the majority of the plasma samples tested (11/20) had no (ID_{50} < 20) or low (ID_{50} < 100) neutralisation activity toward all of the difficult-to-neutralise isolates. Nine participant plasma samples were able to neutralise at least one of the three isolates with ID_{50} values ≥ 100. However the most potent neutralisation was observed for the FRESH1388 isolate which was neutralised by plasma from participants, CAP287 and CAP341, with ID_{50} values > 5000. Plasma from participant CAP287 had the highest neutralisation activity (ID_{50} = 61770) against the FRESH1388 isolate with an ID_{50} approximately 12-fold higher than that of the plasma from participant CAP341 (ID_{50} = 5166). Additionally according to historical data, these plasma samples, from three years post-infection, had neutralisation breadth of 61% (CAP287) and 50% (CAP341) against the 18-virus panel (**Table S2.2**) (Moore *et al*. unpublished data). Therefore, the PBMCs of participant CAP287 were selected for bNAb isolation. Additionally, given the high neutralisation titers toward the FRESH1388 isolate, soluble trimers, were designed using the Env of the FRESH1388 virus, for use as antigen baits in bNAb isolation.

Table 3.2: CAPRISA participant plasmas, from the CAPRISA 002 and 004 cohorts, were screened for neutralisation of the difficult-to-neutralise isolates.

Virus	FRESH1388	PC220898	PC235205
CAPRISA participants	ID_{50}(µg/ml)		
CAP287	61770	28	99
CAP341	5166	176	72
CAP292	148	28	252
CAP314	98	84	108
CAP255	466	20	90
CAP177	96	63	115
CAP037	90	50	104
CAP373	249	33	32
CAP008	74	32	93
CAP357	90	52	34
CAP248	33	20	103
CAP206	41	20	72
CAP312	25	20	95
CAP288	34	20	65
CAP331	29	34	35
CAP267	44	20	35
CAP370	26	53	20
CAP309	36	20	22
CAP322	26	30	20
CAP280	29	20	27

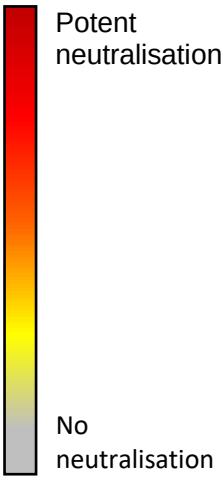

3.3 Design, expression and characterisation of the FRESH1388 trimers

3.3.1 Expression of FRESH1388 trimers

Soluble trimers, based on the subtype C FRESH1388 isolate, were designed with DS-SOSIP.664 stabilising mutations (FRESH1388-WT) (**Figure 3.1A**). Two proline substitutions were added to the design for further stabilisation (Wrapp *et al.*, 2023) (FRESH1388-2P) (**Figure 3.1B**). Following expression in mammalian cells, proteins were purified using nickel-affinity chromatography and SEC. Profiles for each trimer were evaluated against the “gold-standard” BG505 SOSIP.664 trimer (Sanders *et al.*, 2013) which is known to be a stable and well-formed trimer (**Figure 3.1C**). The SEC profiles had three peaks with the first peak containing aggregated protein, followed by a peak containing trimeric protein and lastly a peak with dimers and monomers. Both the FRESH1388-WT and FRESH1388-2P trimers eluted after approximately 55 minutes, comparable with the elution time of the BG505 trimer, confirming that the FRESH1388 trimer was of comparable size to the BG505 trimer. However, the height of the FRESH1388 trimer peaks were much lower compared to the BG505 trimer peak (**Figure 3.1C**). This indicates that the amount of trimer present was much lower, relative to the amount of trimer in the BG505 protein sample. Although the height of the FRESH1388-WT trimer peak was greater than that of the FRESH1388-2P trimer peak, a shift was seen toward more trimer production as opposed to aggregate in the SEC profile of the FRESH1388-2P trimer (**Figure 3.1C**). The FRESH1388-2P trimer was therefore selected as the sorting bait as it formed more trimer than aggregate, compared to the FRESH1388-WT which formed more aggregate than trimer.

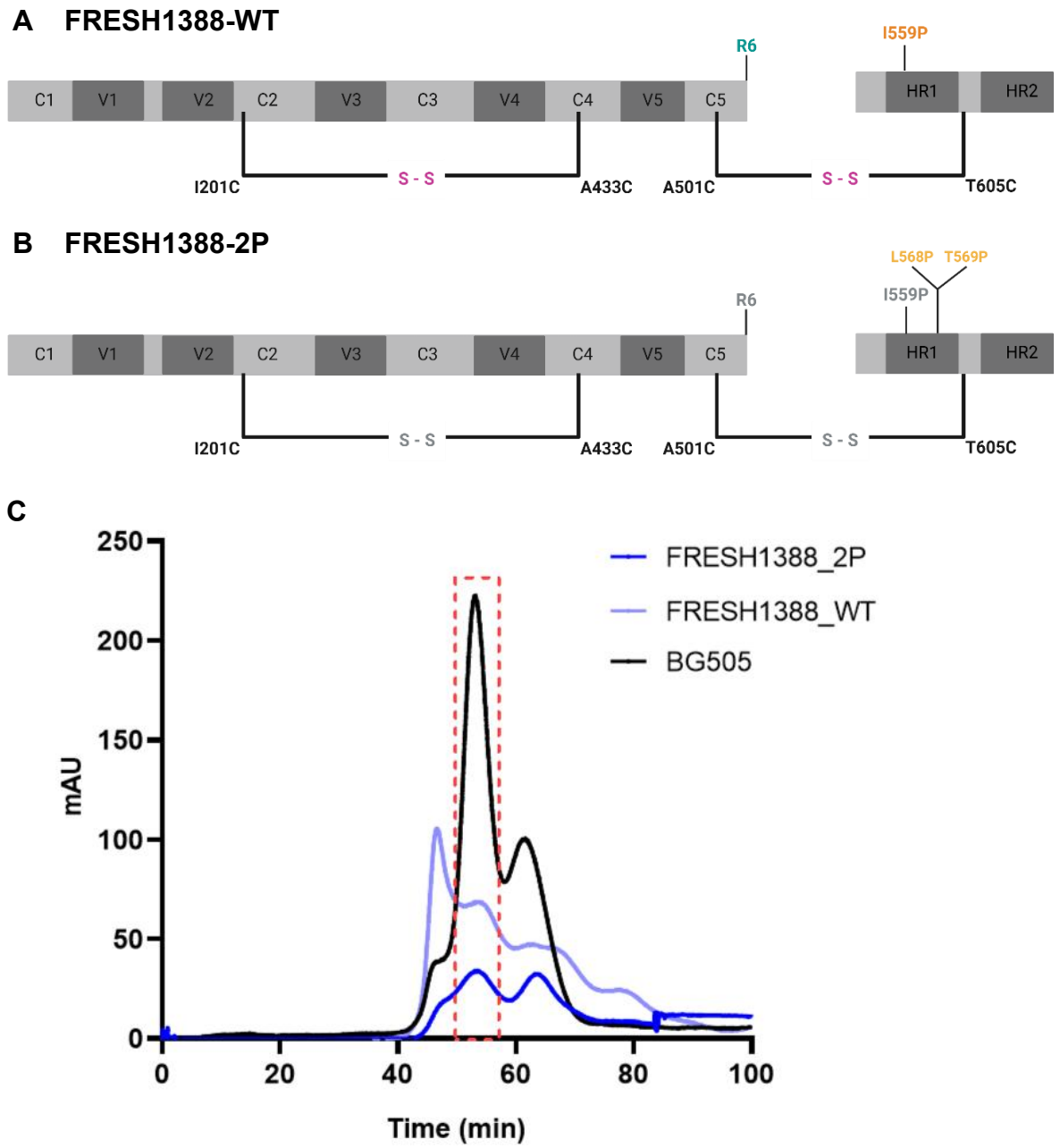

Figure 3.1: Design and size-exclusion chromatography (SEC) profiles of soluble FRESH1388 trimers.
(A) Schematic of the wild type FRESH1388 trimer, FRESH1388-WT, with various stabilising mutations. (B) Additional proline substitutions were added to the wild type trimer, which formed the FRESH1388-2P trimer, for further stabilisation. (C) The SEC profiles of the FRESH1388 SOSIP trimers were generated after elution of proteins using a Superdex 200 HiLoad 16/600 column, and compared with the gold standard BG505 trimer. Trimer peaks are indicated by the red dashed box. Peaks before and after the box are indicative of aggregate and monomers, respectively.

3.3.2 Antigenicity of the FRESH1388-2P trimer

The FRESH1388-2P trimer was characterised using a Luminex BAMA to assess the ability of neutralising and non-neutralising antibodies to bind the trimer, ensuring that the purified trimer retained the antigenic profile of the native envelope protein (**Figure 3.2**). Antibodies that neutralise the FRESH1388 virus (**Table 3.1**) were expected to bind the trimer. The bNAbs used for antigenic analysis targeted the V3-glycan (PGT121 and BG18), V2-apex (CAP256-VRC26.25), gp120/gp41 interface (PGT151) and CD4bs (N6, 1-18 and b12), and the non-bNAbs targeted the CD4i (17b) and V3-loop (3074 and 447-52D). Palivizumab, an antibody targeting the F protein on the respiratory synticial virus (RSV), was expressed and purified in the laboratory, based on published sequences (Johnson *et al.*, 1997), and used as a negative control starting at 5 µg/ml. High binding was observed for the bNAbs that neutralised the FRESH1388 virus (**Figure 3.2**), such as those targeting the V3-glycan (BG18 and PGT121) and CD4bs (N6) all of which had an AUC > 42 000. Lower levels of binding were observed for PGT151 (AUC = 1359) and CAP256-VRC26.25 (AUC = 403), which matches the neutralisation profile of the FRESH1388 isolate as the virus was resistant at the both the interface and V2-apex epitopes. BNAbs 1-18 and b12, did not neutralise the FRESH1388 virus and did not bind the trimer. High binding was observed for 17b (AUC = 12 409), which did not neutralise the FRESH1388 virus, indicating the CD4i epitope may be accessible on the trimer. Additionally, high binding, comparable with that of the V3-glycan bNAbs and N6, was observed for V3-loop targeting antibodies 3074 (AUC = 34 894) and 447-52D (AUC = 157 693). The high level of binding by the 3074 and 447-52D antibodies, indicated that the trimer was in the open conformation or had an exposed V3-loop. These characteristics would hinder the selective isolation of bNAbs because this trimer would select for to the isolation of weakly neutralising antibodies or nNAbs which target this region, and are predominant in the sera of PLWH (de Taeye *et al.*, 2018). Therefore, we aimed to reduce exposure of the V3-loop through the addition of previously defined stabilising mutations before the trimer could be used as a sorting bait.

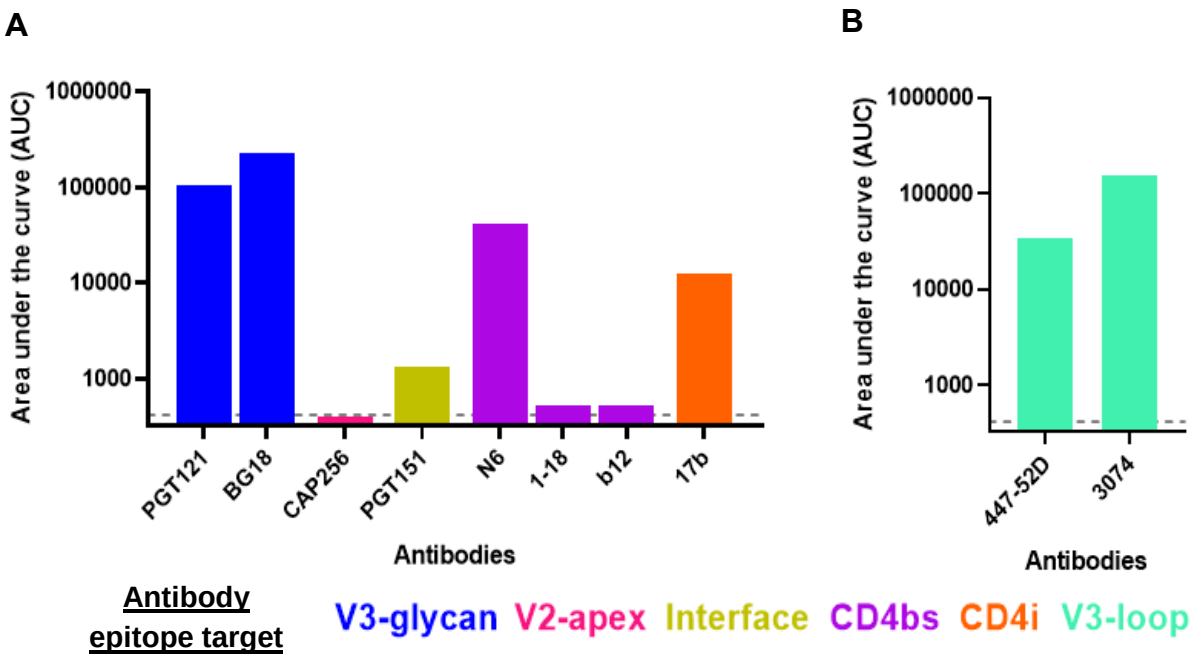

Figure 3.2: Luminex binding data of the various antibodies targeting bNAb and non-bNAb epitopes on the FRESH1388-2P trimer.
The area under the curve (AUC) of the mean fluorescence intensity (MFI) vs concentration, starting at 10 µg/ml followed by a three-fold serial dilution of each antibody. (A) Binding of antibodies previously tested for neutralisation of the FRESH1388 virus and targeted the following epitopes: V3-glycan (PGT121 and BG18), V2-apex (CAP256.VRC26.25), Interface (PGT151), CD4bs (N6, 1-18 and b12) and CD4 inducible site (17b). (B) Binding of V3-loop specific antibodies, 3074 and 447-52D. The binding threshold (dashed line) was determined by palivizumab, an RSV F protein (non-HIV) specific antibody, which was used as a negative control to determine background signal.

3.3.3 Expression of V3-stabilised FRESH1388 trimers

Three additional trimers were designed and expressed with stabilising mutations to increase hydrophobicity in the V3-loop region and reduce the binding of V3 loop-specific antibodies (**Figure 3.3)**. These trimers were FRESH1388-2P-316W (**Figure 3.3A**), FRESH1388-2P_3M (**Figure 3.3B**) and FRESH1388-2P_4M (**Figure 3.3C**) and included the mutations described in 2.2.1. The SEC profiles of the three trimers were compared to previously expressed BG505, however both the FRESH1388-2P_3M and FRESH1388-2P_4M SEC profiles had very small peaks corresponding to the trimer protein peak of BG505 and had aggregate and monomer peaks (**Figure 3.3D**). The FRESH1388-2P-316W SEC profile revealed a prominent trimer peak, indicating a higher proportion of trimer, relative to the other V3- stabilised FRESH1388 trimer peaks. Furthermore this indicates that the 316W mutation improves expression of this trimer.

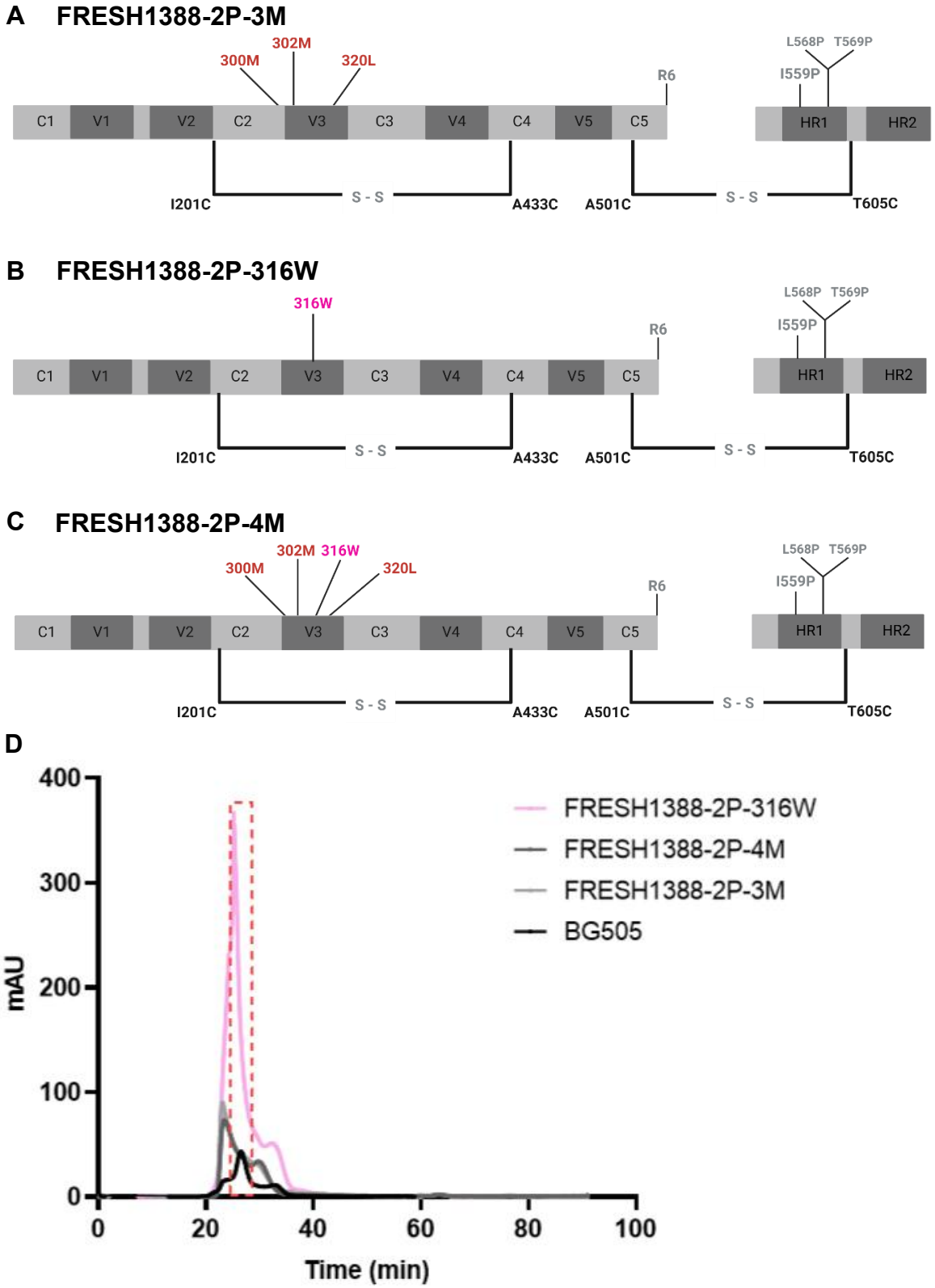

Figure 3.3: Design and purification of the V3- stabilised FRESH1388 trimers. Design schematic of V3- stabilised trimers (A) FRESH1388-2P-316W (316W), (B) FRESH1388-2P-3M (3M) and (C) FRESH1388-2P-4M (4M). (D) SEC profiles of purified FRESH1388 V3-stabilised trimers, overlayed with BG505. Proteins were eluted using a Superdex 200 HiLoad 16/600 column. Trimer peaks are indicated by the red dashed box. Peaks before and after the box are indicative of aggregate and monomers, respectively.

3.3.4 Antigenicity of V3-stabilised FRESH1388 trimers

Antigenic profiles of the V3- stabilised trimers were assessed by Luminex BAMA to ensure the antigenicity was similar to the FRESH1388-2P trimer (**Figure 3.4** and **Figure S3.1**). As an alternative to AUC, the half-maximal effective concentration or (EC_{50}) was calculated for each antibody trimer pair and the EC_{50} of palivizumab, an RSV F protein specific antibody, was averaged for all trimers to determine the threshold of background binding. Binding of the various antibodies, previously tested for neutralisation of the FRESH1388 virus, were compared, by means of EC_{50}, between the FRESH1388-2P trimer and each V3-stabilised trimer: FRESH1388-2P-316W (**Figure 3.4A**), FRESH1388-2P-3M (**Figure 3.4C**) and FRESH1388-2P-4M (**Figure 3.4E**), and confirmed that the trimers were antigenically similar. Furthermore, the fold-difference between the EC_{50} greater than or equal to 2 are highlighted. Additionally, binding of V3-loop specific antibodies to the FRESH1388-2P-316W (**Figure 3.4B**), FRESH1388-2P-3M (**Figure 3.4D**) and FRESH1388-2P-4M (**Figure 3.4F**) trimers were compared to binding of FRESH1388-2P to assess whether the mutations had sufficiently decreased exposure of the V3-loop. Both 3074 and 447-52D showed reduced binding to trimers FRESH1388-2P-316W (**Figure 3.4B**) and FRESH1388-2P-4M (**Figure 3.4F**), while only 3074 had reduced binding to the FRESH1388-2P-3M (**Figure 3.4D**) trimer. This indicates reduced exposure of the V3-loop, specifically for the FRESH1388-2P-316W and FRESH1388-2P-4M trimers. However an overall reduction in binding by all antibodies to the FRESH1388-2P-4M trimer (**Figure 3.4E**) resulted in the selection of the FRESH1388-2P-316W trimer for use as a sorting bait. However, due to time constraints, this experiment has only been completed once and will need to be repeated to confirm the results.

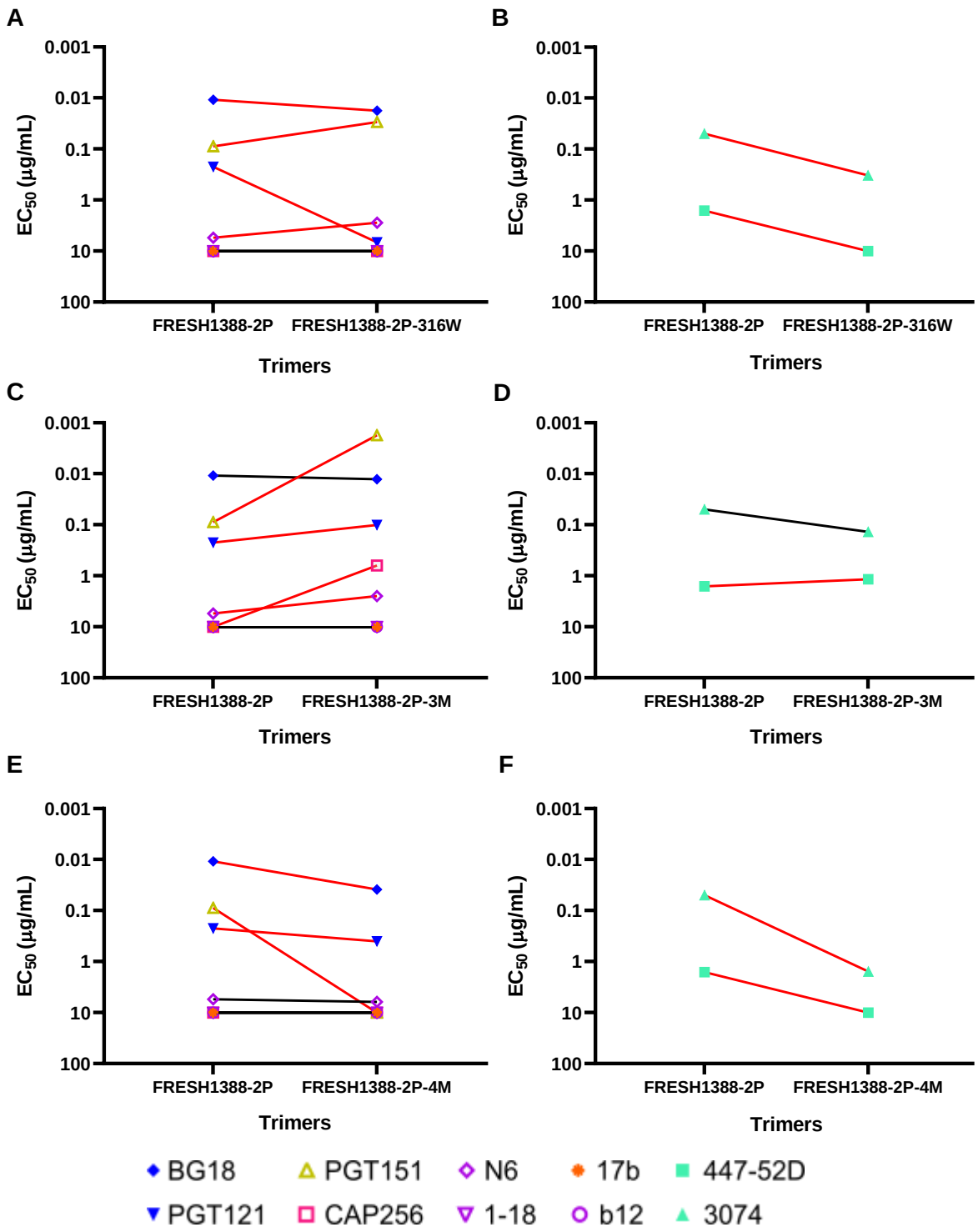

Figure 3.4: Comparative luminex binding data of the bNAb and non-bNAb antibodies to the FRESH1388-2P trimer and V3 stabilised FRESH1388 trimers. Binding of antibodies, which had been tested for neutralisation of the FRESH1388 pseudovirus, were compared between the each V3-stabilised trimers; (A) FRESH1388-2P-316W, (C) FRESH1388-2P-3M and (E) FRESH1388-2P-4M, and the FRESH1388-2P trimer. Additionally the binding of non-bNAbs, targeting the V3-loop, were tested for binding to (B) FRESH1388-2P-316W, (D) FRESH1388-2P-3M and (F) FRESH1388-2P-4M, compared the FRESH1388-2P trimer. Lines between each antibody indicate an increase or decrease in EC_{50}, and the red line indicates if the fold change is equal to or greater than two.

3.3.5 Structural characterisation of the FRESH1388-2P-316W trimer

Next, negative-stain electron-microscopy was used to assess whether the FRESH1388-2P-316W trimer was in the correct, closed conformation (**Figure 3.5**). A BG505 trimer protein sample served as a positive control as it is known to form stable trimers, mainly in the closed conformation (Sanders *et al.*, 2013). After imaging, the Relion software was used to select propeller-like, trimer-shaped particles from the FRESH1388-2P-316W, FRESH1388-2P and BG505 trimer protein preparations (**Figure 3.5A**). The software was used to classify the particles into different bins or classes, based on similarity. This process is known as 2D class averaging. Final 2D class averages for each protein preparation formed five distinct classes (**Figure 3.5B**) and the percentage of trimers in the closed conformation was calculated (**Figure 3.5C**). 96% of the BG505 trimer particles were in the closed conformation, similar to what has previously been reported (de Taeye *et al.*, 2018), while 74% of the FRESH1388-2P-316W and 54% of the FRESH1388-2P trimers were in the closed conformation, thus presenting the bNAb epitopes while concealing nNAb epitopes.

A

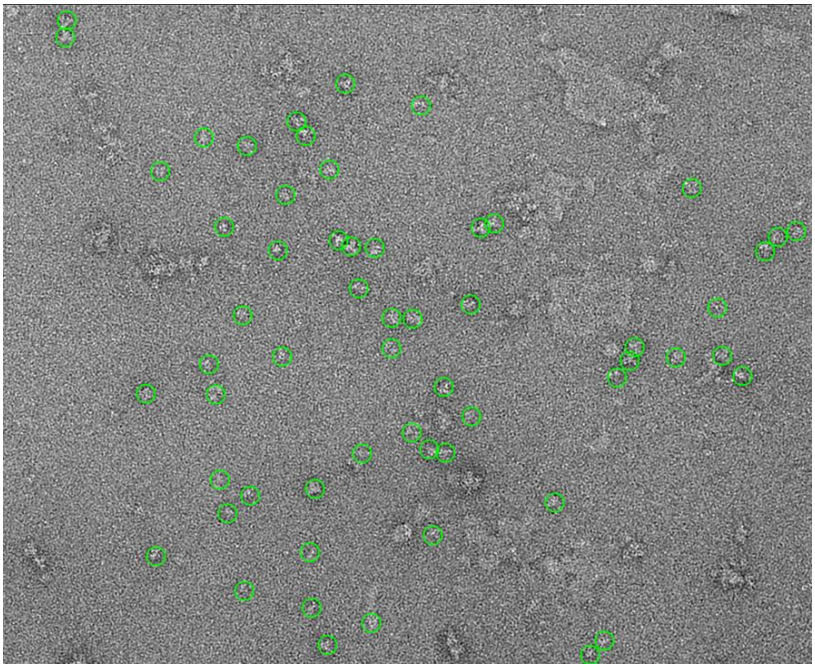

B

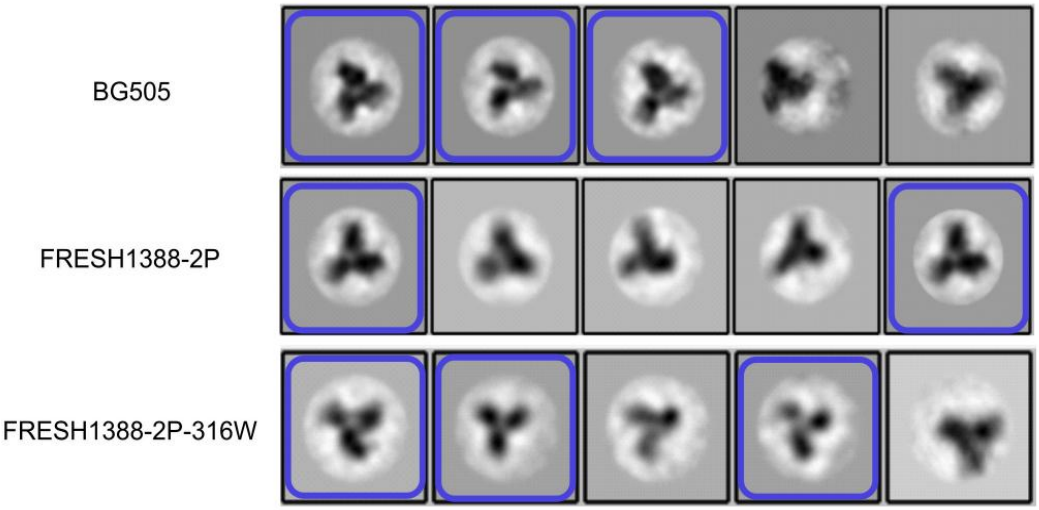

C

HIV-1 trimer	Percentage in the closed conformation
BG505 (positive control)	96%
FRESH1388 2P	53%
FRESH1388 2P 316W	74%

Figure 3.5: Negative-stain electron microscopy of soluble FRESH1388 trimers relative to BG505 trimer.
(A) FRESH1388_2P_316W trimer particles were selected (indicated in green circles) and classified into different 2D-classes based on similarity. (B) 2D-class averaging of BG505, FRESH1388_2P and FRESH1388_2P_316W identified trimers in the closed conformation (indicated in blue squares). The closed conformation trimers were identified by the propeller-like shape. (C) The percentage of trimers in the closed conformation within each sample is shown.

Based on classes of different trimer views and orientations from the 2D class averages, a 3D model of FRESH1388-2P-316W was created using Relion and further refined using ChimeraX, shown from the side (**Figure 3.6A**) and top (**Figure 3.6B)** views. The model generated was mapped using a previously solved BG505 trimer (PDB ID: 8TNG). The final 3D model, resembling the BG505 trimer, exhibited a characteristic propeller shape (**Figure 3.6B**), indicating a well-formed trimer in the closed conformation that presents bNAb epitopes. Moreover, the NS-EM 3D-model was supported by a preliminary cryo-EM 3D reconstruction of the FRESH1388-2P-316W trimer shown from the side (**Figure 3.6C**) and top (**Figure 3.6D)** views. The preliminary structure is at a resolution of 4.9 Å and the propeller-like shape can be seen in the top view (**Figure 3.6D)**. Further refinement of the model will be completed in future studies for more in-depth analysis of compactness, amino acid interactions and degree of similarity to previously solved structures. Structural characterisation using NS-EM and cryo-EM confirmed that the FRESH1388-2P-316W trimer was predominantly in the closed conformation and similar to the well-formed BG505 trimer. The FRESH1388-2P-316W trimer could thus be used to singly-sort B cells from CAPRISA donor CAP287.

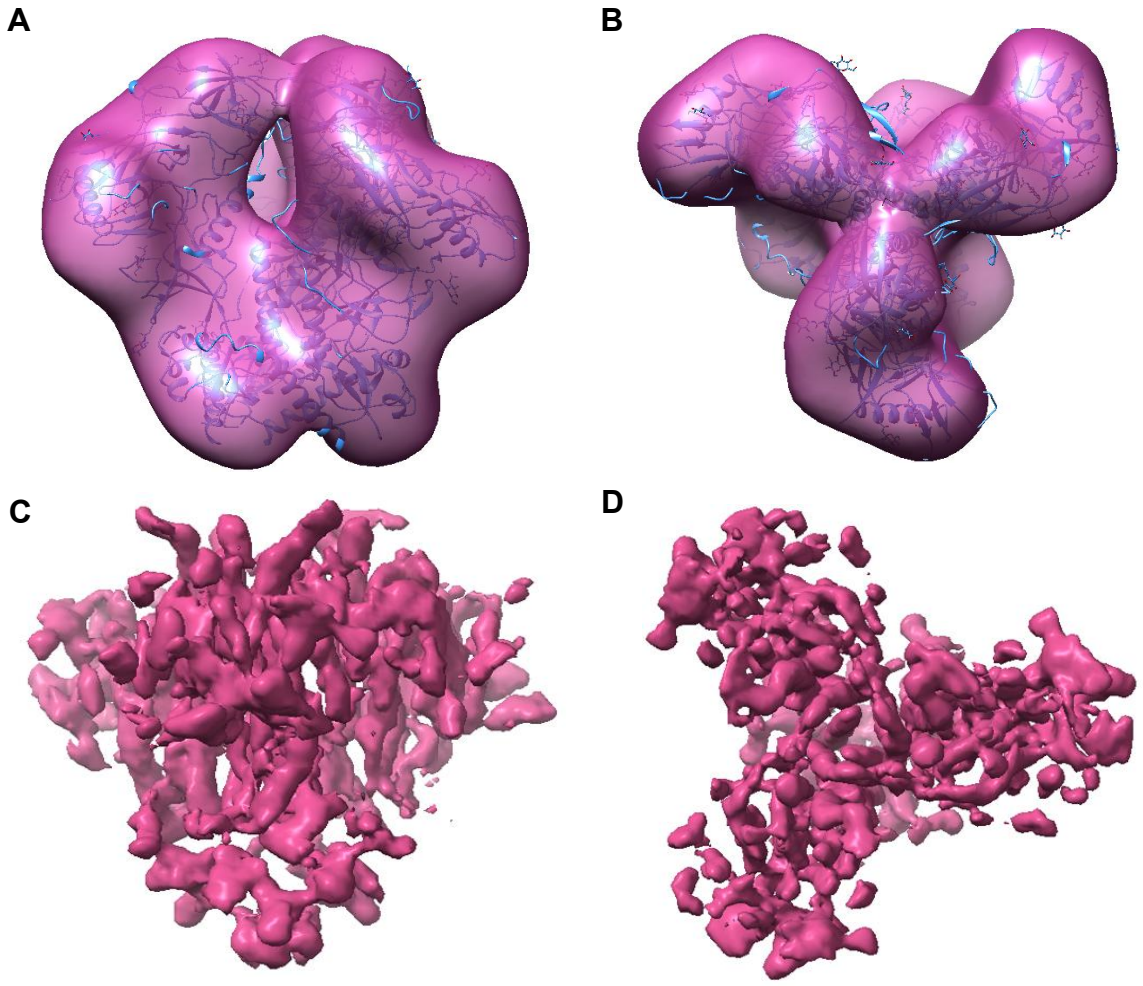

Figure 3.6: 3D models based on particles of the FRESH1388-2P-316W trimer observed through NS-EM and cryo-EM.
(A and B) A 3D model of FRESH1388-2P-316W (pink), generated by particles picked from grids prepared for NS-EM, imaged using the FEI Tecnai F20 field emission cryo-Transmission Electron Microscope (Thermo Fisher Scientific) operating at 200 kVe. The model was created in Relion and was modelled on a previously solved BG505 structure (blue ribbon), PDB: 8TNG, using ChimeraX. (C and D) A preliminary 3D model of FRESH1388-2P-316W produced by particles selected from grids prepared for cryo-EM, imaged using the Titan Krios (Thermo Fisher Scientific) operating at 300kVe. The preliminary reconstruction was generated using Relion. Models are shown from the (A, C) side and (B, D) top views.

3.4 Antibody isolation from sorted B cells of participant CAP287

3.4.1 Isolation of B cells and immunogenetics of paired heavy and light chain sequences

Memory B cells were sorted from cryopreserved PBMCs of CAPRISA donor CAP287, at 172 weeks post-infection. In total 4 479 950 cells were stained with fluorescently labelled markers. Memory B cells were positive for CD19 and CD20 cell surface markers, however negative for CD3, CD14, CD16 and IgD cell surface markers. In the order of the flow cytometry plots, cell selection occurred as follows: lymphocytes, singlets, live cells, B cells and those which did not bind non-specifically to the decoy bait (**Figure 3.7**). Then memory B cells and finally cells specific to select HIV-1 trimers including FRESH1388-2P-316, BG505, CAP255.4D and CE1086C. B cells that bound to either one or multiple HIV-1 trimers were singly sorted, resulting in a total of 252 sorted B cells.

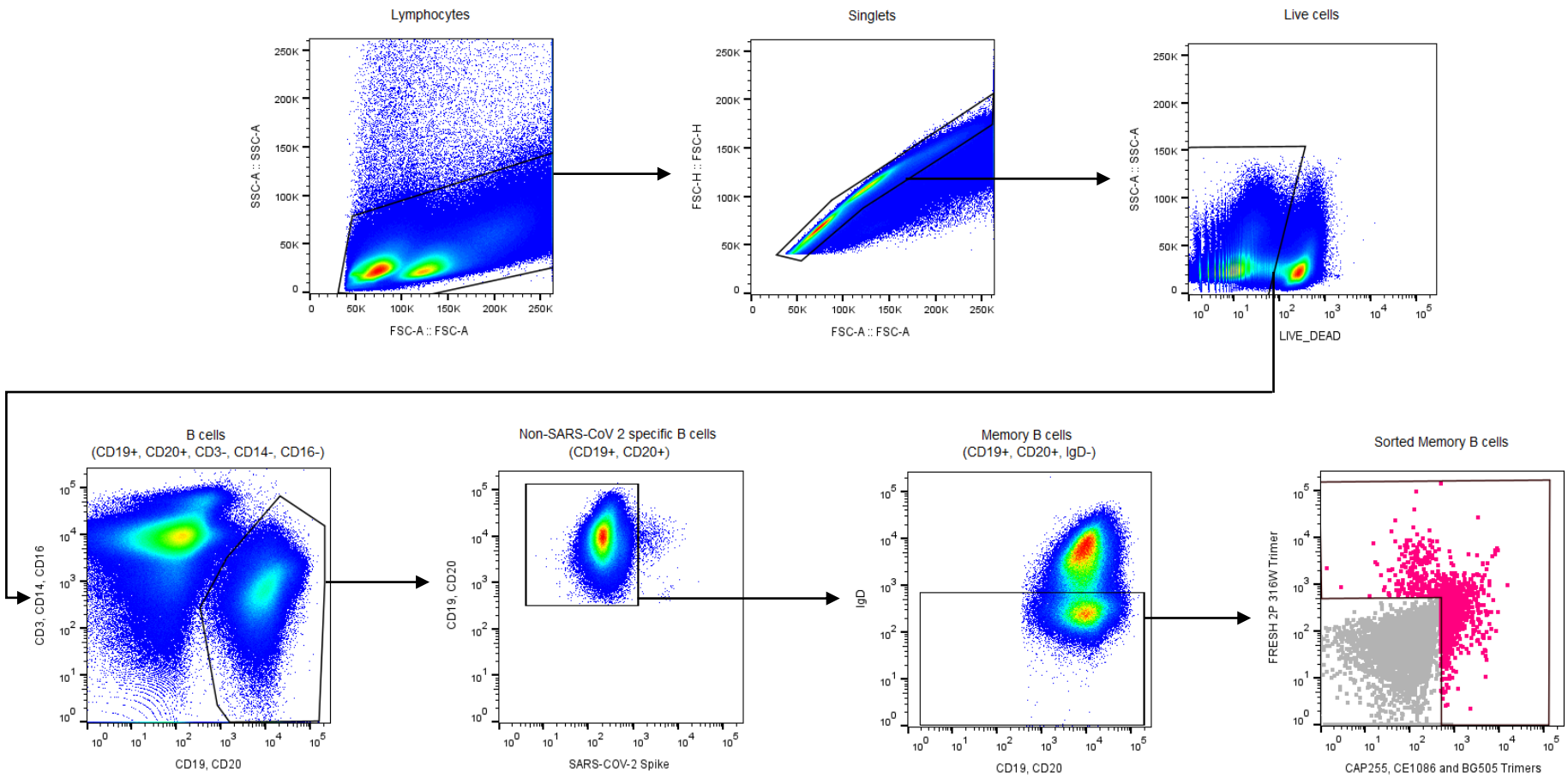

Figure 3.7: Flow cytometry plots of cells sorted from participant CAP287.
Cryopreserved PBMCs from CAP287 were stained with markers to identify trimer-specific cells. The gating strategy included selection for lymphocytes, singlets, live cells, B cells, B cells that did not bind non-specifically to the SARS-CoV-2 spike decoy bait, memory B cells and lastly cells binding to one or more HIV-1 trimers (FRESH1388_2P_316W, CAP255.4D, BG505 and CE1086C). Analysis was done using FlowJo v10.10.0.

Of the 252 sorted B cells, cDNA synthesis led to the recovery of variable regions from 191 B cells, which is 75% of the total sorted cells. Sequencing of the amplified variable heavy and light chain regions was used to further characterise and group the isolated antibodies into clonotypes - B cell receptors (BCR) which were descended from the same ancestral naive B cell BCR. In total 94 paired full-length and functionally rearranged heavy and light chain V(D)J sequences were recovered (**Table S3.1**). A number of V genes were used amongst the heavy and light chain sequences, with the predominant germline V genes used being IGHV3-13 (17.02%) and IGVL2-14 (12.77%) (**Figure 3.8A**). Interestingly, the most used V gene, IGHV3-13, is a rarely used gene in the human repertoire and not commonly found amongst HIV specific antibodies (Boyd *et al.*, 2010; Gidoni *et al.*, 2019; Rodriguez *et al.*, 2023). Distribution of CDRH3 AA length and percentage SHM, showed 51% of antibodies had CDRH3s longer than what is found on average in the naive repertoire (15 AA) and 43% of antibodies had more than 10% SHM, suggesting some of these antibodies could have features associated with bNAbs (Figure 3.8B). Thirteen antibody clonotypes, with more than two members, were identified by spectral clustering, based on the similarity of their heavy chain junctional regions (**Figure 3.8C**). More specifically, three clonotypes identified all used the predominant germline gene, IGHV3-13, including the largest clonotype which contained seven members.

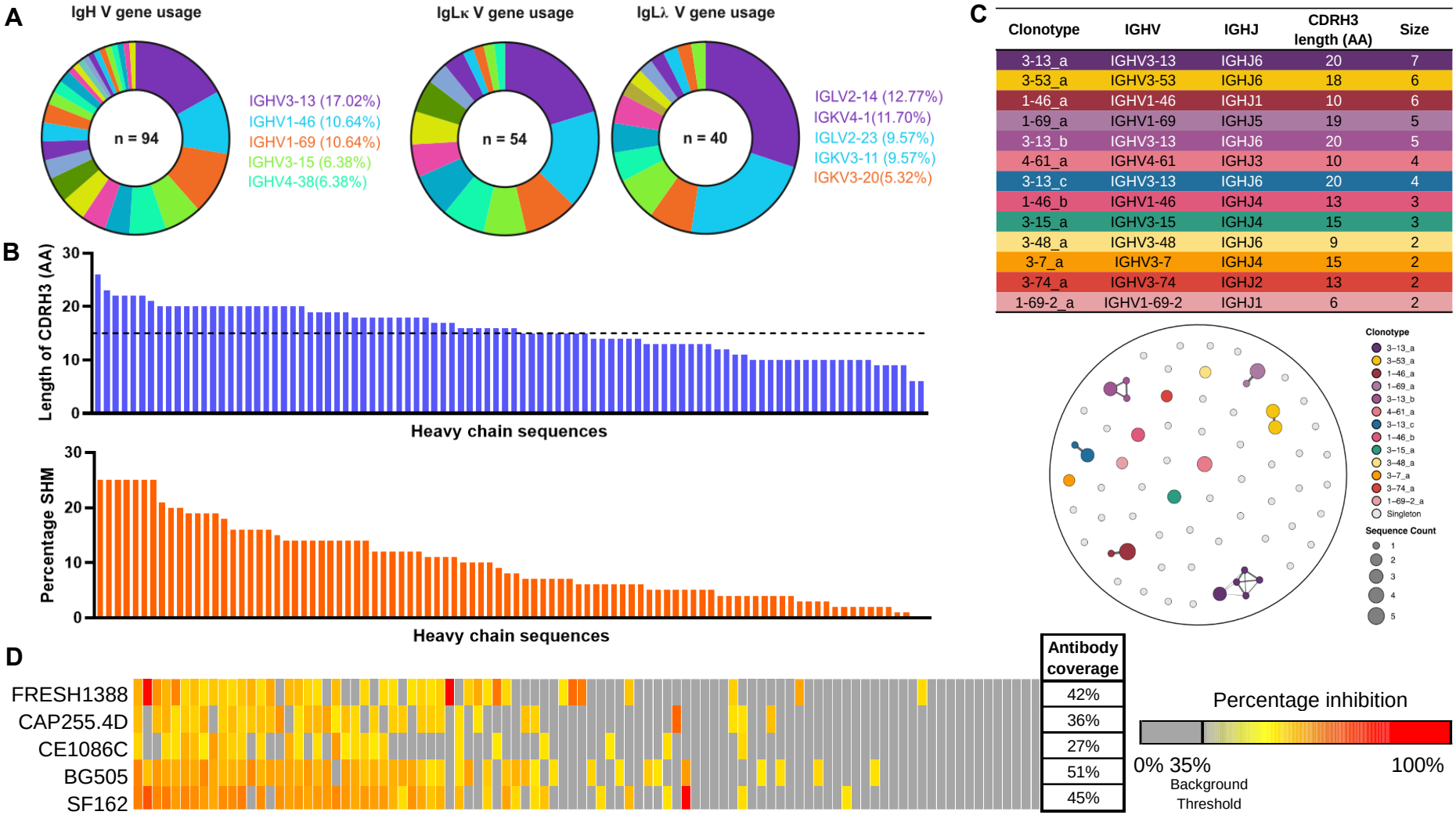

Clonotype	IGHV	IGHJ	CDRH3 length (AA)	Size
3-13_a	IGHV3-13	IGHJ6	20	7
3-53_a	IGHV3-53	IGHJ6	18	6
1-46_a	IGHV1-46	IGHJ1	10	6
1-69_a	IGHV1-69	IGHJ5	19	5
3-13_b	IGHV3-13	IGHJ6	20	5
4-61_a	IGHV4-61	IGHJ3	10	4
3-13_c	IGHV3-13	IGHJ6	20	4
1-46_b	IGHV1-46	IGHJ4	13	3
3-15_a	IGHV3-15	IGHJ4	15	3
3-48_a	IGHV3-48	IGHJ6	9	2
3-7_a	IGHV3-7	IGHJ4	15	2
3-74_a	IGHV3-74	IGHJ2	13	2
1-69-2_a	IGHV1-69-2	IGHJ1	6	2

Figure 3.8: High-throughput neutralisation screening data of expressed antibodies and immunogenetic data of paired heavy and light chain sequences.

(A) Germline V gene usage for the heavy (IgH), kappa light (IgLκ) and lambda light (IgLλ) chains of paired heavy and light chain sequences, with the top five most frequently used genes for each chain indicated. (B) Distribution of percentage SHM and CDRH3 lengths of the heavy chains, with the dotted line indicating the average length of CDRH3 in naïve human repertoires. (C) Spectral clustering of productively rearranged and full length VDJ sequences, based on heavy chain junction region similarity, identified 13 clonotypes with two or more members. (D) Neutralisation screening data, as percentage inhibition of infection, for a subset of expressed antibodies (n = 96).

3.4.2 Preliminary antibody screening

CAP287 antibodies were expressed through transfections of linear cassettes, which were composed of amplified variable regions of both the heavy and light chains along with the antibody constant regions for each chain. From 252 isolated B cells only a subset of 96 antibodies were expressed and screened for neutralisation activity against several pseudoviruses (**Figure 3.8D**). These included SF162 (a tier 1, neutralisation sensitive virus) as well as pseudoviruses BG505, CE1086, CAP255.4D and FRESH1388 (all representing the corresponding viruses from which the HIV soluble sorting antigens were derived). From the antibody supernatants tested, 38/96 contained antibodies that neutralised three or more viruses with a mean percentage inhibition above 35%, which was the background threshold, as determined by the no-template controls (NTC). More specifically, BG505 and CE1086 were neutralised by the most (51%) and the least (27%) number of antibodies, respectively. The difficult-to-neutralise FRESH1388 isolate was neutralised by 42% of the antibodies, suggesting that some potent antibodies, potentially with novel specificities, may have been isolated. Other pseudoviruses, used in screening, including CAP255.4D and the tier 1 virus, SF162 were neutralised by 36% and 45% of the 96 supernatants, respectively. Overall, the screening data successfully showed that several of neutralising antibodies could potentially have breadth and had the ability to neutralise a difficult-to-neutralise isolate.

3.4.3 Antibody selection

Both the sequencing and neutralisation screening data were used to prioritise ten CAP287 antibodies for further functional characterisation (**Table 3.3**). Antibodies that showed neutralisation activity against three or more viruses and had a mean percentage inhibition higher than 35% were favoured. Furthermore antibodies from the observed clonotypes with bNAb features, such as long CDRH3s (>20 AA) and high levels of SHM, were favoured for selection (Yu and Guan, 2014). The selected antibodies came from nine different clonotypes, which used the IGHV3-13, IGHV1-46, IGHV3-74, IGHV1-69, IGHV3-48, IGHV4-38 or IGHV4-4 genes. Due to time constraints, CAP287.160 was not screened for neutralisation activity.

Table 3.3: Immunogenetic and neutralisation screening data of antibodies selected for further characterisation.

		Immunogenetic data						Neutralisation data					
								Percentage inhibition					
Clonotype	Antibody	VH V gene	VH SHM (%)	CDRH3 Length	VL V gene	VL SHM (%)	CDRL3 Length	SF162	BG505 +N332	CE1086	CAP255.4D	FRESH1388	Mean
3-13_a	CAP287.44	IGHV3-13	18,1	20	IGLV2-14	12,6	12	77%	46%	25%	32%	100%	56%
3-13_a	CAP287.17	IGHV3-13	14,4	20	IGLV2-23	9,2	11	57%	46%	42%	34%	40%	44%
3-13_c	CAP287.39	IGHV3-13	16,8	20	IGLV2-14	8,5	11	56%	51%	38%	38%	63%	49%
3-13_b	CAP287.5	IGHV3-13	16,6	20	IGLV2-14	8,1	11	57%	57%	28%	54%	34%	46%
1-46_c	CAP287.49	IGHV1-46	16,4	10	IGKV2-24	12,0	9	63%	54%	51%	44%	41%	51%
1-46_b	CAP287.160	IGHV1-46	5,1	13	IGKV3-15	3,1	10	-	-	-	-	-	-
1-69_a	CAP287.37	IGHV1-69	15,4	19	IGKV4-1	5,9	9	61%	49%	47%	43%	43%	48%
4-38-2_a	CAP287.14	IGHV4-38	7,7	22	IGKV3-20	4,3	9	61%	50%	42%	48%	40%	48%
3-48_a	CAP287.26	IGHV3-48	2,4	9	IGKV1-16	2,1	9	57%	55%	36%	47%	31%	45%
4-4_b	CAP287.34	IGHV4-4	16,7	22	IGKV1-39	9,5	8	50%	42%	23%	42%	42%	40%

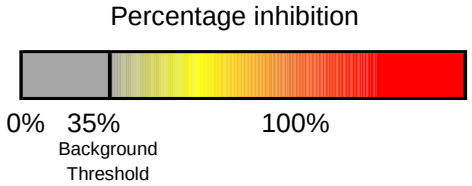

3.4.4 Neutralisation breadth of prioritised CAP287 antibodies

The 10 prioritised CAP287 mAbs were screened for neutralisation activity against a six-virus panel (94UG103, 92BR020, JRCSF, IAVIC22, 93IN905 and 92TH021), and the FRESH1388 virus (**Table 3.5**). The six-virus panel was originally developed by Simek *et al.* (2009) to predict neutralisation breadth against a larger virus panel by participant serum, and includes viruses from subtypes A, B and C and a CRF01_AE recombinant strain. Four antibodies (CAP287.39, CAP287.5, CAP287.44 and CAP287.37) had neutralising activity against the six-virus panel, with neutralisation breadth ranging from 33 to 67%. The broadest antibodies CAP287.44 and CAP287.39, neutralised the six virus panel with neutralisation breadth of 50% and 67%, respectively. However, both these antibodies weakly neutralised the subtype B viruses, JRCSF and 92BR020, respectively, with IC_{50} > 18 µg/ml. Additionally, antibodies CAP287.39, CAP287.44 and CAP287.37 neutralised the difficult-to-neutralise FRESH13888 virus. To further confirm these findings and determine whether these antibodies will be effective against contemporary viruses and additional subtypes the antibodies will be tested against larger and more contemporary virus panels in follow-up studies.

Table 3.4: Neutralisation breadth and potency of the prioritised CAP287 antibodies against a six-virus heterologous panel and FRESH1388.

			Six-virus panel						
		Subtype	A	B	B	C	C	CRF01_AE	C
		Virus	94UG103	92BR020	JRCSF	IAVIC22	93IN905	92TH021	FRESH1388
Clonotype	VH V gene	Antibody	IC50 (µg/ml)						
3-13_a	IGHV3-13	CAP287.44	50	50	20	0,05	0,23	50	0,001
3-13_a	IGHV3-13	CAP287.17	50	50	50	50	50	50	50
3-13_c	IGHV3-13	CAP287.39	50	19	0,22	0,10	0,09	50	0,002
3-13_b	IGHV3-13	CAP287.5	50	50	50	0,002	0,002	50	50
1-46_c	IGHV1-46	CAP287.49	50	50	50	50	50	50	50
1-46_b	IGHV1-46	CAP287.160	50	50	50	50	50	50	50
1-69_a	IGHV1-69	CAP287.37	50	50	50	50	0,05	50	0,38
4-38-2_a	IGHV4-38	CAP287.14	50	50	50	50	50	50	50
3-48_a	IGHV3-48	CAP287.26	50	50	50	50	50	50	50
4-4_b	IGHV4-4	CAP287.34	50	50	45	50	50	50	50

No neutralisation — Potent neutralisation

4 Discussion

Contemporary HIV-1 isolates have shown reduced sensitivity to various bNAbs targeting specific epitopes, due to antigenic drift (Bouvin-Pley *et al.*, 2013; Stefic *et al.*, 2019; Mullick *et al.*, 2021; Mkhize *et al.*, 2023; Sutar *et al.*, 2025). This highlights the need for more bNAbs, with novel binding specificities, that can neutralise currently circulating viruses and specifically those that are difficult-to-neutralise. In this study, difficult-to-neutralise isolates, from PLWH during the early stage of infection, were characterised and a soluble trimer, based on the Env protein of the FRESH1388 virus, was created. In addition to the DS-SOSIP.664 mutations, the final FRESH1388 trimer (FRESH1388-2P-316W) contained a mutation for stabilisation of the V3-region. The FRESH1388 virus was resistant to all bNAbs tested targeting the FP (VRC34, AIRU_F8, DFPHa01), the V2-apex (CAP256-VRC26.25 and ePGDM1400v9) and the gp120-gp41 interface (PGT151) epitopes. Novel antibodies were isolated from a person living with HIV, using the soluble FRESH1388-2P-316W trimer and a subset of antibodies were selected for further characterisation. Four neutralising antibodies, from three different clonal lineages, were identified and had up to 67% neutralisation breadth. Three of these antibodies use a rare germline gene that has been associated with V2-apex targeting antibodies which have an alternative binding mode (Cale *et al.*, 2017) and that could be exploited to target isolates that are resistant to clinically relevant V2-apex bNAbs.

Both single or multiple amino acid mutations within the antibody contact site, on the Env protein, can result in antibody resistance toward a particular epitope (O'Rourke *et al.*, 2012). Such mutations may result in differences between amino acid side-chain interactions which can ultimately lead to structural modifications within the Env protein that may alter epitope recognition or accessibility by the antibody. Furthermore, as previously shown in several studies, although these mutations do not necessarily occur within the antibody binding site, they can still impact the specific epitope (O'Rourke *et al.*, 2012; Moyo *et al.*, 2017; Ferreira *et al.*, 2018). Additionally certain mutations can cause key N-linked glycans to be repositioned or disappear, increasing resistance to glycan-dependent bNAbs (Moore *et al.*, 2012; Lynch *et al.*, 2015a; Moyo *et al.*, 2017).

Contemporary isolates selected from the IAVI ADVANCE Surveillance project had previously been characterised for their bNAb sensitivity. In the present study this was expanded to identify Envs with multi-bNAb class resistance. The neutralisation profile of the FRESH1388 virus was consistent with evidence of reduced bNAb sensitivity observed in recent studies, particularly at the V2-apex and CD4bs epitopes among subtype C isolates (Rademeyer *et al.*, 2016; Mkhize *et al.*, 2023). In addition the FRESH1388 isolate was resistant to bNAbs (that were tested) targeting the FP, suggesting the isolate has multi-bNAb class resistance. During the co-evolution of HIV-1 and host antibody response, genetic variation at the *env* gene occurs, in order to escape NAbs (Arrildt, Joseph and Swanstrom, 2012). The positive selection of viruses that retain mutations preventing neutralisation may have led to these isolates with decreased susceptibility toward NAbs or bNAbs. Thus, as antigenic drift continues, the observed decrease in sensitivity to bNAbs targeting distinct epitopes, could drive the progression toward multi-bNAb class resistance. Previous studies have demonstrated that naturally occurring VRC01-resistant viruses (Lynch *et al.*, 2015b) and b12-resistant clones (Sather *et al.*, 2012) had diminished viral fitness. Moreover this decreased viral fitness was associated with reduced CD4 interaction due to mutations at the CD4bs (Sather *et al.*, 2012; Lynch *et al.*, 2015b). However, as noted by Sutar *et al.* (2025), early isolates with reduced bNAb sensitivity can still continue to transmit and establish infection and therefore, the FRESH1388 virus, an early isolate displaying resistance to multiple bNAb classes, raises important concerns. This present study underscores the need for further characterisation of the viral fitness of early isolates with multi-bNAb class resistance.

In this study two participants, CAP287 and CAP341, with chronic infection and neutralisation breadth of 61% and 50% (Moore *et al*. unpublished), strongly neutralised the FRESH1388 virus. This suggests that previously unmapped participants with breadth may be a good source of novel NAbs, which could potentially neutralise difficult-to-neutralise viruses. For isolation of bNAbs, soluble native-like SOSIP trimers exposing bNAb epitopes are essential. BNAbs including PGDM1400 (Sok *et al.*, 2014), ACS202 (van Gils *et al.*, 2016), AIIMS-P01 (Kumar *et al.*, 2019) and 1-18 (Schommers *et al.*, 2020), were successfully isolated using SOSIP trimer baits based on Env proteins from various isolates with different subtypes. The use of native-like, SOSIP trimers are advantageous due to the reduced exposure of non-desirable

antibody epitopes. However, the MPER epitope is not presented on soluble trimers, due to the truncation beyond residue 664 (Klasse *et al.*, 2013) therefore no MPER-targeting bNAbs could be isolated.

Prior to the selection of the FRESH1388 trimer as a sorting bait, all three difficult-to-neutralise trimers (FRESH1388, PC220898 and PC235205) were expressed, with the DS-SOSIP.664 mutations. However upon additional stabilisation with the 2P substitution (Wrapp *et al.*, 2023), to improve trimer yields, only the FRESH1388 trimer was successfully expressed. This highlights both the difficulty in expressing soluble trimers and that stabilising mutations may not work for all trimers. Alternative stabilising designs, including native flexibly linked (NFL) (Sharma *et al.*, 2015), repair-and-stabilise (RnS) (Rutten *et al.*, 2018) and the recently described interdomain lock (IDL) designs (Zhang *et al.*, 2024) should be explored for the two trimers (PC220898 and PC235205) which were not successfully expressed with the 2P substitution. Additionally many other mutations, described by Torrents de la Peña and Sanders (2018), targeting specific regions on the trimer, could also be explored. A further complication is that stabilising mutations can change the antigenicity and structure of the trimer significantly (Tong *et al.*, 2023). Therefore, stabilisation should be done selectively in order to keep the antigenicity of trimers as close to the native Env as possible. Overall, production of soluble HIV-1 trimers is a difficult process due to the instability and flexibility of the native-trimer, and stabilised trimers should always be assessed to ensure that their antigenicity profile matches that of the virion-associated Env (Binley *et al.*, 2000; Sanders *et al.*, 2002; Julien *et al.*, 2015).

Antigenic analysis of the FRESH1388-2P trimer demonstrated that the V3-loop was highly accessible by nNAbs, 447-52D and 3074, suggesting exposure of the V3-loop. As previously established, during infection, immunological decoys such as gp41 stumps and gp120 monomers are in abundance (Moore *et al.*, 2006) and non-neutralising epitopes are highly exposed on these immunological decoys (Havenar-Daughton, Lee and Crotty, 2017). Therefore, nNAbs are positively selected for and will bind a non-neutralising epitope exposed on the native-Env (Havenar-Daughton, Lee and Crotty, 2017). Immunogens, based on the HIV-1 Env, have been shown to be bound by these nNAbs (Sanders *et al.*, 2013) and several studies have evaluated various stabilisation strategies to reduce the exposure of the non-neutralising

epitopes, involving the V3-loop and CD4i (Julien *et al.*, 2015; Kulp *et al.*, 2017; de Taeye *et al.*, 2018; Torrents de la Peña and Sanders, 2018). Exposure of these nNAb epitopes on a trimer and specifically a bNAb sorting bait is therefore not ideal, as it will result in the isolation of nNAbs. Thus stabilisation within the V3-region of the FRESH1388-2P trimer was essential for the isolation of bNAbs. The 316W mutation used in this study specifically increases hydrophobic interactions, resulting in the loop being positioned closer to the core of the trimer between two protomers and overall increasing trimer stability (de Taeye *et al.*, 2015). This single stabilising mutation was optimal, preserving the antigenicity of the FRESH1388-2P-316W trimer relative to FRESH1388-2P, while reducing binding by the nNAbs 447-52D and 3074, thereby minimizing V3-loop exposure and the likelihood of isolating V3-specific nNAbs. Moreover, compared to the other mutations tested, the 316W amino acid change resulted in superior trimer expression. This may be due to the reduced flexibility and improved thermostability of the trimer, as previously noted by de Taeye *et al*. (2015), which in turn may prevent dissociation of trimer subunits during trimer assembly.

Structural characterization of the FRESH1388-2P-316W trimer was important to determine the conformation of the trimer, given the resistance observed at the trimer-specific epitopes, the V2-apex and interface. A limitation within this project was the partially solved cryo-EM structure of the trimer which could have provided insight into the intricate structural changes emerging within this trimer, relative to other trimers, and potentially resulting in reduced bNAb sensitivity. Future studies should focus on defining the compactness and stability of the difficult-to-neutralise FRESH1388-2P-316W trimer and compare this with other soluble, difficult-to-neutralise trimers and the BG505 SOSIP.664 trimer.

The FRESH1388-2P-316W trimer led to the isolation of 252 antigen specific memory B cells, from which antibodies were isolated, sequenced and screened for neutralising activity. Spectral clustering of the antibody heavy chain V genes identified 13 potential clonal lineages with more than one member. Notably several antibodies used the IGHV1-69, IGHV1-46, and IGHV3-15 genes, which have been used by previously isolated bNAbs including 4E10, 1-18 and 10E8, respectively (Buchacher *et al.*, 1994; Huang *et al.*, 2014; Sok and Burton, 2018; Schommers *et al.*, 2020; Haynes *et al.*, 2023). The IGHV3-13 gene, a rarely used germline gene (Gidoni *et al.*, 2019;

Rodriguez *et al.*, 2023), was the most prevalent V gene among the heavy chains and was identified in three clonal lineages. The prevalence of IGHV3-13 gene in the human repertoire is not extensively known. In a small study, conducted more than a decade ago – in which the naive repertoires of 12 participants were sequenced – the IGHV3-13 gene was found in less than half the participants (n = 5) and was observed in 0.01-0.04% of all sequences of those participants (Boyd *et al.*, 2010). Additionally, the IGHV3-13 gene has been associated with Ebola neutralising antibodies (Corti *et al.*, 2016) and has been found in antibodies produced within a SARS-CoV-2 infected individual (Ma *et al.*, 2022), however the use of this gene has not been widely reported amongst HIV-1 NAbs or bNAbs (Haynes *et al.*, 2023).

The neutralisation activity of the prioritised antibodies was characterised using the six-virus panel and the subtype C FRESH1388 virus. The six-virus panel has been used to screen participant plasma and identify elite neutralisers (Walker *et al.*, 2010, 2011; Landais *et al.*, 2016). Four CAP287 neutralising antibodies stemming from three different clonal lineages, including three different IGHV3-13 lineages and an IGHV1-69 lineage, were identified using this panel. The breadth of these neutralising antibodies ranged from 16% to 67%. However the six-virus panel is limited in subtype variation and panel size, therefore these antibodies should be tested against a larger viral panel, involving more subtypes, for a more conclusive determination of neutralisation breadth. Alternative existing viral panels include the 12-virus global panel (deCamp *et al.*, 2014), CAVD panel (Scheid *et al.*, 2011), Monogram panel (Walker *et al.*, 2011), 40-virus multiclade panel (Rusert *et al.*, 2016), 12-virus clade C panel (Hraber *et al.*, 2017) and 41-virus panel (Hesselman *et al.*, 2025). However the viruses within these panels and the six-virus panel were isolated more than 15 years ago, and therefore may not be a good indicator of breadth against contemporary viruses. As suggested by Mkhize *et al.* (2023), new viral panels, based on viruses from the AMP trials (Corey *et al.*, 2021), would be more representative of circulating strains. Furthermore the neutralising activity of these antibodies against additional difficult-to-neutralise viruses, should be assessed to determine if their coverage of these challenging isolates extends beyond FRESH1388.

Epitope mapping of the CAP287 NAbs is still to be completed, however the IGHV3-13 NAbs may be V2-apex targeting due to similarities with the VRC38 lineage described

by Cale *et al.* (2017). The CAP287 IGHV3-13 lineages had shared germline IGHV and IGHJ genes with VRC38 lineage, isolated from a donor exposed to subtype B infection (Cale *et al.*, 2017). Additionally, all the IGHV3-13 using antibodies of the VRC38 and CAP287 lineages lack tyrosine sulfonation, in particular the 'YYD' motif, which is commonly observed in V2-apex targeting bNAbs and positively influences antibody binding (Andrabi *et al.*, 2015; Haynes *et al.*, 2023). Furthermore moderate neutralisation breadth is a common trait among these antibodies as the VRC38 and CAP287 IGHV3-13 lineages had neutralisation breadth up to 42%, against a 30-virus multi-clade panel (Cale *et al.*, 2017), and up to 67%, against a six-virus panel. Differences within these antibodies can be seen within the CDRH3 and gene usage of the light chains. The IGHV3-13 using CAP287 antibodies have longer CDRH3s (20 AA) compared to the VRC38 lineage (16 AA), and the CDRH3 sequences differ substantially. No similarities were noted for the V and J genes of the light chains. Interestingly, using NS-EM, the VRC38.01 antibody was found to target the V2-apex in a different way than known V2-apex targeting bNAbs, such as PGDM1400 and PG9 (Cale *et al.*, 2017). The shared similarities in heavy chain gene usage and lack of tyrosine sulfonation, could suggest a potential relationship between the VRC38 and CAP287 IGHV3-13 antibodies in terms of their epitope target and/or binding approach. However, further mapping is needed to determine whether the CAP287 mAbs specifically target the V2-apex.

The FRESH1388 virus is resistant to neutralisation by V2-apex bNAbs, CAP256-VRC26.25 and ePGDM1400v9, both of which penetrate the glycan shield using their long, negatively-charged CDRH3s (Andrabi *et al.*, 2015; Haynes *et al.*, 2023). However both CAP287.44 and CAP287.39, which are from the IGHV3-13 lineages share characteristics with the V2-apex targeting VRC38 antibody lineage (Cale *et al.*, 2017), and were able to neutralise the FRESH1388 virus. This further suggests that if the CAP287 antibodies target the V2-apex they may do so in an alternative mode and potentially be used to neutralise viruses that have developed neutralisation resistance to other V2-apex bNAbs. Future work should focus on determining epitope specificity of the CAP287 IGHV3-13 lineage antibodies through binding and neutralisation assays, using epitope knock out mutants, along with structural characterisation, involving NS- and cryo-EM. Additionally, the Env sequence of FRESH1388 virus should be evaluated for mutations and the virus should be assessed for neutralisation

by V2-apex bNAbs not tested, such as CH01, which does not possess a negatively charged CDRH3 that is relied upon by majority of the V2-apex bNAbs. Additionally, the antibodies from the three different IGHV3-13 lineages could have diverged from the same lineage - which could account for the difference in neutralisation coverage and potency between these antibodies. This is likely, considering the extensive SHM and multiple rounds of affinity maturation that bNAbs incur and could impact the sequence and length of the CDRH3 (Klein *et al.*, 2013; Yu and Guan, 2014) which were factored into the spectral clustering of lineages.

Once epitope-specificity of the CAP287 IGHV3-13 lineage antibodies is confirmed then key-residues important for binding and neutralisation, within the IGHV3-13 antibody paratope and Env epitope, can be determined. This will further assist in informing HIV vaccine design strategies. A major focus of the HIV-1 vaccine field has been the design of germline-targeting immunogens that are specifically designed to engage class-specific bNAb precursor cells, such as VRC01-class B cells, and initiate the affinity maturation process toward bNAb development, while reducing binding of non-specific germline precursors (Jardine *et al.*, 2013). IGHV3-13 precursors may not be suitable candidates for designing germline-targeting immunogens, as unlike VRC01-class bNAbs, which share common epitope-binding mechanisms, conserved sequences, and have been identified across multiple individuals (Arnaout *et al.*, 2011), bNAbs utilising the IGHV3-13 gene have been observed in only one additional individual and these do not share sequence features with the CAP287 antibodies, including differences in D and J gene usage and CDR length characteristics (Cale *et al.*, 2017). An alternative vaccine design strategy which may be more amendable for inducing CAP287-like antibody responses, would be an epitope-focused approach, similar to current strategies targeting the V3-glycan epitope (Cai *et al.*, 2017; Zhang *et al.*, 2019). In this approach, immunogens could be designed to elicit bNAbs that target a common epitope while utilising diverse binding mechanisms and angles of approach (Sok *et al.*, 2016), however further binding, neutralisation and structural studies would be required to inform this design approach.

The prevalence of multiple bNAb lineages observed among these isolated CAP287 antibodies could suggest why the mapping of the CAP287 plasma response was inconclusive (Moore *et al*., unpublished). The identification of multiple bNAb lineages

within one donor has been reported in several studies. Firstly, (Bonsignori *et al.*, 2012) isolated two bNAbs, CH01 and VRC-CH31, specific to the V2-apex and CD4bs epitopes, respectively and Krebs *et al.* (2019) described the isolation of three MPER-targeting bNAbs with different levels of neutralisation breadth and modes of recognition. Additionally, Longo *et al.* (2016) isolated four V3-glycan NAb lineages which had similar characteristics and used the same gene families as other V3-glycan targeting antibodies.

The breadth and potency of combinations of bNAbs from different classes have been predicted using modelling tools (Mullick *et al.*, 2021; Mkhize *et al.*, 2023; Sutar *et al.*, 2025). Additionally, combinations of up to three bNAbs, targeting different epitopes, have been tested experimentally (Goo *et al.*, 2012; Bouvin-Pley *et al.*, 2014) and demonstrated improved neutralisation coverage. However, not all isolates are covered with an optimal bNAb combination and decreased neutralisation susceptibility over time highlights the need for more bNAbs, with novel binding mechanisms that can neutralise more resistant viruses. The addition of novel bNAbs, capable of neutralising viruses with reduced bNAb sensitivity, may increase the breadth of any bNAb cocktail and increase coverage of contemporary isolates with reduced sensitivity to various existing bNAbs.

Neutralisation screening was conducted on all CAP287 antibodies produced by mini-transfections and ten antibodies were prioritised (based on neutralisation screening and sequencing data) for further characterisation. A caveat of the neutralisation screening is that different native signal peptides were used for expression of antibodies expressed by mini-transfection, while an optimised signal peptide was used for the antibodies expressed by GenScript, and this may have differentially affected antibody expression (Aw *et al.*, 2018). This may have influenced the neutralisation activity measured in the neutralisation screening and thus could have affected the antibodies prioritised for characterization. Additionally due to time constraints, neutralisation screening was performed on only 50% of the 191 paired antibody sequences. As a consequence, functional antibody sequences that lacked corresponding screening data were likely not prioritised for downstream analysis. Expanding the neutralisation screening to include the remaining sequences could potentially identify additional antibodies that warrant further investigation.

Overall this study demonstrated that a soluble trimer, based on the Env of a difficult-to-neutralise virus, could be used to isolate novel antibodies capable of neutralising a difficult-to-neutralise isolate. Additionally the isolation of antibodies from different lineages using the IGHV1-69 and IGHV3-13 indicates this donor may have developed at least two bNAb lineages. Furthermore the isolation of clonal lineages utilising the infrequently observed IGHV3-13 gene warrants further investigation to establish baseline frequency of this gene segment within the naive BCR repertoire of participant CAP287. Based on the shared germline gene usage with the VRC38 lineage, these antibodies may target the V2-apex, and may do so in an uncommon way much like VRC38 and CH01. Moreover structural characterisation of the antibody-trimer interaction could identify novel binding mechanisms used by these antibodies - which could be used to influence the design of future immunogens in order to elicit antibodies with similar characteristics.

5 Conclusion

The aim of this project was to use SOSIP trimers derived from highly neutralisation-resistant HIV-1 Envs to isolate novel bNAbs from PLWH who had developed neutralisation breadth. Based on neutralisation profiling, the FRESH1388 isolate was confirmed to be resistant to multiple bNAbs and it was hypothesised that the FRESH1388 trimer could isolate antibodies with unique binding specificities due to the inherent resistance to existing bNAbs. Expression and characterization of the soluble FRESH1388-2P-316W trimer enabled the isolation of novel antibodies from participant CAP287. Sequence analysis revealed that the dominant clonal lineage utilized the rarely used IGHV3-13 germline gene, also found in the VRC38 lineage which targets the V2-apex by not using a protruding, anionic CDRH3 to penetrate the glycan shield. Among the isolated antibodies, four exhibited neutralising activity, with neutralisation breadth up to 67%, and three were capable of neutralising a highly resistant viral isolate, FRESH1388. Overall, this study demonstrates that plasma from a donor with broad neutralisation capacity during chronic infection can contain antibodies capable of neutralising resistant viral strains, and that such antibodies can be selectively isolated using a neutralisation-resistant, soluble Env trimer. This study contributes to the broader understanding of bNAb development and highlights the utility of resistant trimers for HIV-1 antibody discovery.

References

1. Abdool Karim, Q. *et al.* (2010) “Effectiveness and Safety of Tenofovir Gel, an Antiretroviral Microbicide, for the Prevention of HIV Infection in Women,” *Science*, 329(5996), pp. 1168–1174. Available at: https://doi.org/10.1126/science.1193748.

2. Abdool Karim, S.S. *et al.* (2009) “HIV infection and tuberculosis in South Africa: an urgent need to escalate the public health response,” *Lancet*, 374(9693), pp. 921–933. Available at: https://doi.org/10.1016/S0140-6736(09)60916-8.

3. Andrabi, R. *et al.* (2015) “Identification of Common Features in Prototype Broadly Neutralizing Antibodies to HIV Envelope V2 Apex to Facilitate Vaccine Design,” *Immunity*, 43(5), pp. 959–973. Available at: https://doi.org/10.1016/j.immuni.2015.10.014.

4. Arrildt, K.T., Joseph, S.B. and Swanstrom, R. (2012) “The HIV-1 Env Protein: A Coat of Many Colors,” *Current HIV/AIDS reports*, 9(1), pp. 52–63. Available at: https://doi.org/10.1007/s11904-011-0107-3.

5. Arts, E.J. and Hazuda, D.J. (2012) “HIV-1 antiretroviral drug therapy,” *Cold Spring Harbor Perspectives in Medicine*, 2(4), p. a007161. Available at: https://doi.org/10.1101/cshperspect.a007161.

6. Aw, R. *et al.* (2018) “A systematic analysis of the expression of the anti-HIV VRC01 antibody in *Pichia pastoris* through signal peptide optimization,” *Protein Expression and Purification*, 149, pp. 43–50. Available at: https://doi.org/10.1016/j.pep.2018.03.013.

7. Bar, K.J. *et al.* (2012) “Early low-titer neutralizing antibodies impede HIV-1 replication and select for virus escape,” *PLoS pathogens*, 8(5), p. e1002721. Available at: https://doi.org/10.1371/journal.ppat.1002721.

8. Bar-On, Y. *et al.* (2018) “Safety and antiviral activity of combination HIV-1 broadly neutralizing antibodies in viremic individuals,” *Nature Medicine*, 24(11), pp. 1701–1707. Available at: https://doi.org/10.1038/s41591-018-0186-4.

9. Barré-Sinoussi, F. *et al.* (1983) “Isolation of a T-lymphotropic retrovirus from a patient at risk for acquired immune deficiency syndrome (AIDS),” *Science (New York, N.Y.)*, 220(4599), pp. 868–871. Available at: https://doi.org/10.1126/science.6189183.

10. Behrens, A.-J. *et al.* (2016) “Composition and Antigenic Effects of Individual Glycan Sites of a Trimeric HIV-1 Envelope Glycoprotein,” *Cell Reports*, 14(11), pp. 2695–2706. Available at: https://doi.org/10.1016/j.celrep.2016.02.058.

11. Bekker, L.-G. *et al.* (2024) “Twice-Yearly Lenacapavir or Daily F/TAF for HIV Prevention in Cisgender Women,” *New England Journal of Medicine*, 391(13), pp. 1179–1192. Available at: https://doi.org/10.1056/NEJMoa2407001.

12. Bhiman, J.N. *et al.* (2015) “Viral variants that initiate and drive maturation of V1V2-directed HIV-1 broadly neutralizing antibodies,” *Nature Medicine*, 21(11), pp. 1332–1336. Available at: https://doi.org/10.1038/nm.3963.

13. Binley, J.M. *et al.* (2000) “A Recombinant Human Immunodeficiency Virus Type 1 Envelope Glycoprotein Complex Stabilized by an Intermolecular Disulfide Bond between the gp120 and gp41 Subunits Is an Antigenic Mimic of the Trimeric Virion-Associated Structure,” *Journal of Virology*, 74(2), pp. 627–643. Available at: https://doi.org/10.1128/JVI.74.2.627-643.2000.

14. Binley, J.M. *et al.* (2002) “Enhancing the Proteolytic Maturation of Human Immunodeficiency Virus Type 1 Envelope Glycoproteins,” *Journal of Virology*, 76(6), pp. 2606–2616. Available at: https://doi.org/10.1128/JVI.76.6.2606-2616.2002.

15. Bonsignori, M. *et al.* (2012) “Two Distinct Broadly Neutralizing Antibody Specificities of Different Clonal Lineages in a Single HIV-1-Infected Donor: Implications for Vaccine Design,” *Journal of Virology*, 86(8), pp. 4688–4692. Available at: https://doi.org/10.1128/jvi.07163-11.

16. Bonsignori, M. *et al.* (2017) “Staged induction of HIV-1 glycan–dependent broadly neutralizing antibodies,” *Science Translational Medicine*, 9(381), p. eaai7514. Available at: https://doi.org/10.1126/scitranslmed.aai7514.

17. Bouvin-Pley, M. *et al.* (2013) “Evidence for a Continuous Drift of the HIV-1 Species towards Higher Resistance to Neutralizing Antibodies over the Course of the Epidemic,” *PLOS Pathogens*, 9(7), p. e1003477. Available at: https://doi.org/10.1371/journal.ppat.1003477.

18. Bouvin-Pley, M. *et al.* (2014) “Drift of the HIV-1 Envelope Glycoprotein gp120 toward Increased Neutralization Resistance over the Course of the Epidemic: a Comprehensive Study Using the Most Potent and Broadly Neutralizing Monoclonal Antibodies,” *Journal of Virology*, 88(23), pp. 13910–13917. Available at: https://doi.org/10.1128/JVI.02083-14.

19. Boyd, S.D. *et al.* (2010) “Individual Variation in the Germline Ig Gene Repertoire Inferred from Variable Region Gene Rearrangements,” *The Journal of Immunology*, 184(12), pp. 6986–6992. Available at: https://doi.org/10.4049/jimmunol.1000445.

20. Buchacher, A. *et al.* (1994) “Generation of human monoclonal antibodies against HIV-1 proteins; electrofusion and Epstein-Barr virus transformation for peripheral blood lymphocyte immortalization,” *AIDS research and human retroviruses*, 10(4), pp. 359–369. Available at: https://doi.org/10.1089/aid.1994.10.359.

21. Buonaguro, L., Tornesello, M.L. and Buonaguro, F.M. (2007) “Human Immunodeficiency Virus Type 1 Subtype Distribution in the Worldwide Epidemic: Pathogenetic and Therapeutic Implications,” *Journal of Virology*, 81(19), pp. 10209–10219. Available at: https://doi.org/10.1128/JVI.00872-07.

22. Cai, H. *et al.* (2017) “Synthetic Three-Component HIV-1 V3 Glycopeptide Immunogens Induce Glycan-Dependent Antibody Responses,” *Cell Chemical Biology*, 24(12), pp. 1513-1522.e4. Available at: https://doi.org/10.1016/j.chembiol.2017.09.005.

23. Cale, E.M. *et al.* (2017) “Virus-like Particles Identify an HIV V1V2 Apex-Binding Neutralizing Antibody that Lacks a Protruding Loop,” *Immunity*, 46(5), pp. 777-791.e10. Available at: https://doi.org/10.1016/j.immuni.2017.04.011.

24. Caniels, T.G. *et al.* (2025) “Precise targeting of HIV broadly neutralizing antibody precursors in humans,” *Science*, p. eadv5572. Available at: https://doi.org/10.1126/science.adv5572.

25. Caskey, M. *et al.* (2015) “Viraemia suppressed in HIV-1-infected humans by broadly neutralizing antibody 3BNC117,” *Nature*, 522(7557), pp. 487–491. Available at: https://doi.org/10.1038/nature14411.

26. Caskey, M. *et al.* (2017) “Antibody 10-1074 suppresses viremia in HIV-1-infected individuals,” *Nature Medicine*, 23(2), pp. 185–191. Available at: https://doi.org/10.1038/nm.4268.

27. Chawla, A. *et al.* (2018) “A Review of Long-Term Toxicity of Antiretroviral Treatment Regimens and Implications for an Aging Population,” *Infectious Diseases and Therapy*, 7(2), pp. 183–195. Available at: https://doi.org/10.1007/s40121-018-0201-6.

28. Chuang, G.-Y. *et al.* (2017) “Structure-Based Design of a Soluble Prefusion-Closed HIV-1 Env Trimer with Reduced CD4 Affinity and Improved Immunogenicity,” *Journal of Virology*, 91(10), pp. e02268-16. Available at: https://doi.org/10.1128/jvi.02268-16.

29. Chun, T.W. *et al.* (1999) “Re-emergence of HIV after stopping therapy,” *Nature*, 401(6756), pp. 874–875. Available at: https://doi.org/10.1038/44755.

30. Cobb, D.A. *et al.* (2020) “Long-acting approaches for delivery of antiretroviral drugs for prevention and treatment of HIV: a review of recent research,” *Expert Opinion on Drug Delivery*, 17(9), pp. 1227–1238. Available at: https://doi.org/10.1080/17425247.2020.1783233.

31. Corey, L. *et al.* (2021) “Two Randomized Trials of Neutralizing Antibodies to Prevent HIV-1 Acquisition,” *New England Journal of Medicine*, 384(11), pp. 1003–1014. Available at: https://doi.org/10.1056/NEJMoa2031738.

32. Corti, D. *et al.* (2016) “Protective monotherapy against lethal Ebola virus infection by a potently neutralizing antibody,” *Science*, 351(6279), pp. 1339–1342. Available at: https://doi.org/10.1126/science.aad5224.

33. De Leys, R. *et al.* (1990) “Isolation and partial characterization of an unusual human immunodeficiency retrovirus from two persons of west-central African origin.,” *Journal of Virology*, 64(3), pp. 1207–1216. Available at: https://doi.org/10.1128/jvi.64.3.1207-1216.1990.

34. deCamp, A. *et al.* (2014) “Global panel of HIV-1 Env reference strains for standardized assessments of vaccine-elicited neutralizing antibodies,” *Journal of Virology*, 88(5), pp. 2489–2507. Available at: https://doi.org/10.1128/JVI.02853-13.

35. Deodhar, S. *et al.* (2022) “Transformation of dolutegravir into an ultra-long-acting parenteral prodrug formulation,” *Nature Communications*, 13(1), p. 3226. Available at: https://doi.org/10.1038/s41467-022-30902-7.

36. Desrosiers, R.C. and Letvin, N.L. (1987) “Animal models for acquired immunodeficiency syndrome,” *Reviews of Infectious Diseases*, 9(3), pp. 438–446. Available at: https://doi.org/10.1093/clinids/9.3.438.

37. de Taeye, S.W. *et al.* (2015) “Immunogenicity of Stabilized HIV-1 Envelope Trimers with Reduced Exposure of Non-neutralizing Epitopes,” *Cell*, 163(7), pp. 1702–1715. Available at: https://doi.org/10.1016/j.cell.2015.11.056.

38. de Taeye, S.W. *et al.* (2018) “Stabilization of the gp120 V3 loop through hydrophobic interactions reduces the immunodominant V3-directed non-neutralizing response to HIV-1 envelope trimers,” *Journal of Biological Chemistry*, 293(5), pp. 1688–1701. Available at: https://doi.org/10.1074/jbc.RA117.000709.

39. Doria-Rose, N.A. *et al.* (2014) “Developmental pathway for potent V1V2-directed HIV-neutralizing antibodies,” *Nature*, 509(7498), pp. 55–62. Available at: https://doi.org/10.1038/nature13036.

40. Doria-Rose, N.A. *et al.* (2016) “New Member of the V1V2-Directed CAP256-VRC26 Lineage That Shows Increased Breadth and Exceptional Potency,” *Journal of Virology*, 90(1), pp. 76–91. Available at: https://doi.org/10.1128/JVI.01791-15.

41. Dudley, D.D. *et al.* (2005) “Mechanism and control of V(D)J recombination versus class switch recombination: similarities and differences,” *Advances in Immunology*, 86, pp. 43–112. Available at: https://doi.org/10.1016/S0065-2776(04)86002-4.

42. Epstein, F.H. and Greene, W.C. (1991) “The Molecular Biology of Human Immunodeficiency Virus Type 1 Infection,” *New England Journal of Medicine*, 324(5), pp. 308–317. Available at: https://doi.org/10.1056/NEJM199101313240506.

43. Ferreira, R.-C. *et al.* (2018) “Structural Rearrangements Maintain the Glycan Shield of an HIV-1 Envelope Trimer After the Loss of a Glycan,” *Scientific Reports*, 8(1), p. 15031. Available at: https://doi.org/10.1038/s41598-018-33390-2.

44. Fischl, M.A. *et al.* (1987) “The Efficacy of Azidothymidine (AZT) in the Treatment of Patients with AIDS and AIDS-Related Complex,” *New England Journal of Medicine*, 317(4), pp. 185–191. Available at: https://doi.org/10.1056/NEJM198707233170401.

45. Frankel, A.D. and Young, J.A. (1998) “HIV-1: Fifteen Proteins and an RNA,” *Annual Review of Biochemistry*, 67, pp. 1–25. Available at: https://doi.org/10.1146/annurev.biochem.67.1.1.

46. Freed, E.O. (2001) “HIV-1 Replication,” *Somatic Cell and Molecular Genetics*, 26(1), pp. 13–33. Available at: https://doi.org/10.1023/A:1021070512287.

47. Frost, S.D.W. *et al.* (2005) “Neutralizing antibody responses drive the evolution of human immunodeficiency virus type 1 envelope during recent HIV infection,” *Proceedings of the National Academy of Sciences of the United States of America*, 102(51), pp. 18514–18519. Available at: https://doi.org/10.1073/pnas.0504658102.

48. Gąciarz, A. and Ruddock, L.W. (2017) “Complementarity determining regions and frameworks contribute to the disulfide bond independent folding of intrinsically

stable scFv," *PLoS ONE*, 12(12), p. e0189964. Available at: https://doi.org/10.1371/journal.pone.0189964.

49. Gallo, R.C. *et al.* (1984) "Frequent Detection and Isolation of Cytopathic Retroviruses (HTLV-III) from Patients with AIDS and at Risk for AIDS," *Science*, 224(4648), pp. 500–503. Available at: https://doi.org/10.1126/science.6200936.

50. Gartner, M.J. *et al.* (2020) "Understanding the mechanisms driving the spread of subtype C HIV-1," *eBioMedicine*, 53, p. 102682. Available at: https://doi.org/10.1016/j.ebiom.2020.102682.

51. Gaynor, R. (1992) "Cellular transcription factors involved in the regulation of HIV-1 gene expression," *AIDS*, 6(4), pp. 347–363. Available at: https://doi.org/10.1097/00002030-199204000-00001.

52. Gidoni, M. *et al.* (2019) "Mosaic deletion patterns of the human antibody heavy chain gene locus shown by Bayesian haplotyping," *Nature Communications*, 10(1), p. 628. Available at: https://doi.org/10.1038/s41467-019-08489-3.

53. van Gils, M.J. *et al.* (2016) "An HIV-1 antibody from an elite neutralizer implicates the fusion peptide as a site of vulnerability," *Nature microbiology*, 2, p. 16199. Available at: https://doi.org/10.1038/nmicrobiol.2016.199.

54. Giudicelli, V. *et al.* (2006) "IMGT/LIGM-DB, the IMGT® comprehensive database of immunoglobulin and T cell receptor nucleotide sequences," *Nucleic Acids Research*, 34(Database issue), pp. D781–D784. Available at: https://doi.org/10.1093/nar/gkj088.

55. Goo, L. *et al.* (2012) "A Combination of Broadly Neutralizing HIV-1 Monoclonal Antibodies Targeting Distinct Epitopes Effectively Neutralizes Variants Found in Early Infection," *Journal of Virology*, 86(19), pp. 10857–10861. Available at: https://doi.org/10.1128/JVI.01414-12.

56. Gorman, J. *et al.* (2016) "Structures of HIV-1 Env V1V2 with broadly neutralizing antibodies reveal commonalities that enable vaccine design," *Nature Structural & Molecular Biology*, 23(1), pp. 81–90. Available at: https://doi.org/10.1038/nsmb.3144.

57. Gray, E.S. *et al.* (2007) “Neutralizing antibody responses in acute human immunodeficiency virus type 1 subtype C infection,” *Journal of Virology*, 81(12), pp. 6187–6196. Available at: https://doi.org/10.1128/JVI.00239-07.

58. Gray, E.S. *et al.* (2011) “The Neutralization Breadth of HIV-1 Develops Incrementally over Four Years and Is Associated with CD4+ T Cell Decline and High Viral Load during Acute Infection,” *Journal of Virology*, 85(10), pp. 4828–4840. Available at: https://doi.org/10.1128/JVI.00198-11.

59. Griffith, S.A. and McCoy, L.E. (2021) “To bnAb or Not to bnAb: Defining Broadly Neutralising Antibodies Against HIV-1,” *Frontiers in Immunology*, 12, p. 708227. Available at: https://doi.org/10.3389/fimmu.2021.708227.

60. Gruell, H. and Schommers, P. (2022) “Broadly neutralizing antibodies against HIV-1 and concepts for application,” *Current Opinion in Virology*, 54, p. 101211. Available at: https://doi.org/10.1016/j.coviro.2022.101211.

61. Guenaga, J. *et al.* (2015) “Well-ordered trimeric HIV-1 subtype B and C soluble spike mimetics generated by negative selection display native-like properties,” *PLoS pathogens*, 11(1), p. e1004570. Available at: https://doi.org/10.1371/journal.ppat.1004570.

62. Gürtler, L.G. *et al.* (1994) “A new subtype of human immunodeficiency virus type 1 (MVP-5180) from Cameroon.,” *Journal of Virology*, 68(3), pp. 1581–1585. Available at: https://doi.org/10.1128/jvi.68.3.1581-1585.1994.

63. Guttman, M. *et al.* (2015) “Antibody potency relates to the ability to recognize the closed, pre-fusion form of HIV Env,” *Nature Communications*, 6, p. 6144. Available at: https://doi.org/10.1038/ncomms7144.

64. Halper-Stromberg, A. *et al.* (2014) “Broadly Neutralizing Antibodies and Viral Inducers Decrease Rebound from HIV-1 Latent Reservoirs in Humanized Mice,” *Cell*, 158(5), pp. 989–999. Available at: https://doi.org/10.1016/j.cell.2014.07.043.

65. Havenar-Daughton, C. *et al.* (2018) “The human naive B cell repertoire contains distinct subclasses for a germline-targeting HIV-1 vaccine immunogen,” *Science*

Translational Medicine, 10(448), p. eaat0381. Available at: https://doi.org/10.1126/scitranslmed.aat0381.

66. Havenar-Daughton, C., Lee, J.H. and Crotty, S. (2017) “Tfh cells and HIV bnAbs, an immunodominance model of the HIV neutralizing antibody generation problem,” *Immunological Reviews*, 275(1), pp. 49–61. Available at: https://doi.org/10.1111/imr.12512.

67. [a]Haynes, B.F., *et al.* (2012) “B-cell-lineage immunogen design in vaccine development with HIV-1 as a case study,” *Nature Biotechnology*, 30(5), pp. 423–433. Available at: https://doi.org/10.1038/nbt.2197.

68. [b]Haynes, B.F., *et al.* (2012) “Immune-correlates analysis of an HIV-1 vaccine efficacy trial,” *The New England Journal of Medicine*, 366(14), pp. 1275–1286. Available at: https://doi.org/10.1056/NEJMoa1113425.

69. Haynes, B.F. *et al.* (2023) “Strategies for HIV-1 vaccines that induce broadly neutralizing antibodies,” *Nature Reviews Immunology*, 23(3), pp. 142–158. Available at: https://doi.org/10.1038/s41577-022-00753-w.

70. Hemelaar, J. (2012) “The origin and diversity of the HIV-1 pandemic,” *Trends in Molecular Medicine*, 18(3), pp. 182–192. Available at: https://doi.org/10.1016/j.molmed.2011.12.001.

71. Hemelaar, J. *et al.* (2019) “Global and regional molecular epidemiology of HIV-1, 1990–2015: a systematic review, global survey, and trend analysis,” *The Lancet Infectious Diseases*, 19(2), pp. 143–155. Available at: https://doi.org/10.1016/S1473-3099(18)30647-9.

72. Hesselman, M.C. *et al.* (2025) “Rare twin cysteine residues in the HIV-1 envelope variable region 1 link to neutralization escape and breadth development,” *Cell Host & Microbe*, 33(2), pp. 279-293.e6. Available at: https://doi.org/10.1016/j.chom.2025.01.004.

73. HIV-CAUSAL Collaboration *et al.* (2010) “The effect of combined antiretroviral therapy on the overall mortality of HIV-infected individuals,” *AIDS*, 24(1), pp. 123–137. Available at: https://doi.org/10.1097/QAD.0b013e3283324283.

74. Hraber, P. *et al.* (2014) “Prevalence of broadly neutralizing antibody responses during chronic HIV-1 infection,” *AIDS*, 28(2), pp. 163–169. Available at: https://doi.org/10.1097/QAD.0000000000000106.

75. Hraber, P. *et al.* (2017) “Panels of HIV-1 Subtype C Env Reference Strains for Standardized Neutralization Assessments,” *Journal of Virology*, 91(19), pp. e00991-17. Available at: https://doi.org/10.1128/JVI.00991-17.

76. Huang, J. *et al.* (2014) “Broad and potent HIV-1 neutralization by a human antibody that binds the gp41-120 interface,” *Nature*, 515(7525), pp. 138–142. Available at: https://doi.org/10.1038/nature13601.

77. Jardine, J.G. *et al.* (2016) “HIV-1 broadly neutralizing antibody precursor B cells revealed by germline-targeting immunogen,” *Science*, 351(6280), pp. 1458–1463. Available at: https://doi.org/10.1126/science.aad9195.

78. Jogiraju, V. *et al.* (2025) “Pharmacokinetics and safety of once-yearly lenacapavir: a phase 1, open-label study,” *Lancet*, 405(10485), pp. 1147–1154. Available at: https://doi.org/10.1016/S0140-6736(25)00405-2.

79. Johnson, S. *et al.* (1997) “Development of a humanized monoclonal antibody (MEDI-493) with potent in vitro and in vivo activity against respiratory syncytial virus,” *The Journal of Infectious Diseases*, 176(5), pp. 1215–1224. Available at: https://doi.org/10.1086/514115.

80. Joyce, M.G. *et al.* (2017) “Soluble Prefusion Closed DS-SOSIP.664-Env Trimers of Diverse HIV-1 Strains,” *Cell Reports*, 21(10), pp. 2992–3002. Available at: https://doi.org/10.1016/j.celrep.2017.11.016.

81. Julg, B. and Barouch, D.H. (2019) “Neutralizing antibodies for HIV-1 prevention,” *Current opinion in HIV and AIDS*, 14(4), pp. 318–324. Available at: https://doi.org/10.1097/COH.0000000000000556.

82. [a]Julien, J.-P., *et al.* (2013) “Broadly Neutralizing Antibody PGT121 Allosterically Modulates CD4 Binding via Recognition of the HIV-1 gp120 V3 Base and Multiple Surrounding Glycans,” *PLOS Pathogens*, 9(5), p. e1003342. Available at: https://doi.org/10.1371/journal.ppat.1003342.

83. [b]Julien, J.-P., *et al.* (2013) “Crystal Structure of a Soluble Cleaved HIV-1 Envelope Trimer,” *Science*, 342(6165), pp. 1477–1483. Available at: https://doi.org/10.1126/science.1245625.

84. Julien, J.-P. *et al.* (2015) “Design and structure of two HIV-1 clade C SOSIP.664 trimers that increase the arsenal of native-like Env immunogens,” *Proceedings of the National Academy of Sciences*, 112(38), pp. 11947–11952. Available at: https://doi.org/10.1073/pnas.1507793112.

85. Kelesidis, T. and Landovitz, R.J. (2011) “Preexposure Prophylaxis for HIV Prevention,” *Current HIV/AIDS Reports*, 8(2), pp. 94–103. Available at: https://doi.org/10.1007/s11904-011-0078-4.

86. Kelley, C.F. *et al.* (2024) “Twice-Yearly Lenacapavir for HIV Prevention in Men and Gender-Diverse Persons,” *New England Journal of Medicine*, 392(13), pp. 1261–1276. Available at: https://doi.org/10.1056/NEJMoa2411858.

87. Kharsany, A.B.M. and Abdool Karim, Q. (2016) “HIV Infection and AIDS in Sub-Saharan Africa: Current Status, Challenges and Opportunities,” *Open AIDS Journal*, 10, pp. 34–48. Available at: https://doi.org/10.2174/1874613601610010034.

88. Khayat, R. *et al.* (2013) “Structural characterization of cleaved, soluble HIV-1 envelope glycoprotein trimers,” *Journal of Virology*, 87(17), pp. 9865–9872. Available at: https://doi.org/10.1128/JVI.01222-13.

89. Klasse, P.J. *et al.* (2013) “Influences on Trimerization and Aggregation of Soluble, Cleaved HIV-1 SOSIP Envelope Glycoprotein,” *Journal of Virology*, 87(17), pp. 9873–9885. Available at: https://doi.org/10.1128/JVI.01226-13.

90. Klein, F. *et al.* (2013) “Somatic Mutations of the Immunoglobulin Framework Are Generally Required for Broad and Potent HIV-1 Neutralization,” *Cell*, 153(1), pp. 126–138. Available at: https://doi.org/10.1016/j.cell.2013.03.018.

91. Kontomanolis, E.N. *et al.* (2017) “The social stigma of HIV-AIDS: society’s role,” *HIV/AIDS (Auckland, N.Z.)*, 9, pp. 111–118. Available at: https://doi.org/10.2147/HIV.S129992.

92. Kulp, D.W. *et al.* (2017) “Structure-based design of native-like HIV-1 envelope trimers to silence non-neutralizing epitopes and eliminate CD4 binding,” *Nature Communications*, 8(1), p. 1655. Available at: https://doi.org/10.1038/s41467-017-01549-6.

93. Kumar, S. *et al.* (2019) “An HIV-1 Broadly Neutralizing Antibody from a Clade C-Infected Pediatric Elite Neutralizer Potently Neutralizes the Contemporaneous and Autologous Evolving Viruses,” *Journal of Virology*, 93(4), pp. e01495-18. Available at: https://doi.org/10.1128/JVI.01495-18.

94. Kumar, S. *et al.* (2024) “Design and immunogenicity of an HIV-1 clade C pediatric envelope glycoprotein stabilized by multiple platforms,” *bioRxiv: The Preprint Server for Biology*, p. 2024.09.14.613016. Available at: https://doi.org/10.1101/2024.09.14.613016.

95. Kumar, S., Singh, S. and Luthra, K. (2023) “An Overview of Human Anti-HIV-1 Neutralizing Antibodies against Diverse Epitopes of HIV-1,” *ACS Omega*, 8(8), pp. 7252–7261. Available at: https://doi.org/10.1021/acsomega.2c07933.

96. Kwong, P.D. and Mascola, J.R. (2018) “HIV-1 Vaccines Based on Antibody Identification, B Cell Ontogeny, and Epitope Structure,” *Immunity*, 48(5), pp. 855–871. Available at: https://doi.org/10.1016/j.immuni.2018.04.029.

97. Landais, E. *et al.* (2016) “Broadly Neutralizing Antibody Responses in a Large Longitudinal Sub-Saharan HIV Primary Infection Cohort,” *PLOS Pathogens*, 12(1), p. e1005369. Available at: https://doi.org/10.1371/journal.ppat.1005369.

98. Landais, E. and Moore, P.L. (2018) “Development of broadly neutralizing antibodies in HIV-1 infected elite neutralizers,” *Retrovirology*, 15(1), p. 61. Available at: https://doi.org/10.1186/s12977-018-0443-0.

99. Leggat, D.J. *et al.* (2022) “Vaccination induces HIV broadly neutralizing antibody precursors in humans,” *Science*, 378(6623), p. eadd6502. Available at: https://doi.org/10.1126/science.add6502.

100. Li, B. *et al.* (2006) “Evidence for Potent Autologous Neutralizing Antibody Titers and Compact Envelopes in Early Infection with Subtype C Human

Immunodeficiency Virus Type 1," *Journal of Virology*, 80(11), pp. 5211–5218. Available at: https://doi.org/10.1128/jvi.00201-06.

101. Liao, H.-X. *et al.* (2013) "Co-evolution of a broadly neutralizing HIV-1 antibody and founder virus," *Nature*, 496(7446), pp. 469–476. Available at: https://doi.org/10.1038/nature12053.

102. Lima, N.S. *et al.* (2022) "Primary exposure to SARS-CoV-2 variants elicits convergent epitope specificities, immunoglobulin V gene usage and public B cell clones," *Nature Communications*, 13(1), p. 7733. Available at: https://doi.org/10.1038/s41467-022-35456-2.

103. Loggerenberg, F. van *et al.* (2008) "Establishing a Cohort at High Risk of HIV Infection in South Africa: Challenges and Experiences of the CAPRISA 002 Acute Infection Study," *PLOS ONE*, 3(4), p. e1954. Available at: https://doi.org/10.1371/journal.pone.0001954.

104. Longo, N.S. *et al.* (2016) "Multiple Antibody Lineages in One Donor Target the Glycan-V3 Supersite of the HIV-1 Envelope Glycoprotein and Display a Preference for Quaternary Binding," *Journal of Virology*, 90(23), pp. 10574–10586. Available at: https://doi.org/10.1128/JVI.01012-16.

105. [a]Lynch, R.M., Wong, P., *et al.* (2015) "HIV-1 fitness cost associated with escape from the VRC01 class of CD4 binding site neutralizing antibodies," *Journal of Virology*, 89(8), pp. 4201–4213. Available at: https://doi.org/10.1128/JVI.03608-14.

106. [b]Lynch, R.M., Boritz, E., *et al.* (2015) "Virologic effects of broadly neutralizing antibody VRC01 administration during chronic HIV-1 infection," *Science Translational Medicine*, 7(319), p. 319ra206. Available at: https://doi.org/10.1126/scitranslmed.aad5752.

107. Lyumkis, D. *et al.* (2013) "Cryo-EM structure of a fully glycosylated soluble cleaved HIV-1 Env trimer," *Science*, 342(6165), pp. 1484–1490. Available at: https://doi.org/10.1126/science.1245627.

108. Ma, J. *et al.* (2022) “Novel skewed usage of B-cell receptors in COVID-19 patients with various clinical presentations,” *Immunology Letters*, 249, pp. 23–32. Available at: https://doi.org/10.1016/j.imlet.2022.08.006.

109. Mansky, L.M. and Temin, H.M. (1995) “Lower in vivo mutation rate of human immunodeficiency virus type 1 than that predicted from the fidelity of purified reverse transcriptase,” *Journal of Virology*, 69(8), pp. 5087–5094. Available at: https://doi.org/10.1128/jvi.69.8.5087-5094.1995.

110. Mascola, J.R. *et al.* (2000) “Protection of macaques against vaginal transmission of a pathogenic HIV-1/SIV chimeric virus by passive infusion of neutralizing antibodies,” *Nature Medicine*, 6(2), pp. 207–210. Available at: https://doi.org/10.1038/72318.

111. Massud, I. *et al.* (2019) “Efficacy of Oral Tenofovir Alafenamide/Emtricitabine Combination or Single-Agent Tenofovir Alafenamide Against Vaginal Simian Human Immunodeficiency Virus Infection in Macaques,” *The Journal of Infectious Diseases*, 220(11), pp. 1826–1833. Available at: https://doi.org/10.1093/infdis/jiz383.

112. McCoy, L.E. and Burton, D.R. (2017) “Identification and specificity of broadly neutralizing antibodies against HIV,” *Immunological Reviews*, 275(1), pp. 11–20. Available at: https://doi.org/10.1111/imr.12484.

113. Mendoza, P. *et al.* (2018) “Combination therapy with anti-HIV-1 antibodies maintains viral suppression,” *Nature*, 561(7724), pp. 479–484. Available at: https://doi.org/10.1038/s41586-018-0531-2.

114. Mkhize, N.N. *et al.* (2023) “Neutralization profiles of HIV-1 viruses from the VRC01 Antibody Mediated Prevention (AMP) trials,” *PLOS Pathogens*, 19(6), p. e1011469. Available at: https://doi.org/10.1371/journal.ppat.1011469.

115. Moldt, B. *et al.* (2012) “Highly potent HIV-specific antibody neutralization in vitro translates into effective protection against mucosal SHIV challenge in vivo,” *Proceedings of the National Academy of Sciences of the United States of*

America, 109(46), pp. 18921–18925. Available at: https://doi.org/10.1073/pnas.1214785109.

116. Montefiori, D.C. (2009) “Measuring HIV neutralization in a luciferase reporter gene assay,” *Methods in Molecular Biology*, 485, pp. 395–405. Available at: https://doi.org/10.1007/978-1-59745-170-3_26.

117. Moody, M.A. *et al.* (2016) “Immune perturbations in HIV-1–infected individuals who make broadly neutralizing antibodies,” *Science Immunology*, 1(1). Available at: https://doi.org/10.1126/sciimmunol.aag0851.

118. Moore, P.L. *et al.* (2006) “Nature of Nonfunctional Envelope Proteins on the Surface of Human Immunodeficiency Virus Type 1,” *Journal of Virology*, 80(5), pp. 2515–2528. Available at: https://doi.org/10.1128/JVI.80.5.2515-2528.2006.

119. Moore, P.L. *et al.* (2011) “Potent and Broad Neutralization of HIV-1 Subtype C by Plasma Antibodies Targeting a Quaternary Epitope Including Residues in the V2 Loop,” *Journal of Virology*, 85(7), pp. 3128–3141. Available at: https://doi.org/10.1128/jvi.02658-10.

120. Moore, P.L. *et al.* (2012) “Evolution of an HIV glycan–dependent broadly neutralizing antibody epitope through immune escape,” *Nature Medicine*, 18(11), pp. 1688–1692. Available at: https://doi.org/10.1038/nm.2985.

121. Moore, P.L. *et al.* (2017) “Ontogeny-based immunogens for the induction of V2-directed HIV broadly neutralizing antibodies,” *Immunological Reviews*, 275(1), pp. 217–229. Available at: https://doi.org/10.1111/imr.12501.

122. Moore, P.L. (2018) “The Neutralizing Antibody Response to the HIV-1 Env Protein,” *Current HIV Research*, 16(1), pp. 21–28. Available at: https://doi.org/10.2174/1570162X15666171124122044.

123. Moyo, T. *et al.* (2017) “Chinks in the armor of the HIV-1 Envelope glycan shield: Implications for immune escape from anti-glycan broadly neutralizing antibodies,” *Virology*, 501, pp. 12–24. Available at: https://doi.org/10.1016/j.virol.2016.10.026.

124. Mullick, R. *et al.* (2021) “Neutralization diversity of HIV-1 Indian subtype C envelopes obtained from cross sectional and followed up individuals against broadly neutralizing monoclonal antibodies having distinct gp120 specificities,” *Retrovirology*, 18(1), p. 12. Available at: https://doi.org/10.1186/s12977-021-00556-2.

125. Munro, J.B. *et al.* (2014) “Conformational dynamics of single HIV-1 envelope trimers on the surface of native virions,” *Science*, 346(6210), pp. 759–763. Available at: https://doi.org/10.1126/science.1254426.

126. Murakami, T. (2008) “Roles of the interactions between Env and Gag proteins in the HIV-1 replication cycle,” *Microbiology and Immunology*, 52(5), pp. 287–295. Available at: https://doi.org/10.1111/j.1348-0421.2008.00008.x.

127. Kimanius, D. *et al.* (2021) “New tools for automated cryo-EM single-particle analysis in RELION-4.0” *Biochemical Journal*, 478(24), pp. 4169–4185. Available at: https://doi.org/10.1042/BCJ20210708.

128. Nouri, N. and Kleinstein, S.H. (2018) “Optimized Threshold Inference for Partitioning of Clones From High-Throughput B Cell Repertoire Sequencing Data,” *Frontiers in Immunology*, 9. Available at: https://doi.org/10.3389/fimmu.2018.01687.

129. Nouri, N. and Kleinstein, S.H. (2020) “Somatic hypermutation analysis for improved identification of B cell clonal families from next-generation sequencing data,” *PLoS computational biology*, 16(6), p. e1007977. Available at: https://doi.org/10.1371/journal.pcbi.1007977.

130. O’Rourke, S.M. *et al.* (2012) “Sequences in Glycoprotein gp41, the CD4 Binding Site, and the V2 Domain Regulate Sensitivity and Resistance of HIV-1 to Broadly Neutralizing Antibodies,” *Journal of Virology*, 86(22), pp. 12105–12114. Available at: https://doi.org/10.1128/jvi.01352-12.

131. Palella, F.J. *et al.* (1998) “Declining Morbidity and Mortality among Patients with Advanced Human Immunodeficiency Virus Infection,” *New England Journal*

of Medicine, 338(13), pp. 853–860. Available at: https://doi.org/10.1056/NEJM199803263381301.

132. Pegu, A. *et al.* (2014) “Neutralizing antibodies to HIV-1 envelope protect more effectively in vivo than those to the CD4 receptor,” *Science Translational Medicine*, 6(243), p. 243ra88. Available at: https://doi.org/10.1126/scitranslmed.3008992.

133. Peng, Y. *et al.* (2023) “Current drugs for HIV-1: from challenges to potential in HIV/AIDS,” *Frontiers in Pharmacology*, 14. Available at: https://doi.org/10.3389/fphar.2023.1294966.

134. Picelli, S. *et al.* (2014) “Full-length RNA-seq from single cells using Smart-seq2,” *Nature Protocols*, 9(1), pp. 171–181. Available at: https://doi.org/10.1038/nprot.2014.006.

135. Plantier, J.-C. *et al.* (2009) “A new human immunodeficiency virus derived from gorillas,” *Nature Medicine*, 15(8), pp. 871–872. Available at: https://doi.org/10.1038/nm.2016.

136. Popovic, M. *et al.* (1984) “Detection, isolation, and continuous production...,” *Science*, 224. Available at: https://doi.org/10.1126/science.6200935.

137. Pugach, P. *et al.* (2015) “A Native-Like SOSIP.664 Trimer Based on an HIV-1 Subtype B env Gene,” *Journal of Virology*, 89(6), pp. 3380–3395. Available at: https://doi.org/10.1128/JVI.03473-14.

138. Punjani, A. *et al.* (2017) “cryoSPARC: algorithms for rapid unsupervised cryo-EM structure determination,” *Nature Methods*, 14(3), pp. 290–296. Available at: https://doi.org/10.1038/nmeth.4169.

139. Rademeyer, C. *et al.* (2016) “Features of Recently Transmitted HIV-1 Clade C Viruses that Impact Antibody Recognition: Implications for Active and Passive Immunization,” *PLOS Pathogens*, 12(7), p. e1005742. Available at: https://doi.org/10.1371/journal.ppat.1005742.

140. Rerks-Ngarm, S. *et al.* (2009) “Vaccination with ALVAC and AIDSVAX to prevent HIV-1 infection in Thailand,” *The New England Journal of Medicine*, 361(23), pp. 2209–2220. Available at: https://doi.org/10.1056/NEJMoa0908492.

141. Richardson, S.I. *et al.* (2018) “HIV-specific Fc effector function early in infection predicts the development of broadly neutralizing antibodies,” *PLOS Pathogens*, 14(4), p. e1006987. Available at: https://doi.org/10.1371/journal.ppat.1006987.

142. Robertson, D.L. *et al.* (2000) “HIV-1 Nomenclature Proposal,” *Science*, 288(5463), pp. 55–55. Available at: https://doi.org/10.1126/science.288.5463.55d.

143. Rodriguez, O.L. *et al.* (2023) “Genetic variation in the immunoglobulin heavy chain locus shapes the human antibody repertoire,” *Nature Communications*, 14(1), p. 4419. Available at: https://doi.org/10.1038/s41467-023-40070-x.

144. Rojas-Celis, V. *et al.* (2019) “New Challenges of HIV-1 Infection: How HIV-1 Attacks and Resides in the Central Nervous System,” *Cells*, 8(10), p. 1245. Available at: https://doi.org/10.3390/cells8101245.

145. Rusert, P. *et al.* (2016) “Determinants of HIV-1 broadly neutralizing antibody induction,” *Nature Medicine*, 22(11), pp. 1260–1267. Available at: https://doi.org/10.1038/nm.4187.

146. Rutten, L. *et al.* (2018) “A Universal Approach to Optimize the Folding and Stability of Prefusion-Closed HIV-1 Envelope Trimers,” *Cell Reports*, 23(2), pp. 584–595. Available at: https://doi.org/10.1016/j.celrep.2018.03.061.

147. Sanders, R.W. *et al.* (2000) “Variable-loop-deleted variants of the human immunodeficiency virus type 1 envelope glycoprotein can be stabilized by an intermolecular disulfide bond between the gp120 and gp41 subunits,” *Journal of Virology*, 74(11), pp. 5091–5100. Available at: https://doi.org/10.1128/jvi.74.11.5091-5100.2000.

148. Sanders, R.W. *et al.* (2002) “Stabilization of the soluble, cleaved, trimeric form of the envelope glycoprotein complex of human immunodeficiency virus type 1,”

Journal of Virology, 76(17), pp. 8875–8889. Available at: https://doi.org/10.1128/jvi.76.17.8875-8889.2002.

149. Sanders, R.W. *et al.* (2013) “A Next-Generation Cleaved, Soluble HIV-1 Env Trimer, BG505 SOSIP.664 gp140, Expresses Multiple Epitopes for Broadly Neutralizing but Not Non-Neutralizing Antibodies,” *PLOS Pathogens*, 9(9), p. e1003618. Available at: https://doi.org/10.1371/journal.ppat.1003618.

150. Sanders, R.W. *et al.* (2015) “HIV-1 VACCINES. HIV-1 neutralizing antibodies induced by native-like envelope trimers,” *Science (New York, N.Y.)*, 349(6244), p. aac4223. Available at: https://doi.org/10.1126/science.aac4223.

151. Sanders, R.W. and Moore, J.P. (2017) “Native-like Env trimers as a platform for HIV-1 vaccine design,” *Immunological Reviews*, 275(1), pp. 161–182. Available at: https://doi.org/10.1111/imr.12481.

152. Sather, D.N. *et al.* (2012) “Broadly Neutralizing Antibodies Developed by an HIV-Positive Elite Neutralizer Exact a Replication Fitness Cost on the Contemporaneous Virus,” *Journal of Virology*, 86(23), pp. 12676–12685. Available at: https://doi.org/10.1128/JVI.01893-12.

153. Scheid, J.F. *et al.* (2011) “Sequence and Structural Convergence of Broad and Potent HIV Antibodies That Mimic CD4 Binding,” *Science*, 333(6049), pp. 1633–1637. Available at: https://doi.org/10.1126/science.1207227.

154. Scheres, S.H.W. (2012) “RELION: Implementation of a Bayesian approach to cryo-EM structure determination,” *Journal of Structural Biology*, 180(3), pp. 519–530. Available at: https://doi.org/10.1016/j.jsb.2012.09.006.

155. Schommers, P. *et al.* (2020) “Restriction of HIV-1 Escape by a Highly Broad and Potent Neutralizing Antibody,” *Cell*, 180(3), pp. 471-489.e22. Available at: https://doi.org/10.1016/j.cell.2020.01.010.

156. Schroeder, H.W. and Cavacini, L. (2010) “Structure and function of immunoglobulins,” *Journal of Allergy and Clinical Immunology*, 125(2 Suppl 2), pp. S41-52. Available at: https://doi.org/10.1016/j.jaci.2009.09.046.

157. Serrão, R. *et al.* (2019) “Non-AIDS-related comorbidities in people living with HIV-1 aged 50 years and older: The AGING POSITIVE study,” *International Journal of Infectious Diseases*, 79, pp. 94–100. Available at: https://doi.org/10.1016/j.ijid.2018.10.011.

158. Sharma, S.K. *et al.* (2015) “Cleavage-independent HIV-1 Env trimers engineered as soluble native spike mimetics for vaccine design,” *Cell reports*, 11(4), pp. 539–550. Available at: https://doi.org/10.1016/j.celrep.2015.03.047.

159. Sharp, P.M. and Hahn, B.H. (2011) “Origins of HIV and the AIDS Pandemic,” *Cold Spring Harbor Perspectives in Medicine*, 1(1), p. a006841. Available at: https://doi.org/10.1101/cshperspect.a006841.

160. Simek, M.D. *et al.* (2009) “Human immunodeficiency virus type 1 elite neutralizers: individuals with broad and potent neutralizing activity identified by using a high-throughput neutralization assay together with an analytical selection algorithm,” *Journal of Virology*, 83(14), pp. 7337–7348. Available at: https://doi.org/10.1128/JVI.00110-09.

161. Simon, F. *et al.* (1998) “Identification of a new human immunodeficiency virus type 1 distinct from group M and group O,” *Nature Medicine*, 4(9), pp. 1032–1037. Available at: https://doi.org/10.1038/2017.

162. Sivay, M.V. *et al.* (2017) “Characterization of HIV Seroconverters in a TDF/FTC PrEP Study: HPTN 067/ADAPT,” *Journal of Acquired Immune Deficiency Syndromes*, 75(3), pp. 271–279. Available at: https://doi.org/10.1097/QAI.0000000000001374.

163. Sok, D. *et al.* (2014) “Recombinant HIV envelope trimer selects for quaternary-dependent antibodies targeting the trimer apex,” *Proceedings of the National Academy of Sciences*, 111(49), pp. 17624–17629. Available at: https://doi.org/10.1073/pnas.1415789111.

164. Sok, D. *et al.* (2016) “A Prominent Site of Antibody Vulnerability on HIV Envelope Incorporates a Motif Associated with CCR5 Binding and Its

Camouflaging Glycans," *Immunity*, 45(1), pp. 31–45. Available at: https://doi.org/10.1016/j.immuni.2016.06.026.

165. Sok, D. and Burton, D.R. (2018) "Recent progress in broadly neutralizing antibodies to HIV," *Nature Immunology*, 19(11), pp. 1179–1188. Available at: https://doi.org/10.1038/s41590-018-0235-7.

166. Song, L. *et al.* (2021) "TRUST4: immune repertoire reconstruction from bulk and single-cell RNA-seq data," *Nature Methods*, 18(6), pp. 627–630. Available at: https://doi.org/10.1038/s41592-021-01142-2.

167. Stefic, K. *et al.* (2019) "Impact of HIV-1 Diversity on Its Sensitivity to Neutralization," *Vaccines*, 7(3), p. 74. Available at: https://doi.org/10.3390/vaccines7030074.

168. Sutar, J. *et al.* (2025) "Distinct region-specific neutralization profiles of contemporary HIV-1 clade C against best-in-class broadly neutralizing antibodies." bioRxiv, p. 2024.12.31.630867. Available at: https://doi.org/10.1101/2024.12.31.630867.

169. Thavarajah, J.J., Hønge, B.L. and Wejse, C.M. (2024) "The Use of Broadly Neutralizing Antibodies (bNAbs) in HIV-1 Treatment and Prevention," *Viruses*, 16(6), p. 911. Available at: https://doi.org/10.3390/v16060911.

170. Tomaras, G.D. *et al.* (2008) "Initial B-cell responses to transmitted human immunodeficiency virus type 1: virion-binding immunoglobulin M (IgM) and IgG antibodies followed by plasma anti-gp41 antibodies with ineffective control of initial viremia," *Journal of Virology*, 82(24), pp. 12449–12463. Available at: https://doi.org/10.1128/JVI.01708-08.

171. Tonegawa, S. (1983) "Somatic generation of antibody diversity," *Nature*, 302(5909), pp. 575–581. Available at: https://doi.org/10.1038/302575a0.

172. Tong, T. *et al.* (2023) "Impact of stabilizing mutations on the antigenic profile and glycosylation of membrane-expressed HIV-1 envelope glycoprotein," *PLOS Pathogens*, 19(8), p. e1011452. Available at: https://doi.org/10.1371/journal.ppat.1011452.

173. Torrents de la Peña, A. and Sanders, R.W. (2018) “Stabilizing HIV-1 envelope glycoprotein trimers to induce neutralizing antibodies,” *Retrovirology*, 15(1), p. 63. Available at: https://doi.org/10.1186/s12977-018-0445-y.

174. Trkola, A. *et al.* (2005) “Delay of HIV-1 rebound after cessation of antiretroviral therapy through passive transfer of human neutralizing antibodies,” *Nature Medicine*, 11(6), pp. 615–622. Available at: https://doi.org/10.1038/nm1244.

175. Tseng, A., Seet, J. and Phillips, E.J. (2015) “The evolution of three decades of antiretroviral therapy: challenges, triumphs and the promise of the future,” *British Journal of Clinical Pharmacology*, 79(2), pp. 182–194. Available at: https://doi.org/10.1111/bcp.12403.

176. Ullah Nayan, M. *et al.* (2023) “Advances in long-acting slow effective release antiretroviral therapies for treatment and prevention of HIV infection,” *Advanced Drug Delivery Reviews*, 200, p. 115009. Available at: https://doi.org/veill.

177. UNAIDS (2024) *2024 global AIDS report — The Urgency of Now: AIDS at a Crossroads* | *UNAIDS*. Available at: https://www.unaids.org/en/resources/documents/2024/global-aids-update-2024 (Accessed: March 4, 2025).

178. Veillette, M. *et al.* (2014) “Conformational Evaluation of HIV-1 Trimeric Envelope Glycoproteins Using a Cell-based ELISA Assay,” *Journal of Visualized Experiments*, (91), p. e51995. Available at: https://doi.org/10.3791/51995.

179. Verkerke, H.P. *et al.* (2016) “Epitope-Independent Purification of Native-Like Envelope Trimers from Diverse HIV-1 Isolates,” *Journal of Virology*, 90(20), pp. 9471–9482. Available at: https://doi.org/10.1128/jvi.01351-16.

180. Walker, L.M. *et al.* (2010) “A Limited Number of Antibody Specificities Mediate Broad and Potent Serum Neutralization in Selected HIV-1 Infected Individuals,” *PLOS Pathogens*, 6(8), p. e1001028. Available at: https://doi.org/10.1371/journal.ppat.1001028.

181. Walker, L.M. *et al.* (2011) “Broad neutralization coverage of HIV by multiple highly potent antibodies,” *Nature*, 477(7365), pp. 466–470. Available at: https://doi.org/10.1038/nature10373.

182. Wei, X. *et al.* (2003) “Antibody neutralization and escape by HIV-1,” *Nature*, 422(6929), pp. 307–312. Available at: https://doi.org/10.1038/nature01470.

183. Weissenhorn, W. *et al.* (1996) “The ectodomain of HIV-1 env subunit gp41 forms a soluble, alpha-helical, rod-like oligomer in the absence of gp120 and the N-terminal fusion peptide,” *The EMBO journal*, 15(7), pp. 1507–1514.

184. WHO (2024) *HIV data and statistics*. Available at: https://www.who.int/teams/global-hiv-hepatitis-and-stis-programmes/hiv/strategic-information/hiv-data-and-statistics (Accessed: March 4, 2025).

185. Wibmer, C.K., Moore, P.L. and Morris, L. (2015) “HIV broadly neutralizing antibody targets,” *Current opinion in HIV and AIDS*, 10(3), pp. 135–143. Available at: https://doi.org/10.1097/COH.0000000000000153.

186. Wiehe, K. *et al.* (2018) “Functional Relevance of Improbable Antibody Mutations for HIV Broadly Neutralizing Antibody Development,” *Cell Host & Microbe*, 23(6), pp. 759-765.e6. Available at: https://doi.org/10.1016/j.chom.2018.04.018.

187. Williams, W.B. *et al.* (2017) “Initiation of HIV neutralizing B cell lineages with sequential envelope immunizations,” *Nature Communications*, 8, p. 1732. Available at: https://doi.org/10.1038/s41467-017-01336-3.

188. Willis, J.R. *et al.* (2025) “Vaccination with mRNA-encoded nanoparticles drives early maturation of HIV bnAb precursors in humans,” *Science*, p. eadr8382. Available at: https://doi.org/10.1126/science.adr8382.

189. Wrapp, D. *et al.* (2023) “Structure-Based Stabilization of SOSIP Env Enhances Recombinant Ectodomain Durability and Yield,” *Journal of Virology*. Edited by G. Silvestri, 97(1), pp. e01673-22. Available at: https://doi.org/10.1128/jvi.01673-22.

190. Wu, X. *et al.* (2011) “Focused Evolution of HIV-1 Neutralizing Antibodies Revealed by Structures and Deep Sequencing,” *Science*, 333(6049), pp. 1593–1602. Available at: https://doi.org/10.1126/science.1207532.

191. Wyatt, R. and Sodroski, J. (1998) “The HIV-1 Envelope Glycoproteins: Fusogens, Antigens, and Immunogens,” *Science*, 280(5371), pp. 1884–1888. Available at: https://doi.org/10.1126/science.280.5371.1884.

192. Yates, N.L. *et al.* (2014) “Vaccine-induced Env V1-V2 IgG3 correlates with lower HIV-1 infection risk and declines soon after vaccination,” *Science Translational Medicine*, 6(228), p. 228ra39. Available at: https://doi.org/10.1126/scitranslmed.3007730.

193. Ye, J. *et al.* (2013) “IgBLAST: an immunoglobulin variable domain sequence analysis tool,” *Nucleic Acids Research*, 41(Web Server issue), pp. W34-40. Available at: https://doi.org/10.1093/nar/gkt382.

194. Yu, L. and Guan, Y. (2014) “Immunologic Basis for Long HCDR3s in Broadly Neutralizing Antibodies Against HIV-1,” *Frontiers in Immunology*, 5, p. 250. Available at: https://doi.org/10.3389/fimmu.2014.00250.

195. Zhang, P. *et al.* (2024) “Design of soluble HIV-1 envelope trimers free of covalent gp120-gp41 bonds with prevalent native-like conformation,” *Cell Reports*, 43(8), p. 114518. Available at: https://doi.org/10.1016/j.celrep.2024.114518.

196. Zhang, R. *et al.* (2019) “PI-6 Construction and analysis of V3 glycopeptide antigens for HIV-1 vaccine design,” *JAIDS Journal of Acquired Immune Deficiency Syndromes*, 81(1), pp. 78–78. Available at: https://doi.org/10.1097/01.qai.0000558039.75095.df.

197. Zhang, Z. *et al.* (2016) “Antiviral Therapy by HIV-1 Broadly Neutralizing and Inhibitory Antibodies,” *International Journal of Molecular Sciences*, 17(11), p. 1901. Available at: https://doi.org/10.3390/ijms17111901.

198. Zhou, T. *et al.* (2013) “Multidonor analysis reveals structural elements, genetic determinants, and maturation pathway for HIV-1 neutralization by VRC01-class

antibodies," *Immunity*, 39(2), pp. 245–258. Available at: https://doi.org/10.1016/j.immuni.2013.04.012.

199. Zhou, T. and Xu, K. (2018) "Structural Features of Broadly Neutralizing Antibodies and Rational Design of Vaccine," in L. Zhang and S.R. Lewin (eds.) *HIV Vaccines and Cure*. Singapore: Springer Singapore (Advances in Experimental Medicine and Biology), pp. 73–95. Available at: https://doi.org/10.1007/978-981-13-0484-2_4.

Appendix A - CAPRISA letter of support

CAPRISA
CENTRE FOR THE AIDS PROGRAMME OF RESEARCH IN SOUTH AFRICA

Generating Knowledge - Impacting Health

Doris Duke Medical Research Institute (2nd floor), 719 Umbilo Road, Private Bag X7, Congella, 4013, Durban, South Africa
tel: +27 31 2604555 | **fax:** +27 31 2604549 | email: **caprisa@caprisa.org** | **www.caprisa.org**

7th March 2023

Prof Clem Penny
Chair: Human Research Ethics Committee (Medical)
Phillip V Tobias Health Sciences Building
29 Princess of Wales Terrace
Parktown
Johannesburg, 2193
South Africa

Dear Prof Penny,

Re: Danielle Martin - MSc study *"Design of soluble HIV-1 Env trimers, from highly neutralization resistant HIV-1 strains, for bNAb isolation"*

In my role as Project Director and Research Clinician at the Centre for the AIDS Programme of Research in South Africa (CAPRISA) and Co-Chair of the CAPRISA 002 Acute Infection Study, I write to confirm that Ms Danielle Martin will have access to stored samples from the CAPRISA 002 and CAPRISA 004 cohorts to carry out the above study for her MSc through the University of the Witwatersrand.

Participants in the CAPRISA 002 and 004 studies have consented to stored specimens being used for additional studies. The CAPRISA 002 BREC approved Specimen Storage Consent (V4.02) attached here, states that: "*We may test your cells, proteins, other chemicals in your body and genes (DNA). Some of the samples will also be tested to see how your nutritional status may be interacting with HIV infection. Your samples may be analysed in laboratories outside of South Africa".*

Ms Danielle Martin's study will be supervised by Prof Penny Moore, Dr Dale Kitchin, Dr Nono Mkhize and Dr Thandeka Moyo-Gwete and represents an extension of our successful collaboration with Prof Moore's laboratory at the National Institute for Communicable Diseases, Johannesburg.

Please do not hesitate to contact me if there are any queries.

Yours sincerely,

Dr Nigel Garrett
MBBS, MRCP, MSc, PhD
Head of Vaccine and Pathogenesis Research, CAPRISA
Honorary Associate Professor in Public Health, University of KwaZulu-Natal
Doris Duke Medical Research Institute (2nd Floor)
Nelson R Mandela School of Medicine, University of KwaZulu-Natal
Durban, South Africa
Tel: +27 31 655 0617 (ECRS) +27 31 655 0518 (DDMRI)
Email: nigel.garrett@caprisa.org

CAPRISA hosts a DSI-NRF Centre of Excellence in HIV Prevention
CAPRISA is the UNAIDS Collaborating Centre for HIV Research and Policy
CAPRISA has a GIZ-funded Epidemic Intelligence Unit
CAPRISA hosts a MRC HIV-TB Pathogenesis and Treatment Research Unit
CAPRISA hosts a DoH-MRC Special Initiative for HIV Prevention Technology
Partner Institutions:
Board of Control: B Ntuli (Chair) · M Rajab (Deputy Chair) · Q Abdool Karim · SS Abdool Karim · AC Bawa · JH Beare · JM Frantz · LP Fried (US) · ST Harrison · TL Jones · ARDH Moosa · M Moshabela · K Naidoo · A Nortier · A Puren · HW Sherwin · LV Theron
Scientific Advisory Board: F Barré-Sinoussi (Chair) · T Quinn (Vice Chair) · P Godfrey-Faussett · R Hayes · J Mascola · Y Pillay · S Swaminathan
Registration number: 2002/024027/08 • PBO number: 930 018 155

Appendix B - Ethics clearance certificate

UNIVERSITY OF THE WITWATERSRAND, JOHANNESBURG

R14/49 Miss Danielle Martin M230710 MED23-05-005

HUMAN RESEARCH ETHICS COMMITTEE (MEDICAL)

CLEARANCE CERTIFICATE NO. M230710 MED23-05-005

NAME: (Principal Investigator)	Miss Danielle Martin
STUDENT/STAFF NO:	2589758
DEGREE:	MSc (Med) Virology
DEPARTMENT:	School of Pathology Department of Virology National Institute for Communicable Diseases
PROJECT TITLE:	Design of soluble envelope trimers from highly neutralization-resistant HIV-1 strains for the isolation of broadly neutralizing antibodies
DATE CONSIDERED:	11/08/2023
DECISION:	Approved unconditionally
CONDITIONS:	
SUPERVISOR:	Dr Thandeka Moyo-Gwete and Dr Dale Kitchin
APPROVED BY:	Prof P Ruff, Chair, HREC (Medical)
DATE OF APPROVAL:	17/01/2024 **EXPIRY DATE:** 17/01/2029

This clearance certificate is valid for 5 years from date of approval. Extension may be applied for.

DECLARATION OF INVESTIGATORS

I/we fully understand the conditions under which I am/we are authorized to carry out the above-mentioned research and I/we undertake to ensure compliance with these conditions. Should any departure be contemplated, from the research protocol as approved, I/we undertake to resubmit the application to the Committee. **I agree to submit a yearly progress report** in July each year until study is closed. Failure to submit annual report will result in ethics clearance certificate suspension. The date for annual re-certification will be one year after the date of convened meeting where the study was initially reviewed. In this case, the study was initially reviewed in July and will therefore be due in the month of July each year. Unreported changes to the application invalidate the clearance given by the HREC (Medical). Email signed copy of this ethics clearance certificate prior to commencing with the study hrec-medical.researchoffice@wits.ac.za

Principal Investigator Signature Date

Appendix C - Turnitin report

Document Viewer

Turnitin Originality Report

Processed on: 27-May-2025 1:05 PM SAST
ID: 2685970010
Word Count: 23633
Submitted: 1

20250526_Dissertation_Danielle Martin_v-1.doc... By Danielle Martin

Similarity Index	Similarity by Source	
1%	Internet Sources:	2%
	Publications:	2%
	Student Papers:	0%

include quoted | include bibliography | excluding matches < 1% | mode: quickview (classic) report | print | download

1% match (Internet from 08-May-2024)
https://wiredspace.wits.ac.za/server/api/core/bitstreams/bbc484a2-3033-4519-8a5a-e4f41d5959d6/content

Appendix D - Supplementary materials

Table S2.1: Neutralisation screening data from the IAVI ADVANCE surveillance study.

	Subtype Year Virus	C 2017 PC220898	C 2008 FRESH1388	D 2009 PC235205
Epitopes	**Antibody**	**Percentage inhibition (%)**		
CD4 binding site	N6	0	100	93
	1-18	0,04	32	68
V2-apex	ePGDM1400V9	100	22	100
	CAP256_VRC26.25	93	22	93
V3-glycan	ePGT121_V1	46	79	9
	BG18	20	100	19
	Mean	43	59	64

Source: Kitchin *et al*. unpublished

Table S2.2: Neutralisation breadth of CAPRISA participant plasma samples tested against an 18-virus panel, covering subtypes A, B and C.

CAPRISA cohort	CAPRISA participant	Plasma samples		
		Year 2	Year 3	Year 4
		Neutralization breadth (%)		
002	8	33	39	ND
	37	28	50	44
	177	28	56	56
	206	39	44	44
	248	17	56	72
	255	56	61	ND
	267	11	39	50
	280	ND	ND	56
004	287	56	61	56
	288	17	39	ND
	292	28	56	66
	309	28	33	39
	312	44	61	33
	314	44	ND	ND
	322	39	44	ND
	331	ND	33	56
	341	39	44	50
	357	56	44	ND
	370	33	ND	ND
	373	ND	39	ND

Source: Gray et al., 2007; Moore et al. unpublished data
ND – not determined

Table S2.3: Primers used in the RATPIg workflow to amplify BCR sequences and construct linear expression cassettes.

Primer Name	Sequence
VRC_CMV_FWD	CCATTGCATACGTTGTATCCATATC
VRC_CMV_SPLICE_TSO_REV	TATGTACTCTGCGTTGATACCACTGCTTCGACGGTGACTGCA GAAAAGAC
IgHC_FWD	CATCGGTCTTCCCCCTG
IgLC_FWD	GTGGCTGCACCATCTGTC
TBGH_REV	TTAAAATTCTATGATTTCTCTCATTACTTC
A-tag TSO	/5Me-isodC//iisodG//iMe-isodC/AAGCAGTGGTATCAACGCAGAGTACATArGrGrG
Primer II A	AAGCAGTGGTATCAACGCAGAGT
TSoligo2_polydT	CAAGCAGAAGACGGCATACGAGTTTTTTTTTTTTTTTTTTTTTTTTTTTTTTTT(V:33333400)(N:25252525)
TSoligo2	CAAGCAGAAGACGGCATACGAG
IgG	GCCAGGGGGAAGACCGATGGGCCCTTGGTGGA
IgK	GCGGGAAGATGAAGACAGATGGTGCAGCCAC
IgL	GGCCTTGTTGGCTTGAAGCTCCTCAGAGGAGGG
IgA	GAGGCTCAGCGGGAAGACCTTGGGGCTGGTCGG

Table S2.4: cDNA synthesis reaction mixture for a single well.

Reagent	Volume (µl)
5× Ultra Low First-Strand Buffer	4
TSO (100uM)	0,48
Recombinant RNase Inhibitor	0,5
SMARTScribe Reverse Transcriptase	2
dNTP Mix (10mM)	2
DTT (100mM)	0,5
Nuclease free H_2O	0,52

Table S2.5: cDNA synthesis reaction parameters.

Step	Cycles	Temperature (°C)	Time
1	1	42	90 min
2	1	70	10 min
3	1	4	hold

Table S2.6: cDNA amplification reaction mixture for a single well.

Reagent	Volume (µl)
2× SeqAmp PCR Buffer	25
PCR Primer II A (100uM)	0,15
TSoligo2 primer (100uM)	0,15
SeqAmp DNA Polymerase	1
Nuclease free H_2O	3,7

Table S2.7: cDNA amplification reaction parameters.

Step	Cycles	Temperature (°C)	Time
1	1	95	1 min
2	22	98	10 s
		65	30 s
		68	3 min
3	1	72	10 min

Table S2.8: Ig enrichment reaction mixture for a single well.

Ig enrichment heavy chains		Ig enrichment light chains	
Reagent	**Volume (µl)**	**Reagent**	**Volume (µl)**
2x SuperFi II MM	10	2x SuperFi II MM	10
Primer IIA (100 uM)	0,08	Primer IIA (100 uM)	0,08
IgG (100 uM)	0,04	IgK (100 uM)	0,04
IgA (100 uM)	0,04	IgL (100 uM)	0,04
H2O	2,84	H2O	2,84
cDNA	7	cDNA	7

Table S2.9: Ig enrichment reaction parameters.

	Ig enrichment heavy chains			Ig enrichment light chains		
Step	**Cycles**	**Temperature (°C)**	**Time**	**Cycles**	**Temperature (°C)**	**Time**
1	1	98	30 s	1	98	30 s
2	30	98	10 s	25	98	10 s
		60	10 s		60	10 s
		72	30 s		72	30 s
3	1	72	3 min	1	72	3 min
4	1	4	hold	1	4	hold

Table S2.10: Isolation of cassette fragments reaction mixture for a single well.

Reagent	Volume (µl)
2× SuperFi II mastermix	25
Fwd primer (10 uM)	2,5
Rev Primer (10 uM)	2,5
Donor Plasmid	1
Water, nuclease-free	19

Table S2.11: Isolation of cassette fragments reaction parameters.

Step	Cycles	Temperature (°C)	Time
1	1	98	1 min
2	20	98	30 s
		60	10 s
		72	1 min
3	1	72	5 min
4	1	4	hold

Table S2.12: Amplification of cassette fragments reaction mixture for a single well.

Reagent	Volume (µl)
2× SuperFi II mastermix	25
Fwd primer (10 uM)	2,5
Rev Primer (10 uM)	2,5
1ng/uL Template	1
Water, nuclease-free	19

Table S2.13: Amplification of cassette fragments reaction parameters.

Step	Cycles	Temperature (°C)	Time
1	1	98	1 min
2	30	98	30 s
		60	10 s
		72	1 min
3	1	72	5 min
4	1	4	hold

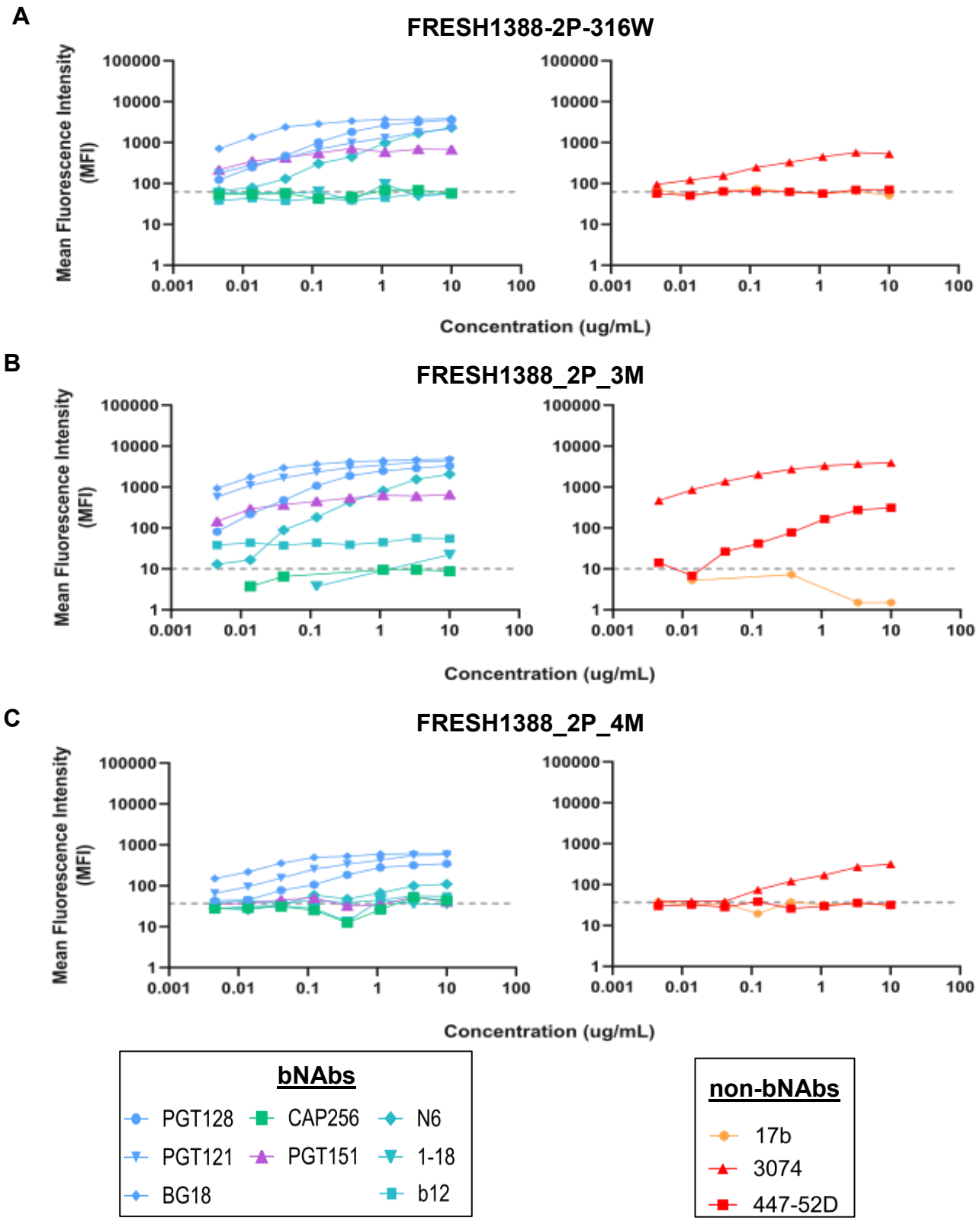

Figure S3.1: Luminex binding data of the bNAb and non-bNAb antibodies to the V3 stabilised FRESH1388 trimers. Binding of bNAbs (left) and non-bNAb (right) to the V3 stabilised trimers: (A) FRESH1388_2P_316W, (B) FRESH1388_2P_3M and (C) FRESH1388_2P_4M. Palivizumab was used to set the threshold for low binding. The dotted line indicates the binding activity of palivizumab, at the highest concentration tested (10 µg/mL).

Table S3.1: Immunogenetics of CAP287 BCRs where paired, functionally rearranged, full-length V(D)J sequences were recovered.

Clonal lineage	Antibody name	IGHV	IGHJ	CDRH3 **length (AA)**	Percentage **SHM**	IGLV/**IGKV**	IGLJ/**IGKJ**	CDRL3 **length (AA)**	Percentage **SHM**
3-13_a	CAP287.16	IGHV3-13	IGHJ6	20	14,4	IGKV1-39	IGKJ1	9	1,7
	CAP287.17	IGHV3-13	IGHJ6	20	14,4	IGLV2-23	IGLJ3	11	8,7
	CAP287.19	IGHV3-13	IGHJ6	20	22,0	IGLV2-14	IGLJ3	12	9,6
	CAP287.44	IGHV3-13	IGHJ6	20	18,9	IGLV2-14	IGLJ3	12	14,7
	CAP287.50	IGHV3-13	IGHJ6	20	14,4	IGKV1-12	IGKJ3	9	4,2
	CAP287.92	IGHV3-13	IGHJ6	20	19,6	IGLV2-14	IGLJ3	12	9,6
	CAP287.98	IGHV3-13	IGHJ6	20	20,6	IGLV2-14	IGLJ3	12	8,2
1-46_a	CAP287.156	IGHV1-46	IGHJ1	10	25,6	IGKV1-5	IGKJ4	8	2,8
	CAP287.166	IGHV1-46	IGHJ1	10	25,6	IGKV2-24	IGKJ1	9	10,3
	CAP287.168	IGHV1-46	IGHJ1	10	25,6	IGKV2-24	IGKJ1	9	10,3
	CAP287.169	IGHV1-46	IGHJ1	10	25,9	IGKV3-11	IGKJ1	11	4,5
	CAP287.170	IGHV1-46	IGHJ1	10	25,6	IGKV2-24	IGKJ1	9	10,3
	CAP287.172	IGHV1-46	IGHJ1	10	25,6	IGKV4-1	IGKJ3	9	6,1
3-13_b	CAP287.128	IGHV3-13	IGHJ6	20	16,3	IGLV1-51	IGLJ3	11	2,4
	CAP287.29	IGHV3-13	IGHJ6	20	16,3	IGLV2-23	IGLJ3	11	8,7
	CAP287.41	IGHV3-13	IGHJ6	20	16,3	IGLV2-14	IGLJ3	11	7,9
	CAP287.5	IGHV3-13	IGHJ6	20	16,1	IGLV2-23	IGLJ3	11	8,7
	CAP287.69	IGHV3-13	IGHJ6	20	17,0	IGKV3-11	IGKJ2	11	1,0
1-69_a	CAP287.37	IGHV1-69	IGHJ5	19	15,4	IGKV4-1	IGKJ3	9	6,3
	CAP287.65	IGHV1-69	IGHJ5	19	14,4	IGKV3-11	IGKJ4	9	2,1
	CAP287.82	IGHV1-69	IGHJ5	19	14,4	IGKV4-1	IGKJ3	9	3,6
	CAP287.84	IGHV1-69	IGHJ5	19	14,4	IGKV4-1	IGKJ3	9	3,6
	CAP287.85	IGHV1-69	IGHJ5	19	14,4	IGLV6-57	IGLJ3	11	5,1
3-13_c	CAP287.39	IGHV3-13	IGHJ6	20	21,0	IGLV2-14	IGLJ3	11	8,5

	CAP287.77	IGHV3-13	IGHJ6	20	19,6	IGKV3-20	IGKJ2	10	4,8
	CAP287.78	IGHV3-13	IGHJ6	20	19,6	IGLV2-14	IGLJ3	11	8,1
	CAP287.80	IGHV3-13	IGHJ6	20	19,6	IGKV4-1	IGKJ4	9	3,0
3-53_a	CAP287.62	IGHV3-53	IGHJ6	18	12,7	IGKV3-11	IGKJ5	10	3,8
	CAP287.63	IGHV3-53	IGHJ6	18	12,7	IGLV2-23	IGLJ3	11	8,7
	CAP287.73	IGHV3-53	IGHJ6	18	12,7	IGLV3-21	IGLJ3	11	6,9
	CAP287.86	IGHV3-53	IGHJ6	18	12,7	IGLV2-14	IGLJ3	11	12,5
4-61_a	CAP287.1	IGHV4-61	IGHJ3	10	6,8	IGLV2-23	IGLJ3	10	8,8
	CAP287.12	IGHV4-61	IGHJ3	10	6,8	IGLV2-23	IGLJ3	10	5,8
	CAP287.2	IGHV4-61	IGHJ3	10	6,8	IGKV4-1	IGKJ2	9	2,6
	CAP287.30	IGHV4-61	IGHJ3	10	6,8	IGLV2-14	IGLJ2	10	4,1
3-15_a	CAP287.144	IGHV3-15	IGHJ4	15	7,9	IGKV2-30	IGKJ4	9	0,7
	CAP287.149	IGHV3-15	IGHJ4	15	7,9	IGKV3-11	IGKJ4	10	0,4
	CAP287.158	IGHV3-15	IGHJ4	15	7,9	IGLV3-27	IGLJ2	9	4,3
1-46_b	CAP287.159	IGHV1-46	IGHJ4	13	5,1	IGKV1-8	IGKJ3	9	2,8
	CAP287.160	IGHV1-46	IGHJ4	13	5,1	IGKV3-15	IGKJ5	10	3,1
	CAP287.163	IGHV1-46	IGHJ4	13	5,1	IGKV4-1	IGKJ4	9	7,6
1-69-2_a	CAP287.100	IGHV1-69-2	IGHJ1	6	11,1	IGKV3-15	IGKJ1	9	7,4
	CAP287.116	IGHV1-69-2	IGHJ1	6	11,1	IGKV2-28	IGKJ5	9	3,0
3-48_a	CAP287.26	IGHV3-48	IGHJ6	9	2,4	IGKV1-16	IGKJ3	9	2,1
	CAP287.27	IGHV3-48	IGHJ6	9	2,4	IGLV2-23	IGLJ3	11	8,7
3-7_a	CAP287.129	IGHV3-7	IGHJ4	15	5,4	IGKV3-20	IGKJ1	9	3,2
	CAP287.142	IGHV3-7	IGHJ4	15	5,4	IGKV3-20	IGKJ1	9	3,2
3-74_a	CAP287.164	IGHV3-74	IGHJ2	13	10,8	IGKV2-28	IGKJ2	9	4,3
	CAP287.165	IGHV3-74	IGHJ2	13	10,8	IGKV4-1	IGKJ4	9	7,6
1-18_a	CAP287.90	IGHV1-18	IGHJ4	15	3,0	IGKV1-5	IGKJ5	9	2,8
1-24_a	CAP287.70	IGHV1-24	IGHJ5	16	5,4	IGLV1-40	IGLJ2	11	1,7
1-46_c	CAP287.49	IGHV1-46	IGHJ1	10	25,0	IGKV2-24	IGKJ1	9	12,0
1-69_b	CAP287.57	IGHV1-69	IGHJ3	18	6,5	IGKV1-33	IGKJ4	11	3,1
1-69_c	CAP287.40	IGHV1-69	IGHJ4	20	8,5	IGKV4-1	IGKJ4	9	2,6
1-69D_a	CAP287.60	IGHV1-69	IGHJ2	16	6,8	IGLV3-21	IGLJ3	11	6,9

2-5_a	CAP287.89	IGHV2-5	IGHJ6	26	3,4	IGLV1-51	IGLJ3	11	2,4
2-70_a	CAP287.166	IGHV2-70	IGHJ4	12	2,0	IGKV3-15	IGKJ1	11	2,4
3-11_a	CAP287.83	IGHV3-11	IGHJ4	16	6,5	IGLV6-57	IGLJ3	11	5,1
3-15_b	CAP287.33	IGHV3-15	IGHJ3	17	4,4	IGKV1-33	IGKJ5	9	2,1
3-15_c	CAP287.20	IGHV3-15	IGHJ4	9	12,3	IGKV3-11	IGKJ2	9	12,4
3-15_d	CAP287.55	IGHV3-15	IGHJ4	12	12,8	IGKV3-11	IGKJ4	9	4,2
3-20_a	CAP287.104	IGHV3-20	IGHJ4	23	0,0	IGKV1-17	IGKJ2	9	0,0
3-21_a	CAP287.66	IGHV3-21	IGHJ4	17	5,7	IGLV2-14	IGLJ3	11	9,3
3-23_a	CAP287.93	IGHV3-23	IGHJ3	16	10,2	IGKV4-1	IGKJ3	9	6,1
3-23D_a	CAP287.99	IGHV3-23	IGHJ4	13	8,6	IGKV4-1	IGKJ3	9	6,1
3-23D_b	CAP287.110	IGHV3-23	IGHJ4	18	14,2	IGKV1-5	IGKJ1	9	1,0
3-30-5_a	CAP287.147	IGHV3-30	IGHJ4	14	4,7	IGLV1-44	IGLJ2	12	3,1
3-30-5_b	CAP287.175	IGHV3-30	IGHJ6	15	7,4	IGLV1-44	IGLJ2	11	9,2
3-48_b	CAP287.4	IGHV3-48	IGHJ4	16	5,1	IGKV3-11	IGKJ2	10	1,8
3-48_c	CAP287.122	IGHV3-48	IGHJ6	16	3,4	IGLV3-1	IGLJ2	10	3,2
3-49_a	CAP287.132	IGHV3-49	IGHJ4	14	7,0	IGKV1-9	IGKJ5	9	4,2
3-66_a	CAP287.8	IGHV3-66	IGHJ3	14	0,7	IGLV2-23	IGLJ3	10	0,3
3-7_b	CAP287.134	IGHV3-7	IGHJ4	11	2,7	IGKV2-30	IGKJ2	9	0,7
3-7_c	CAP287.147	IGHV3-7	IGHJ6	14	10,5	IGKV2-30	IGKJ4	9	0,7
3-74_b	CAP287.174	IGHV3-74	IGHJ4	14	4,7	IGKV1-12	IGKJ4	10	3,2
4-30-4_a	CAP287.6	IGHV4-30-4	IGHJ6	10	2,3	IGKV3-20	IGKJ1	9	2,4
4-30-4_b	CAP287.153	IGHV4-30-4	IGHJ6	21	1,0	IGLV3-16	IGLJ3	10	4,2
4-34_a	CAP287.139	IGHV4-34	IGHJ3	22	7,8	IGKV2-28	IGKJ2	9	4,3
4-38-2_a	CAP287.14	IGHV4-38-2	IGHJ1	22	4,1	IGKV3-20	IGKJ4	9	4,9
4-38-2_b	CAP287.59	IGHV4-38-2	IGHJ4	11	9,1	IGLV2-14	IGLJ3	11	10,2
4-38-2_c	CAP287.114	IGHV4-38-2	IGHJ4	13	3,4	IGKV2-28	IGKJ5	9	3,0
4-38-2_d	CAP287.51	IGHV4-38-2	IGHJ4	14	6,4	IGLV6-57	IGLJ3	9	8,9
4-38-2_e	CAP287.45	IGHV4-38-2	IGHJ4	18	11,3	IGLV1-51	IGLJ2	11	6,4
4-38-2_f	CAP287.109	IGHV4-38-2	IGHJ4	18	14,6	IGLV7-46	IGLJ1	9	10,3
4-39_a	CAP287.155	IGHV4-39	IGHJ4	9	4,4	IGKV1-5	IGKJ4	8	2,8
4-39_b	CAP287.24	IGHV4-39	IGHJ4	10	1,0	IGLV2-11	IGLJ3	11	3,4

4-39_c	CAP287.135	IGHV4-39	IGHJ6	22	4,4	IGLV2-14	IGLJ1	11	3,4
4-4_a	CAP287.108	IGHV4-4	IGHJ3	10	11,5	IGKV1-12	IGKJ4	9	5,2
4-4_b	CAP287.34	IGHV4-4	IGHJ6	22	14,7	IGKV1-39	IGKJ5	8	9,5
4-59_a	CAP287.35	IGHV4-59	IGHJ6	18	2,7	IGLV3-25	IGLJ3	10	3,2
5-10-1_a	CAP287.18	IGHV5-10-1	IGHJ4	13	4,1	IGLV3-25	IGLJ3	11	3,8
5-51_a	CAP287.136	IGHV5-51	IGHJ4	16	2,7	IGKV3-11	IGKJ4	9	1,1
5-51_b	CAP287.58	IGHV5-51	IGHJ5	17	4,4	IGLV2-23	IGLJ3	11	8,7
5-51_c	CAP287.101	IGHV5-51	IGHJ6	15	4,1	IGLV7-43	IGLJ3	10	3,1